



4-2016

Geochemical and Petrological Characterizations of Peridotite and Related Rocks in Marquette County, Michigan

Andrew Lloyd Sasso
Western Michigan University

Follow this and additional works at: https://scholarworks.wmich.edu/masters_theses



Part of the Geochemistry Commons, and the Geology Commons

Recommended Citation

Sasso, Andrew Lloyd, "Geochemical and Petrological Characterizations of Peridotite and Related Rocks in Marquette County, Michigan" (2016). *Masters Theses*. 687.

https://scholarworks.wmich.edu/masters_theses/687

This Masters Thesis-Open Access is brought to you for free and open access by the Graduate College at ScholarWorks at WMU. It has been accepted for inclusion in Masters Theses by an authorized administrator of ScholarWorks at WMU. For more information, please contact wmu-scholarworks@wmich.edu.



GEOCHEMICAL AND PETROLOGICAL CHARACTERIZATIONS OF PERIDOTITE
AND RELATED ROCKS IN MARQUETTE COUNTY, MICHIGAN

by
Andrew Lloyd Sasso

A thesis submitted to the Graduate College
in partial fulfillment of the requirements
for the degree of Master of Science
Geosciences
Western Michigan University
April 2016

Thesis Committee:

Joyashish Thakurta, Ph.D., Chair
Robb Gillespie, Ph.D.
Mohamed Sultan, Ph.D.

GEOCHEMICAL AND PETROLOGICAL CHARACTERIZATIONS OF PERIDOTITE AND RELATED ROCKS IN MARQUETTE COUNTY, MICHIGAN

Andrew Lloyd Sasso, M.S.

Western Michigan University, 2016

This study characterizes the following rock units in Marquette County, Michigan in terms of geochemistry and petrology: (1) Presque Isle Peridotite, (2) Deer Lake Peridotite, (3) Yellowdog Peridotite, and (4) Black Rock Point Gabbro. Analyses were conducted to determine if any petrological or geochemical relationships exist between these units, and to assess the potential of these units to host magmatic sulfide deposits.

The generated data and chosen geotectonic proxies indicate that Black Rock Point Gabbro and Deer Lake Peridotite crystallized from unrelated magmas, probably during the formation of the Great Lakes Tectonic Zone (2.7-1.85 Ga). No evidence was found which suggest that either unit hosts a magmatic sulfide deposit.

Investigation has also revealed a great deal of similarity between the Presque Isle and Yellowdog Peridotite units. Trace element comparisons, along with the use of geotectonic proxies (when considered in conjunction with Yellowdog Peridotite's known age of $1107.2 \text{ Ma} \pm 5.7\text{Ma}$) suggest the possibility that both units crystallized from a similar parent magma during the Midcontinent Rift event (1.1 Ga). Microprobe analysis revealed comparable Ni-depletion in both units. These findings suggest the possibility that Presque Isle Peridotite may be regarded as a prospective location for a magmatic sulfide deposit similar to that hosted by the Yellowdog Peridotite.

Copyright by
Andrew Lloyd Sasso
2016

ACKNOWLEDGMENTS

I wish to thank my primary advisor Dr. Joyashish Thakurta for his patient guidance from the conception of this project, through its completion and for giving me the opportunity to peruse an advanced degree at Western Michigan University. I would also like to express my gratitude for the help and encouragement of the two other members of my thesis committee, Dr. Robb Gillespie and Dr. Mohamed Sultan. Additional, thanks are extended to the Western Michigan University, Graduate College for their financial support.

Further acknowledgement goes to Tony Boxleiter and Ben Hinks for their assistance in the field. And, to Tom Howe for supplying me with equipment.

Thanks also go out to Bob Mahin, of Lundin Mining, for allowing me to collect samples from the Eagle Mine, and for providing me with a geological map of the Eagle Mine area. Melanie Humphrey, of the DEQ for allowing me to access the Marquette core storage facility in order to collect samples. And, Dr. John Fournelle of University of Wisconsin, Madison, for his help with electron microprobe analysis.

To close, I wish to express my most sincere gratitude to my parents, Tony and Holly Sasso, for all of the support, and encouragement which they have provided throughout the undertaking of this project. I also wish to thank all of my friends who have lent their encouragement.

Andrew Lloyd Sasso

TABLE OF CONTENTS

ACKNOWLEDGMENTS	ii
LIST OF TABLES	vii
LIST OF FIGURES	ix
LIST OF ABBREVIATIONS.....	xiv
CHAPTER	
I. INTRODUCTION	1
Research Areas	1
Presque Isle	1
Deer Lake.....	3
Black Rock Point	3
Yellowdog Peridotite-Eagle Mine	3
Peridotite	4
Ophiolites.....	5
Cumulates	6
Magmatic Sulfide Deposits.....	8
Marquette County: Geologic Background.....	10
Great Lakes Tectonic Zone.....	10

Table of Contents-continued

CHAPTER		
	Midcontinent Rift.....	12
	Purpose.....	15
	Previous Work	15
II.	GEOLOGICAL SETTING	17
	Presque Isle Peridotite	17
	Deer Lake Peridotite	19
	Black Rock Point Gabbro	20
	Yellowdog Peridotite	21
III.	METHODS	24
	Field Methods	24
	Petrology and Petrography.....	27
	Geochemistry	29
	Geological Mapping	30
IV.	RESULTS	32
	Petrographic Description	32

Table of Contents-continued

CHAPTER

Presque Isle Peridotite.....	32
Deer Lake Peridotite	37
Black Rock Point Gabbro	41
Yellowdog Peridotite	44
Geochemistry.....	47
X-ray Fluorescence Spectrometry.....	48
Inductively Coupled Plasma Mass Spectrometry	50
Electron Microprobe	56
Presque Isle Peridotite.....	56
Yellowdog Peridotite	60
Black Rock Point Gabbro	65
Data Analysis.....	70
V. DISCUSSION.....	73
Petrology.....	73
Geological Mapping	76

Table of Contents-continued

CHAPTER	
Presque Isle Peridotite.....	76
Deer Lake Peridotite	77
Black Rock Point Gabbro	78
Geochemistry	79
Electron Microprobe	79
Major and Minor Trace Elements	82
Geotectonic Proxies	85
Conclusion	89
Deer Lake Peridotite	89
Black Rock Point Gabbro	91
Presque Isle Peridotite and Yellowdog Peridotite	92
Future Work.....	95
REFERENCES	97

LIST OF TABLES

1. Yellowdog Samples	24
2. Presque Isle Samples.....	25
3. Deer Lake Samples	26
4. Black Rock Point Samples.....	27
5. List of Thin Sections.....	28
6. Whole Rock Geochemistry.....	48
7. Select Base Metal Concentrations	49
8. Trace Element Geochemistry.....	50
9. MQT-14-004 Olivine	56
10. MQT-14-004 Pyroxene.....	58
11. EA-15-002 Olivine.....	60
12. EA-15-002 Pyroxene	62
13. EAUG0012-86.43m Olivine.....	63
14. EAUG0012-86.43m Pyroxene.....	64
15. BRP-14-006 Pyroxene	65

List of Tables-continued

16. BRP-14-006 Plagioclase	68
17. MgO/(MgO+FeO) Ratio of Parental Magma	79

LIST OF FIGURES

1. Geographic map of Marquette County and its location in the state of Michigan.....	1
2. Modified map of the four research areas and their surrounding geology. Adapted from Simms (1992).	2
3. IUGS classification tables for ultramafic rocks. Peridotite shown in yellow. (Woolley, 1996)	4
4. Diagram of the Bay of Islands Ophiolite, Newfoundland. From Blatt et al. (2006).....	6
5. Graphical representation of cumulate rock formation.	7
6. Simplified map of Great Lakes Tectonic Zone. From Sims et al. (1993).....	11
7. Basic diagram of Midcontinent Rift. From Stein et al. (2014).	12
8. Cross section of Midcontinent Rift showing intrusion of molten material along rift margins. Created by Prime Meridian Resources.	13
9. Geological map of Presque Isle. From Gair and Thaden (1968).	17
10. Geological map of the Deer Lake area. From Clark, Cannon, and Klassner (1975).	19

List of Figures-continued

11. Geological map of Black Rock Point showing sample locations from May2014 and May 2015.....	20
12. Map showing locations of the Yellowdog Peridotite and its surrounding rock units. Adapted form (Dunlop, 2013) by Bob Mahin of Lundin Mining.....	23
13. Photo of sample MQT-15-002.....	33
14. Field photo from eastern side of Presque Isle, showing Presque Isle Peridotite as it appears in outcrop.....	33
15. Photomicrograph of MQT-14-003. Olivine chadacrysts surrounded by pyroxene oikocrysts.....	35
16. Photomicrograph of MQT-14-001. Serpentine after olivine pseudomorphs.....	35
17. Reflected light photomicrograph of MQT-14-011.Sulfide inclusions in olivine indicated by red arrows.....	35
18. Reflected light photomicrograph of MQT-15-002. Pyrrhotite (grey), chalcopyrite (dark yellow), pentlandite (bright yellow).....	36
19. Photo of sample DLP-15-006.Hand Sample of low alteration Deer Lake Peridotite.....	37
20. Deer Lake Peridotite outcrop, Verde Antique Quarry. Highly altered region of Deer Lake Peridotite Andrew Sasso (6') for scale.....	37

List of Figures-continued

21. Photomicrograph of DLP-15-006. Bastite oikocrysts (PX) surround serpentine after olivine chadacrysts.	39
22. Photomicrograph of DLP-15-006. Bastite oikocrysts (PX) surround serpentine after olivine chadacrysts (OL).	40
23. Black Rock Point Gabbro. Photo of hand sample BRP-14-005.	41
24. Black Rock Point Gabbro outcrop.	42
25. Photomicrograph from BRP-14-005 showing plagioclase and clinopyroxene crystals. Plagioclase lath indicated by red arrow is partially enclosed within clinopyroxene.	43
26. Photomicrograph form BRP-14-005. Spene is visible at the center of the image.	43
27. Photo of sample EA-15-002. Yellowdog Peridotite hand sample.	44
28. Outcrop of Yellowdog Peridotite at “Eagle Rock” (Eastern intrusion at the Eagle Mine Site).	45
29. Photomicrograph of EA-15-001 Showing olivine, and pyroxene with interstitial plagioclase.	46
30. Photomicrograph from EA-15-001. Poikilitic texture of pyroxene oikocrysts surrounding olivine chadacrysts.	47

List of Figures-continued

31. Pyroxene quadrilateral showing pyroxene compositions for all samples analyzed via electron microprobe.	71
32. Plot of olivine compositions for East Eagle, Eagle, and Presque Isle.	72
33. Comparison of sulfides from Presque Isle Peridotite (A) and Yellowdog Peridotite (B).....	74
34. IUGS classification scheme for gabbro. (Woolley, 1996).....	75
35. Geological map-Presque Isle. Adapted from Gair and Thaden (1968).	76
36. Geological map-Deer Lake area. Adapted from Clark, Cannon, and Klassner (1975).....	77
37. Geological map-Black Rock Point showing sample locations from May 2014 and 2015.	78
38. Ni-content vs. Fo m% plot. After, Ding et al. (2010).Blue curve: Model of equilibrium crystallization. Green curve: Model of fractional crystallization.....	80
39. Minor trace element spider plot normalized to primitive mantle. After McDonough and sun (1995).	82
40. Immobile element spider plot. Normalized to NMORB. After Sun & McDonough 1989 in Pearce (2014).....	83

List of Figures-continued

41. Rare earth element spider plot. After McDonough and Sun (1995).	84
42. Visual explanation of Th-Nb, Nb-Yi, and Ti-Yb proxy indicators. From Pearce (2008).....	85
43. Nb/Yb-Th/Yb plot. Ratio plot highlighting Th-Nb Proxy.	87
44. TiO ₂ /Yb-Nb/Yb plot. One sample from each site is represented. Ratio plot highlighting Ti-Yb proxy.	88

LIST OF ABBREVIATIONS

µm	Micrometer
BRP	Black Rock Point Area
DLP	Deer Lake Area
EA	Eagle East Intrusion
E-MORB	Enriched Mid-Ocean Ridge Basalt
EPMA	Electron Probe Micro-Analysis
EUG	Eagle Intrusion
ft	Feet
Ga	Giga annum (Billion years)
GLTZ	Great Lakes Tectonic Zone
GPS	Global Positioning System
ICP-MS	Inductively Coupled Plasma Mass Spectrometry
IUGS	International Union of Geological Sciences
km	Kilometer
LOI	Loss on Ignition
LREE	Light Rare Earth Element
m	Meter
Ma	Mega annum (Million years)
Meso-Prot.	Mesoproterozoic
Mg#	Magnesium Number
mi	Mile
MORB	Mid-Ocean Ridge Basalt
MQT	Presque Isle Area
N-MORB	Normal Mid-Ocean Ridge Basalt
OIB	Ocean Island Basalt
ppm	parts-per million
REE	Rare Earth Element
SEM	Scanning Electron Microscope
Spn	Sphene
USGS	United States Geological Survey
wt. %	Weight percent
XRF	X-ray Fluorescence Spectrometry

LIST OF MINERAL ABBREVIATIONS

Ab	albite ($\text{NaAlSi}_3\text{O}_8$)
Ac	acmite or aegirine ($\text{NaFeSi}_2\text{O}_6$)
An	anorthite ($\text{CaAl}_2\text{Si}_2\text{O}_8$)
Ccp	chalcopyrite
Cpx	clinopyroxene
Fa	fayalite (Fe_2SiO_4)
Fo	forsterite (Mg_2SiO_4)
Fs	ferrosilite (MgSiO_3)
En	enstatite (MgSiO_3)
Hbl	hornblende ($\text{Ca}_2(\text{Mg, Fe, Al})_5(\text{Al, Si})_8\text{O}_{22}(\text{OH})_2$)
Mag	magnetite
Ol	olivine ($(\text{Mg, Fe})_2\text{SiO}_4$)
Opx	orthopyroxene
Or	orthoclase feldspar (KAlSi_3O_8)
Pn	pentlandite
Pl	plagioclase feldspar ($\text{NaAlSi}_3\text{O}_8$ to $\text{CaAl}_2\text{Si}_2\text{O}_8$)
Px	pyroxene
Po	pyrrhotite
Wo	wollastonite (CaSiO_3)

CHAPTER I

INTRODUCTION

Research Areas

Marquette County is located in the north central portion of Michigan's Upper Peninsula (Figure 1). With an area of 1,821.5 square miles, Marquette is the largest county in the state of Michigan. This study focuses on four locations, and more specifically, four separate lithological units within this county. These four rock units have been mapped as peridotite by past researchers. They are located at: (1) Presque Isle, (2) Deer Lake, (3) Black Rock Point, and (4) the Eagle Mine site, on the Yellowdog Plains. These locations are shown in Figure 2.

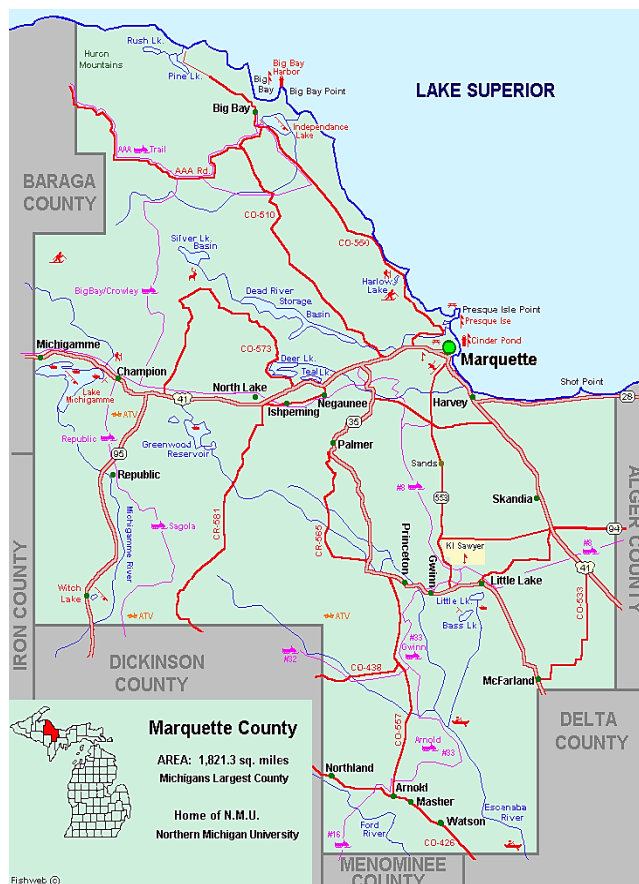
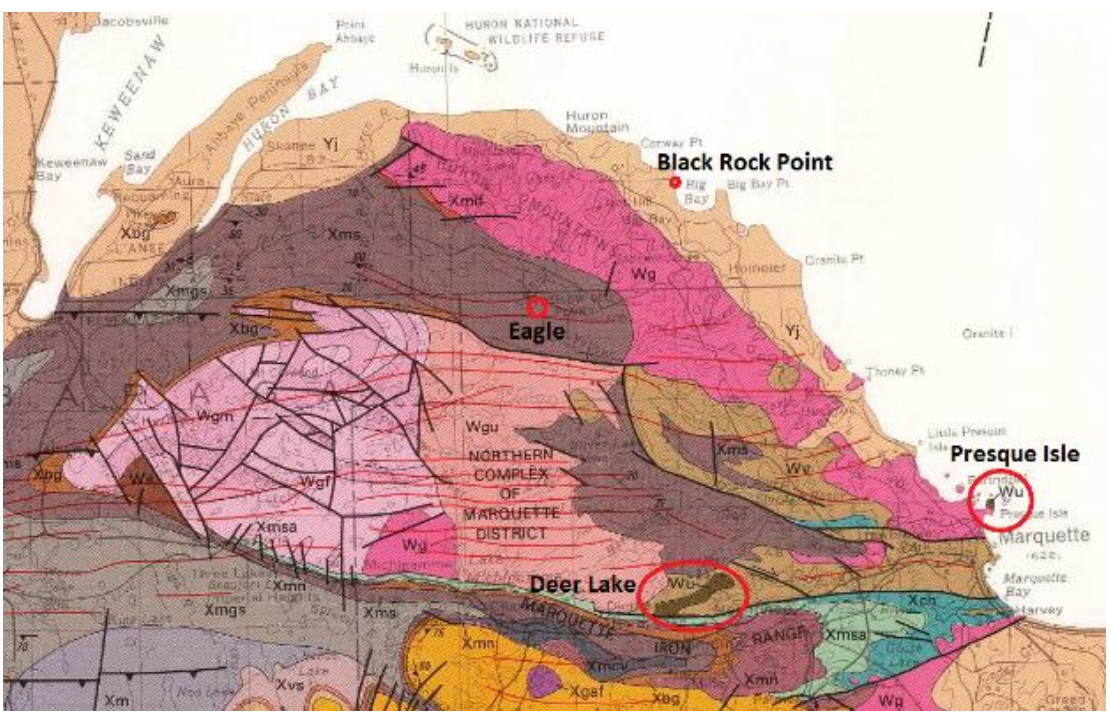


Figure 1
Geographic map of Marquette County and its location in the state of Michigan.

Presque Isle

Presque Isle is a “tied” island in Lake Superior, connected to the mainland by a tombolo composed of lacustrine sediments. Located just north and east of the city of Marquette, Presque Isle has an exposed surface area of 323 acres and a maximum elevation of 724 ft near its center. Although originally designated as a government

lighthouse reservation, Presque Isle has been designated as a park since being deeded to the city of Marquette in July of 1886. Today, Presque Isle is ringed by a paved road. It is Marquette County’s most popular destination for outdoor recreation and sightseeing.



Scale

1:500,000

- Wv** **Metabasalt (Late Archean)**—Derived from mafic to intermediate pyroclastic rocks and massive to pillowed lava flows. Unit mapped as Ramsay Formation by Prinz (1981) south of Gogebic Range; mapped as Mona Schist and Kitchi Schist in northern complex of Marquette district
 - Wu** **Ultramafic rocks (Late Archean)**—Includes serpentine bodies at Deer Lake and Presque Isle, northern complex of Marquette district
 - Xms** **Gray to black slate**—Strongly cleaved. Represents lower stratigraphic part of formation
 - Wg** **Granitic rocks (Late Archean)**—Massive to weakly foliated, medium- to coarse-grained tonalite and granodiorite in northern complex of Marquette district
- Fault intruded by narrow dike

Figure 2
Modified map of the four research areas and their surrounding geology. Adapted from Simms (1992).

Deer Lake

Deer Lake is a dammed lake located approximately 2 miles north of Ishpeming Michigan, and 12 miles west of downtown Marquette. The lake has a surface area of 950 acres, a surface elevation of 1,389ft, and a maximum depth of 35ft. There are a number of small islands scattered throughout the basin. Both low-lying, wetland areas and rugged, hilly terrain (dotted with outcrops) can be found in the lake's immediate surroundings. Deer Lake is another of Marquette County's more popular locations for outdoor recreational activities such as fishing, canoeing, and hiking.

Black Rock Point

Black rock point, also known as Black Rock Cape, is a small rocky point which juts due east into Big Bay (Lake Superior) off Salmon Trout Point. This point is located approximately 2.5 miles north of the unincorporated community of Big Bay, and approximately 26.5 miles north of Marquette. The point can be reached by traveling north from Marquette on county road 550 for 28 miles, then following county road Kf north for approximately 3 miles, followed by a hike of approximately 1 mile to the northeast. Due to its remote location and inaccessibility, the point is visited infrequently, and has never before been the subject of any geologic study.

Yellowdog Peridotite-Eagle Mine

The last location to be addressed by the project is the Yellowdog Peridotite located at the Eagle Mine site near the center of the Yellowdog Plains. This area is located approximately 9 miles southwest of Big Bay, and approximately 27 miles

northwest of Marquette. It consists of a solitary outcrop, known as Eagle Rock, which is now surrounded by the surface infrastructure of the Eagle Mine operation.

Peridotite

Peridotite is a plutonic, ultramafic rock type characterized by a mineralogical composition dominated by 40-100 vol% Olivine (Woolley, 1996). Other mafic minerals such as pyroxenes and amphiboles account for most of the rock's remaining volume. Additionally, minerals such as plagioclase, garnet, chromite, and spinel often comprise a minor fraction of the rock volume. These rocks are typically coarse grained and dark colored. Peridotites are believed to be the dominant rock type found in Earth's upper mantle; however, they are relatively rare at the surface. The extrusive equivalent of peridotite is komatiite.

Peridotite is classified based on its mineralogical composition, and constitutes all rocks composed

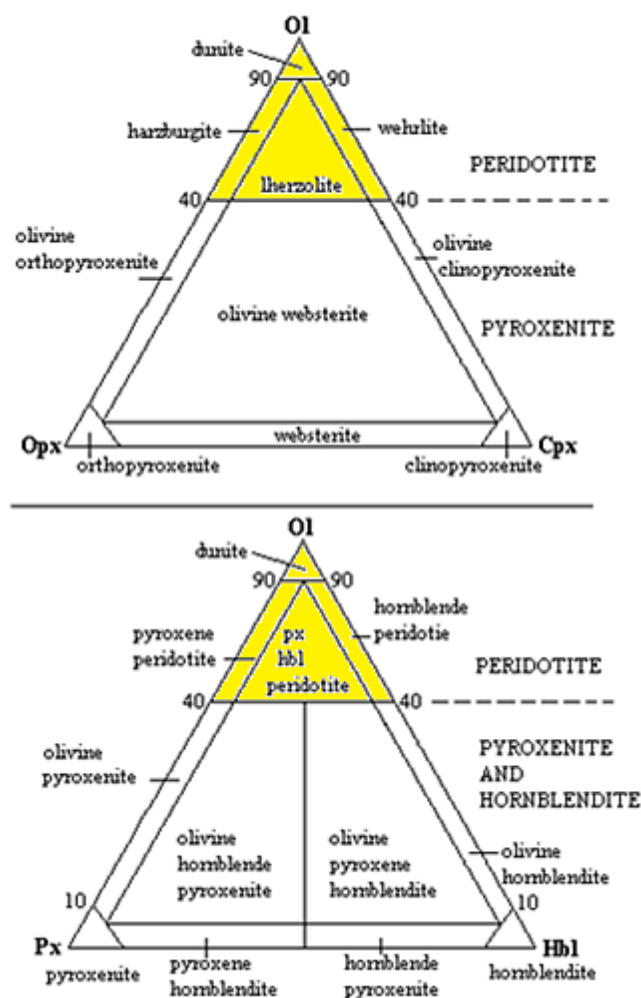


Figure 3
IUGS classification tables for ultramafic rocks. Peridotite shown in yellow. (Woolley, 1996)

of a minimum of 40 vol% olivine. Dunite is a peridotite composed of a minimum of 90% olivine, with minerals such as pyroxene, chromite and spinel constituting its remaining bulk. Harzburgite is a peridotite composed of 40-90 vol% olivine, whose pyroxene fraction is at least 95 vol% orthopyroxene minerals. Similarly, wehrlite is composed of 40-90 vol% olivine, with a pyroxene fraction represented by no less than 95 vol% clinopyroxene minerals. Lherzolite is the most common variety of peridotite, it is composed of 40-90 vol% olivine, and a pyroxene fraction ranging between 95 vol% clinopyroxene, and 95 vol% orthopyroxene. Ultramafic rocks composed of less than 40 vol% olivine include pyroxenite and hornblendite. These ultramafic classes have compositions dominated by pyroxene and amphibole. Pyroxenite and hornblendite are subdivided, in the same fashion as peridotites, based on the chemistry and abundance of their dominant mafic minerals. Figure 3 is the standard classification table for ultramafic rocks developed by the International Union of Geological Sciences, it provides a visual description of the ultramafic classification scheme.

All peridotites found at or near The Earth's surface originate from one of two sources: (1) Ophiolites or (2) Cumulates.

Ophiolites

Peridotites may have formed within The Earth's upper mantle and subsequently been emplaced within the upper crust by tectonic processes (such as accretion during subduction). Such sequences are termed ophiolites. Ophiolites are defined as thrust sheets of ancient oceanic crust and upper mantle rock which has been abducted over, and accreted onto the edge of the continental crust during the course of orogeny (Dalik et al., 2003). Ophiolites are easily identified by their standard lithological sequence, known as a

Typical Ophiolite Suite. This sequence, from the top down is: (1) Deep sea sediments, (2) pillow basalt, (3) sheeted dike complex, (4) isotropic gabbro, (5) layered gabbro, (6) Mantle peridotite (Coleman, 1977).

One example of this sequence is shown in Figure 4.

Peridotites found in ophiolites formed as part of the upper mantle but have since been tectonically emplaced within the upper crust. Typical peridotite of this type can be found at Bay of Islands, Newfoundland (Figure 4) and at the Semail Ophiolite, Oman.

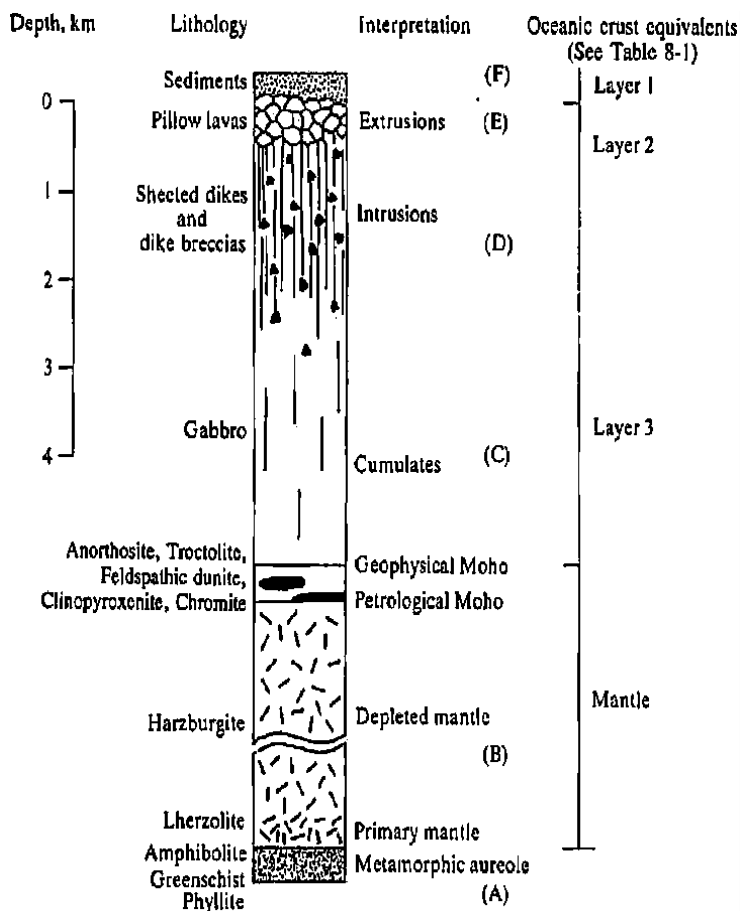


Figure 4

Diagram of the Bay of Islands Ophiolite, Newfoundland.

From Coleman (1977).

Cumulates

Peridotites may also be formed as cumulates. Cumulates are the result of differential crystallization and subsequent accumulation of olivine and pyroxene from a mafic or ultramafic melt which formed deep within The Earth and has intruded the crust.. The deep origin of such a mafic melt generally results from convective melting due to a mantle plume (Wagner et al., 1960). When these magmas intrude into the crust, pressure

and temperature decrease, and this causes crystallization to begin. High temperature minerals such as olivine and pyroxene will be the first to crystallize. They will settle due to their high density and accumulate at the base of the magma chamber. The exact temperature at which crystallization occurs depends on the pressure, and the FeO/MgO ratio of the parent melt. Continued accumulation of mainly mafic minerals will result in the formation of a substantial ultramafic pluton. Remaining parent melt, having been depleted of mafic material, will eventually cool and crystallize, resulting in a zone of the same pluton less mafic than its associated cumulate. Figure 5 depicts this process.

Typical peridotites of this type can be found in the Bushveld Igneous Complex, South Africa and the Bovine Igneous Complex, Baraga County, Michigan.

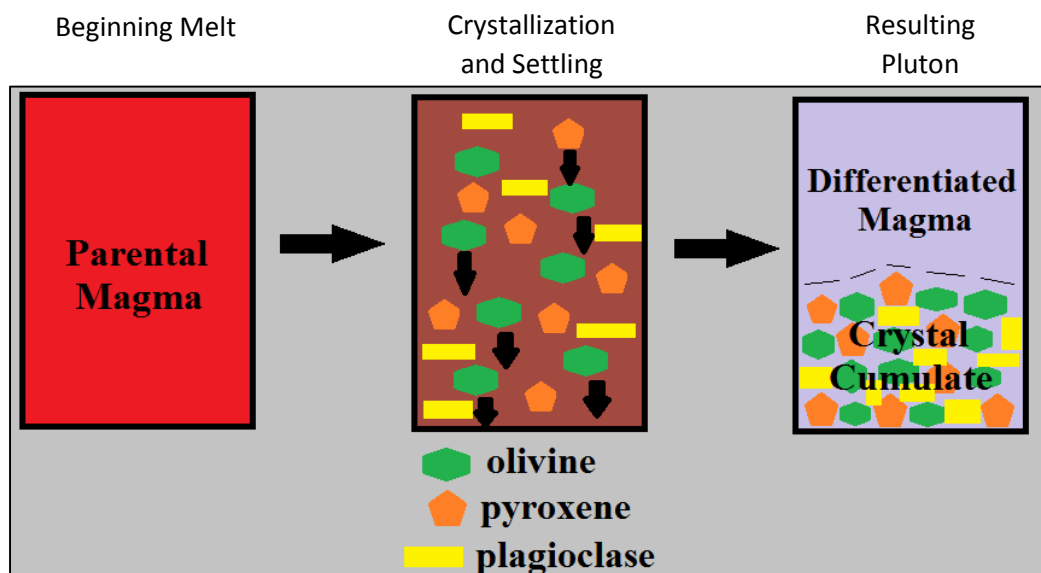


Figure 5
Graphical representation of cumulate rock formation.

Olivine and pyroxene, as discussed above, are the chief mineral components of peridotite and crystallize under conditions of high temperature and pressure. Once

emplaced within the crust (even more so when exposed at the surface) these high pressure minerals quickly become unstable. Interaction with hydrothermal fluids near the surface leads to hydration of these primary ferromagnesian minerals. This process results in their alteration to secondary serpentine group minerals which are stable at, and near, atmospheric temperature and pressure. This low temperature alteration process (0-500°C), is known as serpentinization. Other common alteration minerals include brucite, chlorite talc, magnesite and calcite (Evans, 1977).

Magmatic Sulfide Deposits

Magmatic sulfide deposits can be defined as “substantial” concentrations of sulfide minerals in ultramafic or mafic rocks, which have been derived from immiscible sulfide liquids (Foose et al, 1986). These deposits are important sources of copper, nickel and platinum group elements. They are mined worldwide.

Magmatic sulfide deposits can be divided into two basic categories: (1) Those rich in sulfide containing high concentrations of nickel and copper, and (2) those relatively sulfide poor, but containing high concentrations of platinum group elements (Naldrett, 1999). The Eagle Ni-Cu-PGE deposit, located in Marquette County, is of the former variety. This will be the focus of this study.

Formation of economic magmatic sulfide deposits is dependent upon three key factors (Naldrett, 1999):

(1) The host magma must become saturated in sulfide, allowing for the segregation of an immiscible sulfide liquid. Because the segregation of a sulfide liquid and its subsequent

basal accumulation is not normally observed during the cooling and crystallization of mafic magmas, sulfide saturation of the parent melt must be required for such an occurrence. Mafic magmas are generally not sulfide saturated when they form in the upper mantle, or begin crustal intrusion; therefore, a significant source of sulfur must be encountered, and allowed to contaminate such a melt, for sulfide saturation to be reached.

(2) Sulfides must be allowed to react with a volume of magma sufficient for the concentration of chalcophile elements such as Fe, Ni, Cu, and platinum group elements, to an economic level. Economic magmatic sulfide deposits will only form when the parent melt is of sufficient volume and has a metal-rich chemistry. The parent melt must also continue interaction with the immiscible sulfide liquid even after segregation in order for the sulfide liquid to attain economic levels of chalcophile element enrichment. Ultramafic melts, which contain the highest fraction of metallic chalcophile elements, and lowest silica concentration, best meet these conditions, and are therefore the ideal parent magma for magmatic sulfide genesis. Mafic melts are likewise considered excellent hosts for magmatic sulfide formation. This explains why magmatic sulfide deposits are invariably found in association with ultramafic, and mafic rock units

(3) Once formed, crystalline sulfides must become concentrated in significant abundance, in order to constitute an ore body.

Schulz et al. (2010), states that magmatic sulfide deposits are generally related to a range of olivine-bearing, mantle-derived magmas, which may result in a variety of lithologies. Parental magmas of magmatic sulfide hosts, are typically under saturated in sulfur and relatively enriched in Cu, Ni, and PGEs. These parent melts are also enriched in other strongly incompatible elements such as K, P, Ba, Sr, Pb, Th, Nb, and light REEs.

Marquette County: Geologic Background

Great Lakes Tectonic Zone

The Great Lakes Tectonic Zone (GLTZ) is a 1,400 km long crustal boundary which extends from present-day South Dakota, eastward to the vicinity of Sudbury Ontario. It passes directly through Marquette County, Michigan, where it is well exposed. The GLTZ separates the “Northern Complex” greenstone, granite terrain of the southern Superior Craton, to the north side, from “Southern Complex” gneiss terrain to the south. It is interpreted as a Late-Archean continent-continent collision zone formed during the Kenoran Orogeny (2.7-2.5 Ga). The Minnesota River Valley terrane, during this time, collided with, and overrode, the Superior Craton. This resulted in the formation of the GLTZ, and also produced widespread deformation and metamorphism in the vicinity of the boundary. The initial formation of the GLTZ was followed by a period of extension (2.4-2.1 Ga). Following this series of events, a second major episode of compression occurred during the Penokean Orogeny (1.85-1.83 Ga), which occurred to the southwest of the main event. Even today, minor activity is infrequently observed along the GLTZ. Documented earthquakes have occurred as recently as 1975. The GLTZ in Marquette County, appears as a 2 km wide zone of northwest-striking, metamorphic rock, separating the distinctly different lithologies of the northern and southern complexes (Sims, 1991). Figure 6 shows a simplified map of the GLTZ as it extends through Minnesota, Wisconsin, and western Upper Michigan (including Marquette County).

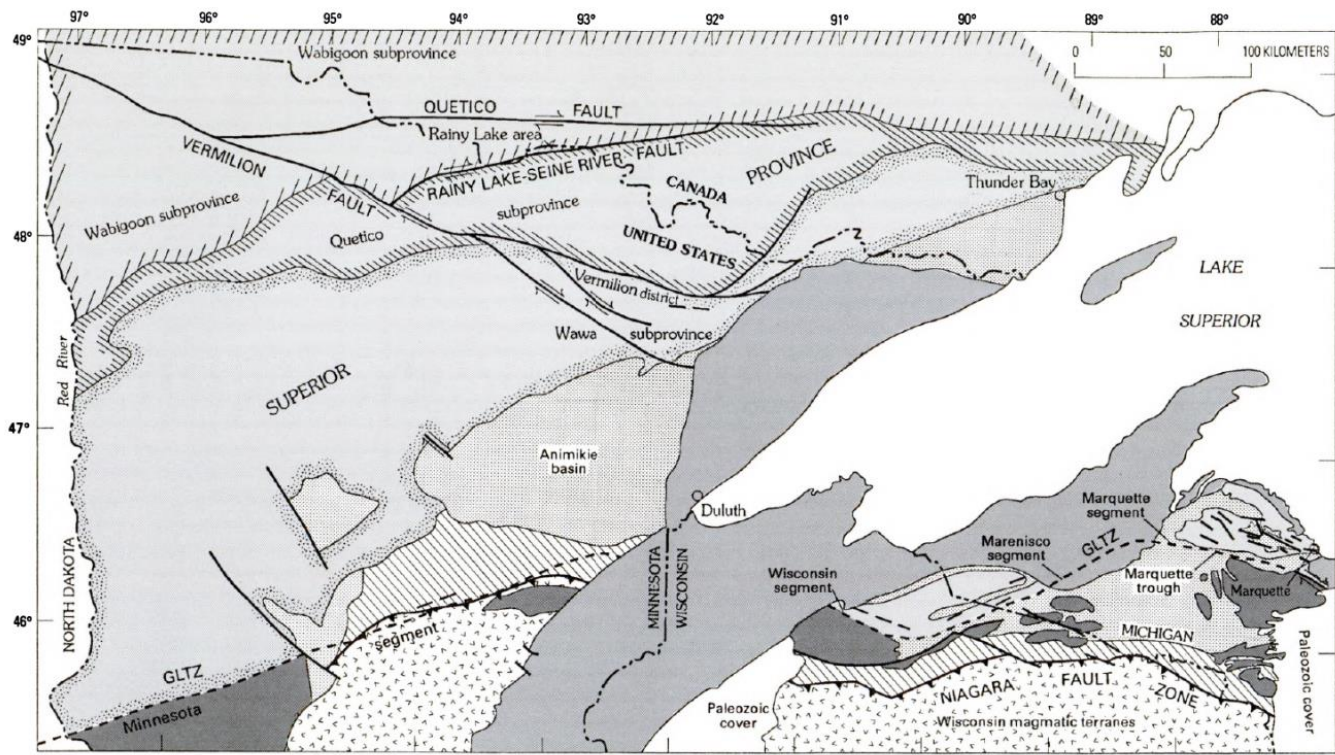
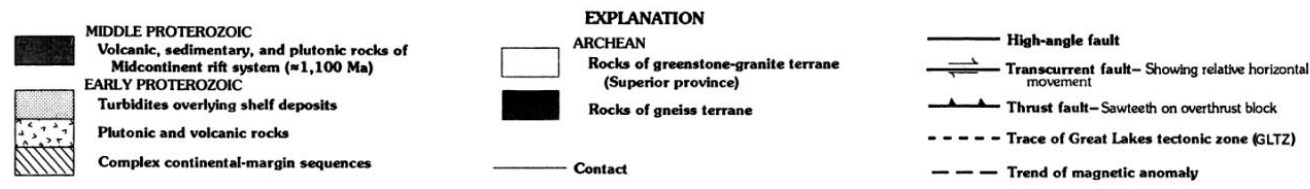


Figure 6
Simplified map of Great Lakes Tectonic Zone.
From Sims et al. (1993).



The Midcontinent Rift

The Midcontinent rift is a failed continental rift system which formed 1.1 billion years ago during the Mesoproterozoic. It is conventionally thought that formation of the rift was caused by a mantle plume. Creating a triple junction with its nexus at Lake Superior (Stein et al., 2014). Only two arms of the rift

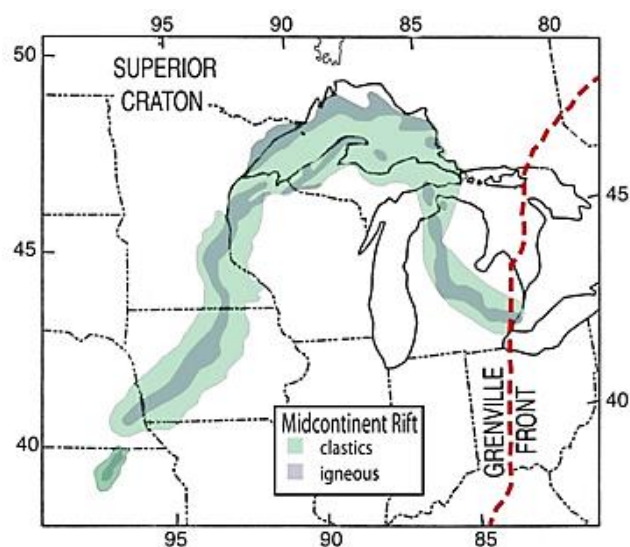


Figure 7
Simplified diagram of Midcontinent Rift.
From Stein et al. (2014).

are well developed. One arm extends southwest from Lake Superior, and can be followed to its point of termination in present-day Kansas. The second arm extends southeast where it is covered by sediments of the Michigan Basin. The poorly developed third arm extends northward where igneous materials associated with its formation can be observed in the vicinity of Lake Nipigon in present-day Ontario, Canada. Although the cause of the rift's failure is not known, compression to the southeast due to the Grenville Orogeny is one possible explanation (Schmus, 1985). Figure 7 shows a generalized diagram of the rift system.

Rocks in the Lake Superior region associated with the rift comprise a series of plutonic, volcanic, and clastic sedimentary units dating from 1.0 Ga to 1.2 Ga. These are collectively referred to as the "Keweenaw Supergroup". The primary feature in Marquette county associated with the rift is a massive swarm of mafic dikes which trend east-west, parallel to the rift axis. These features formed by intrusion of molten material

into the crust along the margins of the rift. Figure 8 shows a generalized interpretation of the relationship of these features to the rift system.

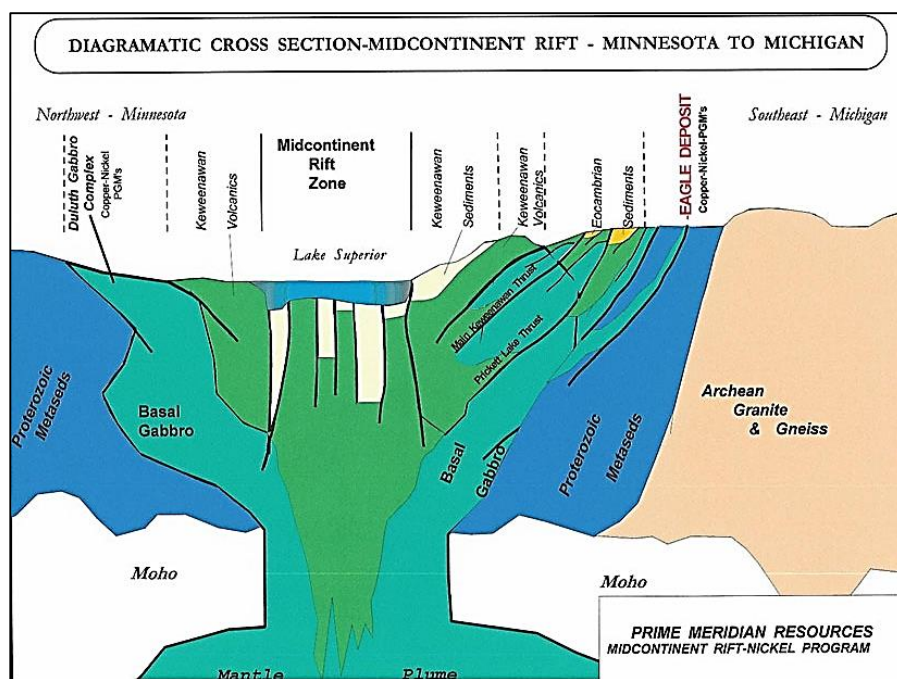


Figure 8

Cross section of Midcontinent Rift showing intrusion of molten material along rift margins.

Purpose

Previous researchers have mapped peridotite rock units at four locations across Marquette County, Michigan. These units are found at: (1) Presque Isle, (2) Deer Lake, (3) Eagle Mine, and (4) Black Rock point. The locations of these sites are shown in Figure 2.

Exploration by Kennecott in 2005 discovered a world class magmatic sulfide deposit hosted within the Yellowdog Peridotite. This discovery has since been developed into the current Eagle Mine site. Discovery of a magmatic sulfide deposit in association with one of the Marquette County peridotite units has raised two significant questions.

Could an as yet undiscovered magmatic sulfide deposit, similar to that found in association with the Yellowdog Peridotite, exist in association with any other Marquette County peridotite unit? Secondly, can a petrological or geochemical relationship be established between any of Marquette County's peridotite units?

Both the Yellowdog Peridotite and associated magmatic sulfide deposit have been studied extensively since the 2005 discovery. Radiometric dating of the peridotite returned an age of 1107.2 ± 5.7 Ma (Ding et al., 2010). These results imply that the peridotite, along with its associated magmatic sulfide deposit, formed during the midcontinent rift event.

Although a number of previous studies have been conducted out at both the Deer Lake, and the Presque Isle peridotite units, no radiometric dates have been obtained for either unit. Previous researchers have collected and analyzed an abundance of petrological and geochemical data for all but the Black Rock Point unit. Despite this effort, no formal petrological or geochemical comparisons have been established to correlate the units.

These two questions (above) are significant, not only due to their economic implications, but also due to advancing the collective understanding of geologic history in Marquette County. It has been the goal of this study to answer these questions through the characterization, and subsequent comparison, of Marquette County's peridotite units in terms of both petrology and geochemistry. A digital geologic map of each peridotite has also been created. This was done to fully visualize the scope and surrounding geology of each peridotite unit.

Previous Work

Marquette County is perhaps best known for the Marquette Iron range. Since its discovery in 1844, by William A. Burt, the range has been continuously mined. Due to the presence, and the substantial value of this large iron range, the area has been the focus of extensive mineral exploration during the past 170 years. This exploration has led to the discovery of numerous economic minerals and native element deposits. More than 380 mines and prospects have been established in Marquette County.

The most recent mine established in Marquette County is the Eagle Mine, located on the Yellowdog Plains. This mine is owned and operated by Lundin Mining Corporation. The mine's primary target resources are nickel and copper in the form of magmatic sulfides. Lundin also expects to recover minor quantities of platinum, palladium, and cobalt. The primary ore deposit is estimated to be approximately 4.1 million metric tons. It is hosted by the Yellowdog Peridotite, an ultramafic intrusion dating to 1.1Ga, the time of the Midcontinent Rift event. Ore being extracted at the mine has been found to contain 3.6 wt. % nickel, and 2.9 wt. % copper. Nearly 8 billion U.S. dollars' worth of ore is expected to be extracted during the project's projected 8 year mining life (Owen & Meyer, 2014). The Eagle mine began production on September 23, 2014. Eagle's discovery and development has set a precedent for economic mineral deposits associated with peridotite intrusions in Marquette County.

Klanser et al. (1979), characterized this rock unit, prior to the discovery of economic ore deposit associated with the Yellowdog Peridotite. Since then, numerous other papers and technical reports have been published regarding the geology of the area,

primarily by Kennecott Exploration, Rio-Tinto, Lundin Mining Corporation, and the consulting firm Wardell-Armstrong.

Previous geologic research has also taken place at both the Presque Isle and Deer Lake sites. The earliest identification of peridotite at Deer Lake was made by Van Heise in 1895. Rossell et al. (1983) also conducted a detailed study of the Deer Lake Peridotite which was first to identify two petrologically distinct rock types within the unit.

Presque Isle has been the subject of numerous theses and research projects since the late 19th century. The earliest attempt to characterize Presque Isle's geology was made by Wadsworth (1884). Wadsworth's work formed the foundation for all subsequent work on the island's geology. There is a section on the Presque Isle Peridotite that appears in the 1895 paper "Preliminary Report on the Marquette Iron-Bearing District of Michigan" by Van Heise. The most recent detailed report on Presque Isle's geology was written by Lewan et al. (1972). A less detailed follow up to Lewan's work was conducted by Rick Lantz (1982).

No previous research has been conducted in the vicinity of Black Rock Point, and very little mention has been made of the site in any previous publications or unpublished works. The point was mapped as serpentinitized peridotite by Case and Gair, 1985; however Black Rock Point is never specifically mentioned in the report. During mapping for this study, it was quickly discovered that no peridotite actually exists at Black Rock Point. The area is actually composed of two main rock types separated by diabase dikes of Keweenaw age. The southernmost and most prominent of the major types, is a large mafic body of gabbro. The other main rock type present is a felsic, heavily veined gneiss.

CHAPTER II GEOLOGICAL SETTING

Presque Isle Peridotite

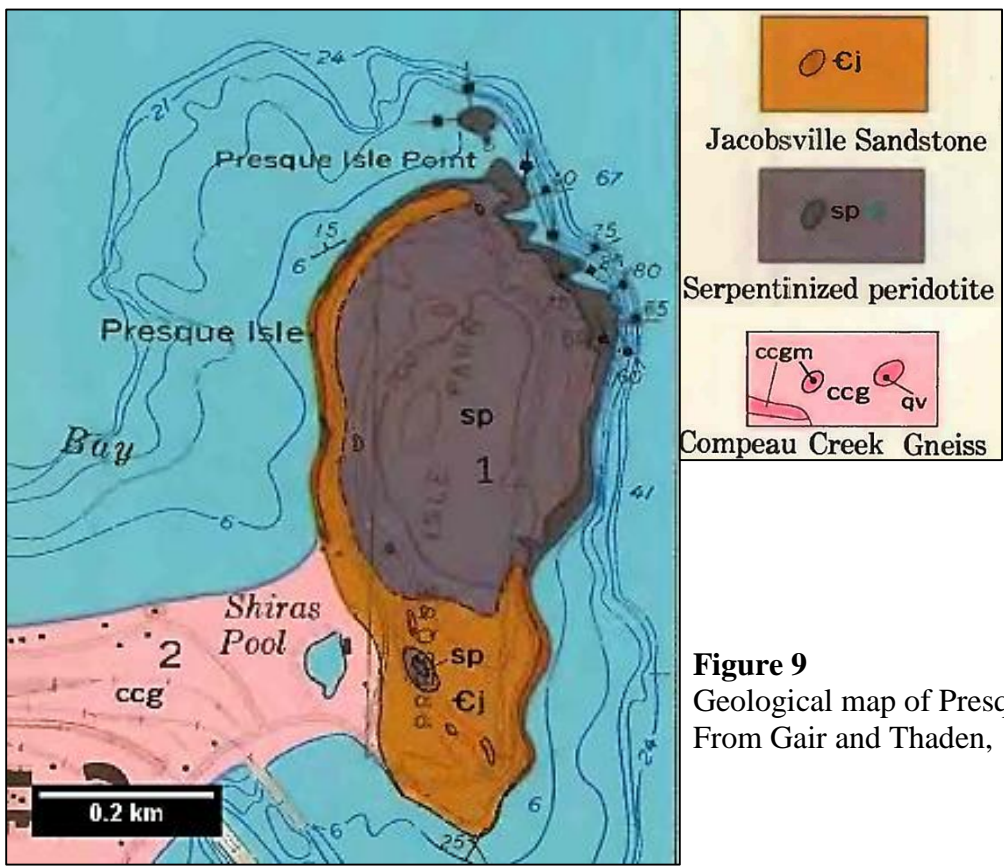


Figure 9
Geological map of Presque Isle
From Gair and Thaden, 1968.

Serpentinized peridotite at Presque Isle, makes up approximately two thirds of the island's 323 acre area. This peridotite shows varying degrees of alteration, but appears to be moderately to heavily serpentinized at most locations. It is likely that this peridotite unit dates to the late Archean or early Proterozoic; however, its composition and variable alteration makes determination of its exact age challenging. Gair and Thaden (1968) have hypothesized that the peridotite could have formed as late as 1.1 Ga in the early stages of the Midcontinent Rift event.

Jacobsville Sandstone unconformably overlies the peridotite and constitutes the remaining third of Presque Isle. The Jacobsville Sandstone is notable being the youngest unit in the Keweenawan series.

Lewan et al. (1972), noted the peridotites at this site form a tear drop shaped mass approximately 1500 meters long and 700 meters wide. Peridotite forms the major basement rock at this site. It is heavily fractured and often cut by veins of serpentine, or carbonate minerals emplaced by hydrothermal activity. Sulfides such as chalcopyrite and galena are visible in these veins at some locations. Prominent peridotite outcrops exist along Presque Isle's northern and eastern shoreline, although the majority of the peridotite is covered by either glacial material or Jacobsville Sandstone. These outcrops, in some areas, form cliffs greater than 100 feet in height. Jacobsville Sandstone is a common unit across Marquette County's Lake Superior shoreline; however, near its contact with the peridotite at Presque Isle, the unit displays an atypical appearance. The Jacobsville Sandstone and its basal conglomerate in particular, overlie the peridotite in a nonconformity. They are heavily cut by carbonate veins similar to those found in the peridotites. The basal conglomerate consists of angular fragments of chert, cemented in a matrix of fine quartz sand. It is likely that the conglomerate is derived from the underlying alteration zone (Lewan, 1972). Locally, the sandstone is seen to contain rounded cobbles of the peridotite (Lantz, 1982).

Peridotite is not seen in contact with any major rock units other than the Jacobsville as its exposure is surrounded by Lake Superior. However it is assumed by observing the geology of the surrounding islands and mainland, that the unit is hosted by the Compeau Creek Gneiss or basement granite on the "Northern Complex".

Deer Lake Peridotite

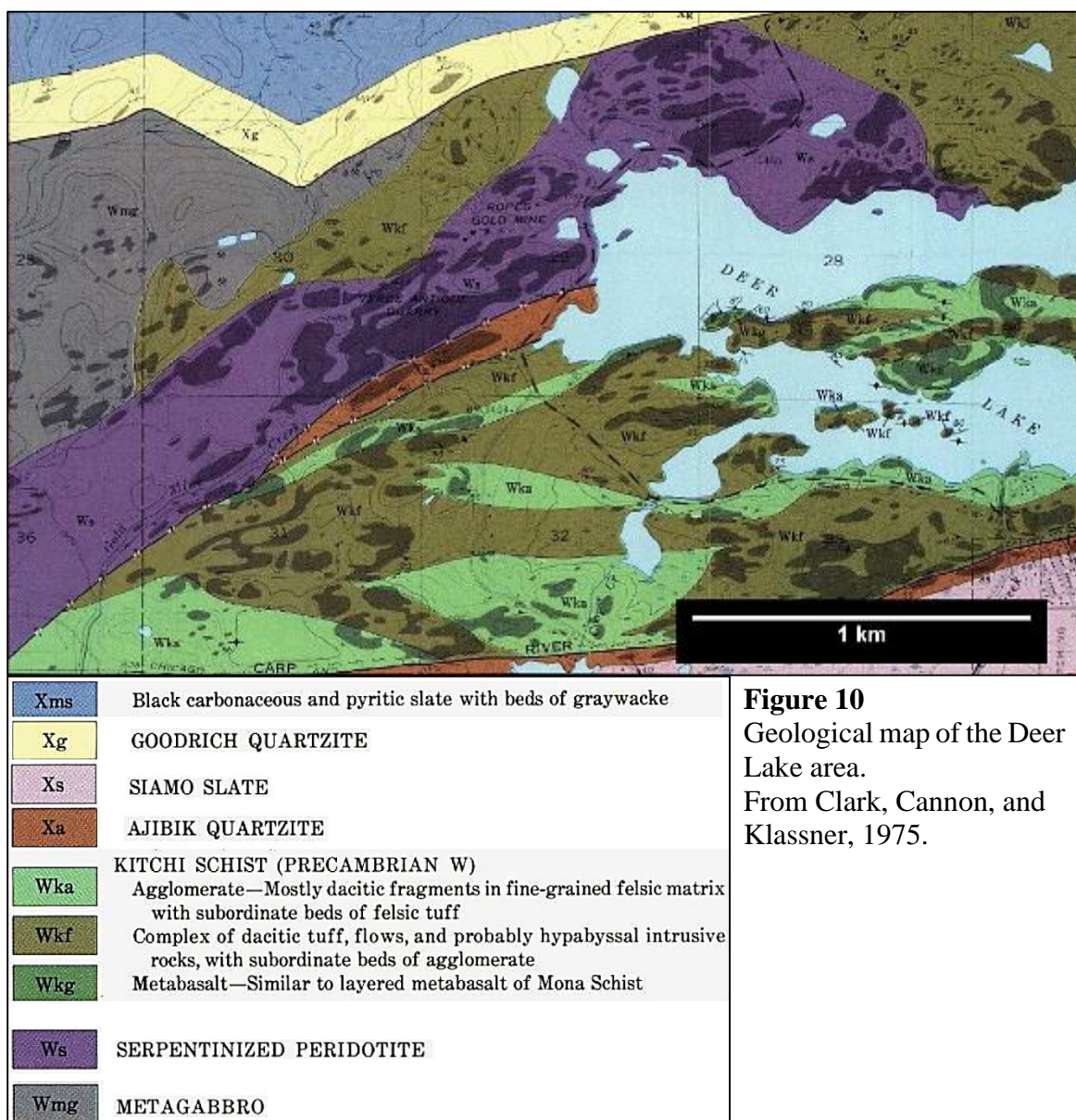


Figure 10
Geological map of the Deer Lake area.
From Clark, Cannon, and Klassner, 1975.

The Deer Lake Peridotite is located within the Ishpeming Greenstone Belt. It is bounded to the south by the east west trending Great Lakes Tectonic Zone. The unit is approximately 8km long and 1km wide. Deer Lake Peridotite displays variable degrees of alteration, but is generally heavily to entirely serpentized. It is hosted by the Kitchi Schist which consists of: (1) A lower mafic member of metamorphosed basalts, diabbases, and gabbros, and (2) upper member of andesites, coarse dacitic pyroclastics, berrecias,

and fine grained tuffs. The Kitchi Schist is overlain by the Mona Schist which has been dated to 2.7 Ga. This unit consists of pillow basalts and felsic pyroclastic rocks. There has been some debate as to whether the sequence between the Kitchi and the Mona is conformable. (Morgan and DeCristoforo, 1974 Rossell, 1983). The Deer Lake Peridotite is truncated by the Great Lakes Tectonic Zone on its south western margin. This can be observed in Figure 2. Truncation of the unit by the Carp River Falls Shear Zone, which represents the northern margin of the GLTZ in Marquette County, suggests that it must have been emplaced prior to, or during, formation of the GLTZ (2.7-1.85 Ga).

Black Rock Point Gabbro

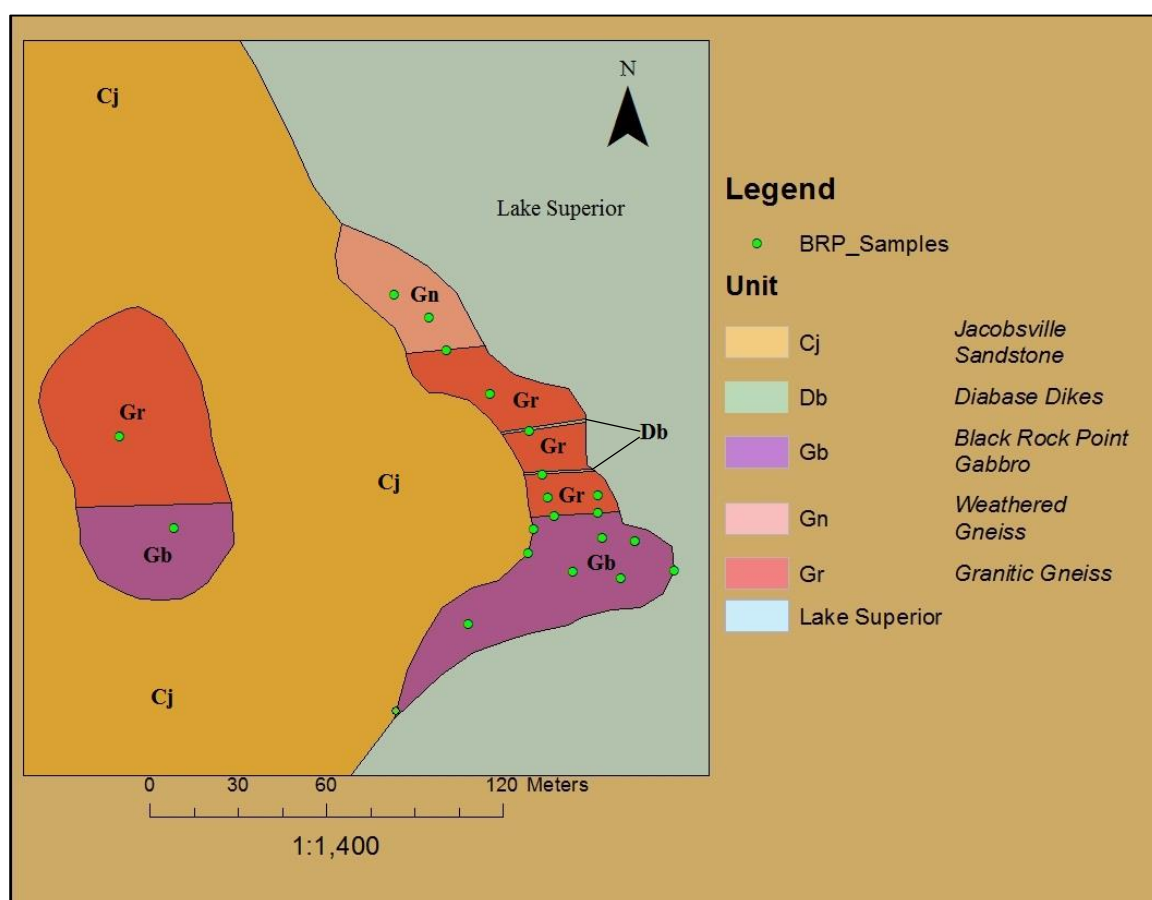


Figure 11
Geological map-Black Rock Point showing sample locations, samples collected during May 2014 and May 2015.

This small, remote point which juts into Lake Superior just north of Big Bay is composed of two main rock units, one mafic, and one felsic as described earlier. The felsic unit has been cut by two mafic dikes which are probably of Keweenawan age. Other than the relatively small exposure of Black Rock Point, the entire unit is overlain by a thick layer of Jacobsville Sandstone which forms cliffs greater than 50 ft high. Field mapping during May 2015 led to the discovery of additional outcrops of gabbro and granite located above the sandstone cliffs.

Yellowdog Peridotite

The Yellowdog Peridotite is located near the center of the Yellowdog Plains, an area of Pleistocene glacial outwash. This ultramafic intrusion is associated with the Mesoproterozoic dike swarm found trending east-to-west across Marquette County and the surrounding region. The Yellowdog Peridotite formed during the Midcontinent Rift event (1.1 Ga). This is confirmed through the use of U-Pb baddeleyite age dating (Ding et al., 2010) which determined an age of $1107.2 \text{ Ma} \pm 5.7 \text{ Ma}$. This peridotite occurs as distinct western and eastern intrusions, referred to as “Eagle” and “Eagle East”. Although the two intrusions are conventionally thought to be connected beneath the surface, exploration drilling has thus far failed to confirm this. The Eagle East intrusion rises the surrounding glacial outwash plain to form a prominent knob. Approximately 650 m to the west of this outcrop is the western or “Eagle” intrusion. This portion of the peridotite intrusion has no surficial outcrop. Both intrusions have a strike length of approximately 530 m and dip steeply to the north. These intrusions are keel shaped and range from approximately 75m wide near the surface to 5 m in width at a depth of 300 m. Both

intrusions host world class magmatic sulfide deposits rich in nickel and copper, along with notable amounts of platinum group elements (PGE). The deposit is actively mined as Lundin Mining Corporation's Eagle Mine (Owen and Meyer, 2013).

The Yellowdog Peridotite is situated at the east most end of the Baraga Basin, the northern most basin of Paleoproterozoic sediments in Michigan (Owen and Meyer, 2013). The host (basement) rock is a gneiss-greenstone complex dating to more than 2.5 Ga. It is overlain by the Marquette Range Supergroup which dates to approximately 2 Ga (Klasner et al., 1979). These rock units are shown in map form in Figure 12.

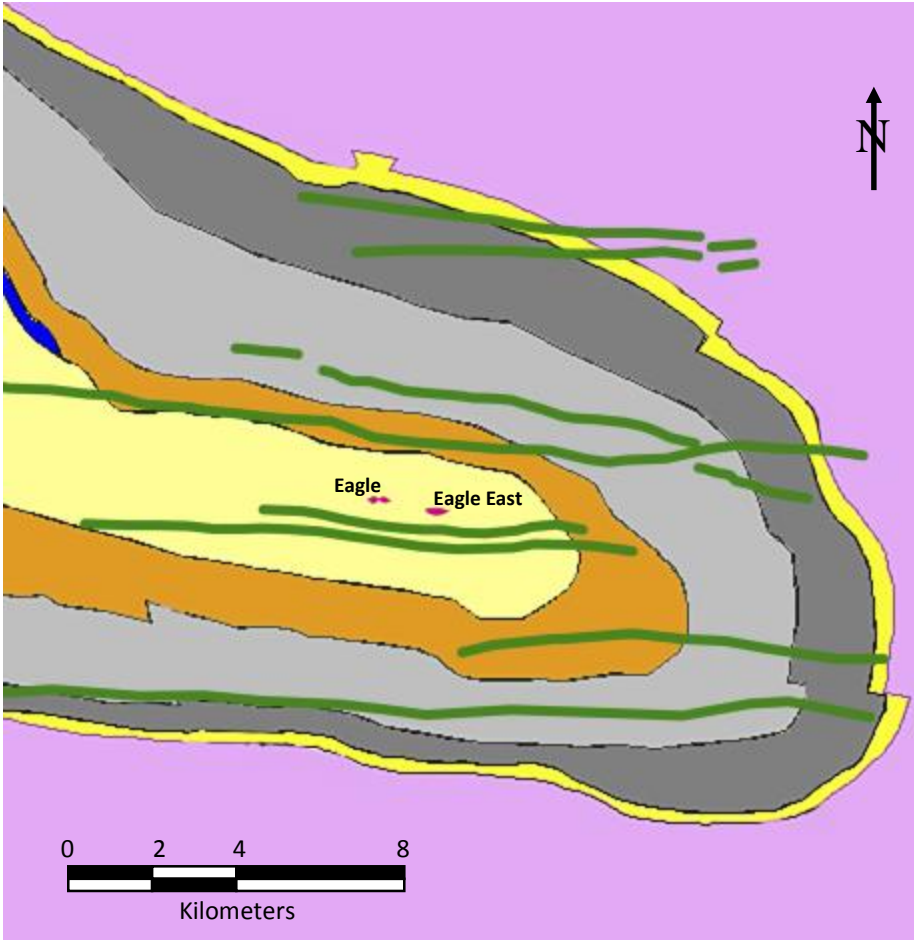


Figure 12
 Map showing locations of the Yellowdog Peridotite and its surrounding rock units. Adapted form (Dunlop, 2013) by Bob Mahin of Lundin Mining.

Meso-Proterozoic		Mafic Dike (interpreted from magnetics)	Largely gabbros and diabases
		Peridotite	Eagle and Eagle East intrusions
Proterozoic		Upper Fossum Creek	Fine grained muddy turbidites
		Deformation Zone	Graphitic phyllite and quartz-graphite schist
		Lower Fossum Creek	Pelitic slate
		Upper Graywacke	Sandy turbidites and black slates
		Lower Slate	Chert-siderite BIF and black slates
		Goodrich Quartzite	Argillite/quartzite
Archean		Granitic Gneiss	

CHAPTER III

METHODS

Field Methods

Field work was conducted during May, 2014 (with the exception of the Eagle site). Various hand samples of both the targeted rock units, and the surrounding lithologies, were collected from each area. Coordinates for each sample location were recorded using a handheld GPS device. Tables 1-4 list samples collected from each field area by sample number, rock type, and sampling location. MQT samples are from Presque Isle, DLP samples are from Deer Lake, BRP samples are from Black Rock Point, EA samples are from the Eagle East intrusion, and EUG samples are from the Eagle intrusion. Local field mapping was also conducted to better define their outcrops and delineate boundaries between major rock units. Important geologic contacts and other notable features such as veins, dikes and areas of sulfide mineral occurrence was also mapped and recorded.

Additional field work was conducted at all research areas during May, 2015. Mapping continued at the Deer Lake site to better delineate the extent of the Deer Lake Peridotite. Samples were collected from beneath the eastern intrusion of the Yellowdog Peridotite from within the Eagle Mine. Additional hand sample collection and minor map adjustments also occurred at the Presque Isle, and Black Rock Point sites.

Table 1: Yellowdog Samples

Sample Number	Rock Type	Latitude	Longitude
EA-15-001	peridotite	46° 44' 47.21"N	87° 52' 57.60"W
EA-15-002	peridotite	46° 44' 47.21"N	87° 52' 57.60"W
EUG00140 200.85m	peridotite		Core
EAUG0012-86.43m	peridotite		Core

Table 2: Presque Isle Samples

Sample Number	Rock Type	Latitude	Longitude
MQT-14-001	peridotite	46° 35' 35.52"N	87° 22' 48.53"W
MQT-14-013	conglomerate	46° 35' 35.70"N	87° 22' 54.42"W
MQT-14-019	Jacobsville Sandstone	46° 35' 13.82"N	87° 23' 9.22"W
MQT-14-017	conglomerate	46° 35' 35.70"N	87° 22' 54.42"W
MQT-14-004	peridotite	46° 35' 28.09"N	87° 22' 41.10"W
MQT-14-006	peridotite	46° 35' 34.38"N	87° 22' 49.48"W
MQT-14-022	calcite, pyrite, galena	46° 35' 32.82"N	87° 22' 48.22"W
MQT-14-022	peridotite	46° 35' 26.10"N	87° 22' 37.85"W
MQT-14-026	chert vein	46° 35' 27.24"N	87° 22' 38.16"W
MQT-14-005	peridotite	46° 35' 32.78"N	87° 22' 48.50"W
MQT-14-007	peridotite	46° 35' 34.49"N	87° 22' 49.20"W
MQT-14-018	conglomerate	46° 35' 35.70"N	87° 22' 54.42"W
MQT-14-009	peridotite	46° 35' 28.08"N	87° 22' 41.10"W
MQT-14-024	calcite, pyrite, galena	46° 35' 32.34"N	87° 22' 47.34"W
MQT-14-003	peridotite	46° 35' 23.46"N	87° 22' 37.86"W
MQT-14-021	peridotite	46° 35' 27.12"N	87° 22' 38.52"W
MQT-14-023	calcite, pyrite, galena	46° 35' 32.34"N	87° 22' 47.34"W
MQT-14-011	peridotite	46° 35' 27.36"N	87° 22' 38.76"W
MQT-14-008	peridotite	46° 35' 36.27"N	87° 22' 47.40"W
MQT-14-015	conglomerate	46° 35' 35.70"N	87° 22' 54.42"W
MQT-14-025	calcite, pyrite, galena	46° 35' 32.82"N	87° 22' 48.45"W
MQT-14-016	conglomerate	46° 35' 28.23"N	87° 23' 8.96"W
MQT-14-020	feldspathic dike	46° 35' 33.05"N	87° 23' 3.29"W
MQT-14-012	peridotite inclusion	46° 35' 35.58"N	87° 22' 56.59"W
MQT-14-010	Jacobsville Sandstone	46° 35' 21.39"N	87° 23' 8.65"W
MQT-14-014	conglomerate	46° 35' 35.70"N	87° 22' 54.42"W
MQT-15-002	peridotite	46° 35' 28.00"N	87° 22' 40.70"W
MQT-15-001	diabase?	46° 35' 34.70"N	87° 23' 00.10"W

Table 3: Deer Lake Samples

Sample Number	Rock Type	Latitude	Longitude
DLP-14-006	peridotite	46° 31' 45.00"N	87° 42' 50.09"W
DLP-14-007	Kitchi Schist	46° 31' 59.82"N	87° 40' 06.14"W
DLP-14-003	peridotite	46° 32' 03.66"N	87° 41' 36.66"W
DLP-14-005	peridotite	46° 32' 03.66"N	87° 41' 36.66"W
DLP-14-008	peridotite	46° 31' 44.42"N	87° 42' 46.48"W
DLP-14-002	peridotite	46° 32' 05.89"N	87° 41' 48.10"W
DLP-14-007	peridotite	46° 32' 03.86"N	87° 41' 48.88"W
DLP-15-001	peridotite	46° 32' 03.84"N	87° 41' 35.64"W
DLP-15-002	Kitchi Schist	46° 32' 16.60"N	87° 40' 50.30"W
DLP-15-004	Kitchi Schist	46° 31' 58.40"N	87° 40' 09.90"W
DLP-15-005	Kitchi Schist	46° 31' 53.22"N	87° 40' 54.60"W
DLP-15-006	peridotite	46° 31' 53.40"N	87° 40' 30.40"W
DLP-15-007	Kitchi Schist	46° 31' 57.30"N	87° 40' 30.10"W
DLP-15-010	peridotite	46° 31' 45.39"N	87° 42' 48.30"W
DLP-15-012	peridotite	46° 31' 38.00"N	87° 43' 16.90"W
DLP-15-013	peridotite	46° 31' 38.30"N	87° 43' 17.10"W
DLP-15-014	peridotite	46° 31' 04.09"N	87° 46' 02.90"W
DLP-15-015	gabbro	46° 31' 04.09"N	87° 46' 02.90"W
DLP-15-016	Kitchi Schist	46° 31' 06.50"N	87° 46' 07.30"W
DLP-15-017	peridotite	46° 32' 25.00"N	87° 41' 40.60"W
DLP-15-018	quartzite	46° 32' 29.50"N	87° 41' 38.80"W
DLP-15-019	Kitchi Schist	46° 32' 26.70"N	87° 41' 33.10"W
DLP-15-020	Kitchi Schist	46° 31' 42.30"N	87° 43' 15.20"W
DLP-15-021	Kitchi Schist	46° 31' 19.80"N	87° 44' 03.18"W
DLP-15-022	peridotite	46° 31' 21.20"N	87° 44' 06.58"W
DLP-15-025	Kitchi Schist	46° 31' 34.90"N	87° 45' 20.10"W
RS 1515E-2 556ft	peridotite		core
RS 1515E-2 562ft	peridotite		core
RS 1515E-2 1784ft	peridotite		core
RS 1515E-2 1298ft	peridotite		core
RS 1515E-2 2015ft	peridotite		core

Table 4: Black Rock Point Samples

Sample Number	Rock Type	Latitude	Longitude
BRP-14-006	gabbro	46° 50' 59.75"N	87° 44' 05.96"W
BRP-14-008	gabbro	46° 51' 00.05"N	87° 44' 06.44"W
BRP-14-015	Jacobsville Sandstone	46° 50' 59.94"N	87° 44' 07.14"W
BRP-14-007	gabbro	46° 51' 00.23"N	87° 44' 06.70"W
BRP-14-005	gabbro	46° 50' 59.88"N	87° 44' 06.15"W
BRP-14-013	gneiss	46° 51' 00.36"N	87° 44' 06.78"W
BRP-14-010	diabase	46° 51' 01.20"N	87° 44' 07.56"W
BRP-14-007	gabbro	46° 50' 59.44"N	87° 44' 06.43"W
BRP-14-003	gabbro	46° 50' 59.70"N	87° 44' 06.24"W
BRP-14-004	gabbro	46° 51' 00.18"N	87° 44' 06.36"W
BRP-14-002	gabbro	46° 50' 59.45"N	87° 44' 06.80"W
BRP-14-006	gabbro	46° 51' 00.12"N	87° 44' 06.51"W
BRP-14-001	gabbro	46° 51' 00.36"N	87° 44' 06.60"W
BRP-14-008	gneiss	46° 51' 02.92"N	87° 44' 08.83"W
BRP-14-012	gneiss	46° 51' 01.52"N	87° 44' 07.65"W
BRP-14-009	gabbro	46° 51' 00.32"N	87° 44' 06.73"W
BRP-14-016	diabase	46° 51' 00.72"N	87° 44' 07.20"W
BRP-15-001	gabbro	46° 51' 00.00"N	87° 44' 06.50"W
BRP-15-002	gneiss	46° 50' 59.00"N	87° 44' 09.60"W
BRP-15-003	gneiss	46° 50' 59.00"N	87° 44' 09.60"W
BRP-15-004	gneiss	46° 50' 59.00"N	87° 44' 09.60"W
BRP-15-005	gneiss	46° 50' 59.00"N	87° 44' 09.60"W
BRP-15-006	diabase	46° 51' 00.60"N	87° 44' 07.80"W
BRP-15-007	gneiss	46° 51' 00.50"N	87° 44' 07.10"W
BRP-15-008	diabase	46° 51' 01.30"N	87° 44' 07.40"W
BRP-15-009	gneiss	46° 51' 03.50"N	87° 44' 11.50"W
BRP-15-010	Jacobsville Sandstone	46° 51' 03.50"N	87° 44' 11.50"W
BRP-15-011	gneiss	46° 51' 02.72"N	87° 44' 08.98"W
BRP-15-012	gabbro	46° 51' 00.10"N	87° 44' 13.90"W
BRP-15-013	gneiss	46° 51' 01.10"N	87° 44' 14.80"W

Petrology and Petrography

After the 2014 field season, ten hand samples were selected, cut and sent to Spectrum Petrographics Inc. for thin section preparation. Samples were selected for each site to be representative of the major rock units found at those locations. Five of these

samples represented several different rock units from the various sample locations around Presque Isle, two were from distinctly different peridotite samples collected in the vicinity of Deer Lake, and three were from the Black Rock Point site (two samples were gabbro and one was a mafic dike).

This process was repeated for samples collected during the 2015 field season. Thirteen samples were selected, cut and sent to Vancouver Petrographics Ltd. for thin section preparation.

All thin sections collected from both the 2014 and 2015 seasons were analyzed in plane polarized, cross polarized, and reflected light using a Leica DM 750P petrographic microscope. This petrological analysis was conducted to create a detailed description of each unit's mineralogical and textural characteristics. A list of these sections is available in Table 5. MQT=Presque Isle, BRP=Black Rock Point, EA=Yellowdog (Eagle Mine), DLP=Deer Lake.

Table 5: List of Thin Sections

Thin Section Number	Rock Type
MQT-14-001	peridotite
MQT-14-003	peridotite
MQT-14-007	highly altered peridotite
MQT-14-011	peridotite
MQT-14-014	conglomerate
MQT-14-016	conglomerate
MQT-14-018	conglomerate
MQT-15-001	diabase?
MQT-15-002	peridotite

Table 5: Continued

Thin Section Number	Rock Type
BRP-14-005	gabbro
BRP-14-006	gabbro
BRP-14-010	diabase
BRP-15-012	gabbro
EA-15-001	peridotite
EA-15-002	peridotite
EA-15-003	peridotite
EUG0012-86.43m	peridotite
DLP-14-002	Mona Schist
DLP-14-006	Mona Schist
DLP-15-006	peridotite type1
DLP-15-015	gabbro
DLP-562ft	peridotite type2
DLP-1784ft	peridotite type2

Geochemistry

Samples from each study area were also selected to undergo geochemical analysis. Geochemical data reported in this study are the result of three separate analytical techniques employed by two separate laboratories.

Eleven Samples were sent to Geoscience Laboratories, located in Sudbury Ontario. Samples MQT-15-002, BRP-14-005, EA-15-001, and DLP-1784 were analyzed using X-Ray Fluorescence Spectrometry (XRF). These samples were first crushed and pulverized to a grain size of $<75\mu\text{m}$, before being mixed with a flux, and heated to approximately 1000°C . This resulted in the production of a fused glass disc. This disc, which is representative of the sample's original chemistry, is free of any mineral structure, and is ideal for XRF analysis.

In preparation for analysis employing Inductively Coupled Plasma Mass Spectrometry (ICP-MS) samples, MQT-15-002, MQT-14-003, MQT-14-011, 14EA331H 1141.9m, 04EA054 86.05m, EA-15-001, EA-15-003, BRP-15-012, BRP-14-005, DLP-15-006, and DLP-1784 were first crushed and pulverized before being fully dissolved in a closed vessel multi acid digestion. The resulting solution was then ready to be analyzed using ICP-MS.

Electron microprobe analysis (EPMA) was conducted at the University of Wisconsin-Madison's Eugene Cameron Electron Microprobe Lab, under the supervision of Dr. John Fournelle. The instrument used was a Cameca SX50 microprobe. Polished thin sections BRP-14-005, MQT-14-003, EA-15-001, and EAUG0012-86.43m were first sterilized and carbon coated to increase their conductivity. Next, the slides were examined using a scanning electron microscope (SEM). This device allowed for observation of the thin sections in much greater detail and at higher magnification than is possible with a standard petrographic microscope. Following (SEM) imaging, the slides were loaded into the electron microprobe. The Electron microprobe was able to target the most pristine grains of the primary minerals remaining in each sample. The Deer Lake Peridotite was excluded from this portion of the study because a thin section containing a sufficient fraction of primary minerals could not be produced.

Geological Mapping

Data collected during field work were first compiled and digitized along with data collected from previous work at each site. These digitized data include unit boundaries, important structural features, outcrop locations, hand sample locations, and unit

descriptions. This includes information for both the units directly addressed in this study and those in their immediate vicinity.

Digitization was accomplished through the use of ESRI-Arc GIS software. Digitized data were then incorporated into the appropriate maps within the GIS software. Layers containing the relevant data could then be used as overlays atop the topographic base map for each study area. Then, by applying a digital elevation model available from the USGS online database, a new geological map could be created for each research site. The resulting maps contain all data collected during the field portion of this study. It also includes all relevant data recorded by previous researchers, making these maps an ideal accompaniment to the petrological and geochemical analyses and interpretations which follow.

CHAPTER IV

RESULTS

Petrographic Description

Presque Isle Peridotite

Presque Isle Peridotite is best described as a medium-to fine-grained lherzolite (peridotite composed of ≥ 40 vol% olivine, and whose pyroxene component is made up of both orthopyroxene and clinopyroxene). Since its formation, the unit has undergone significant alteration. Remaining primary minerals range from $<5\%$ to $>30\%$ depending upon sampling location. The unit's altered fraction is generally composed of serpentine in the form of rounded pseudomorphs after olivine (these are generally recognizable as rounded crystals displaying irregular cracks), and pyroxene-bastite (serpentine pseudomorphs after clinopyroxene). Other secondary minerals such as hematite, magnetite, goethite, carbonates, and quartz constitute 1-2% of the unit. Sulfides such as pyrite and galena also account for 1-2%.

Presque Isle Peridotite, in outcrop, weathers to a brownish green color. Hand samples from Presque Isle Peridotite display a greenish black coloration on fresh surfaces, and a phaneritic texture. However, individual crystals are difficult to distinguish in areas where the rock displays higher degrees of alteration. This is due to the presence of numerous hydrothermal veins filled by serpentine, quartz, calcite, carbonate minerals, or sulfide minerals (such as pyrite and galena).



Figure 13

Photo of sample MQT-15-002

- Hand Sample-Lightly serpentinized Presque Isle Peridotite.
- Note visible phaneritic texture and brownish weathering rind.



Figure 14

Field photo from eastern side of Presque Isle, showing Presque Isle Peridotite as it appears in outcrop.

Thin sections MQT-14-001, MQT-14-003, MQT-14-011, and MQT-15-002 are Presque Isle Peridotite, and display approximately 60-98% alteration minerals. Alteration is primarily observed in the form of serpentine after olivine pseudomorphs with clinopyroxene-bastite filling the interstitial areas is the unit's principal mineral assemblage. Where primary minerals that are still present are composed primary of olivine surrounded by pyroxene grains. The unit exhibits a cumulate texture consisting of subhedral to euhedral olivine with interstitial pyroxene. There is a poikilitic texture that can be observed in some cases, with olivine chadacrysts are surrounded by pyroxene oikocrysts. This texture is shown in Figure 15. Primary minerals can best be observed in thin sections MQT-14-003, and MQT-14-011. Small crystals of spinel and sulfide minerals can also be observed in thin sections of this rock type regardless of alteration level. Sulfide Minerals are commonly observed as inclusions within olivine crystals as shown in Figures 17 and 18.

Thin section MQT-15-002 shows significant sulfide mineralization in the form of pentlandite, and chalcopyrite, which has crystallized in association with magnetite, as seen in Figure 18. Pentlandite is distinguished by its light yellowish cream reflection color, from its supergene equivalent, violarite, which reflects grey to pink (Pracejus, 2008).

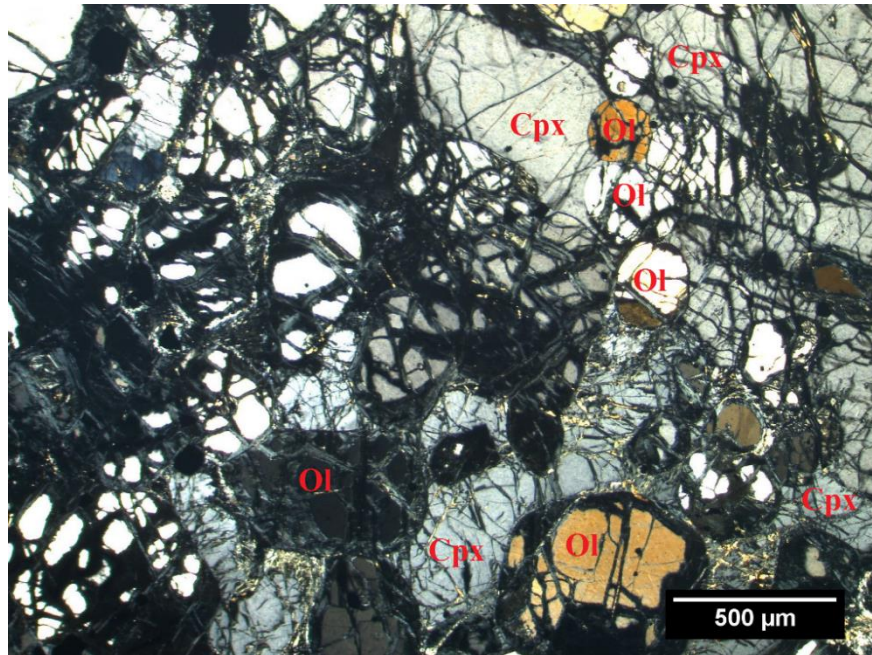


Figure 15

Photomicrograph of MQT-14-003

Olivine chadacrysts surrounded by pyroxene oikocrysts.

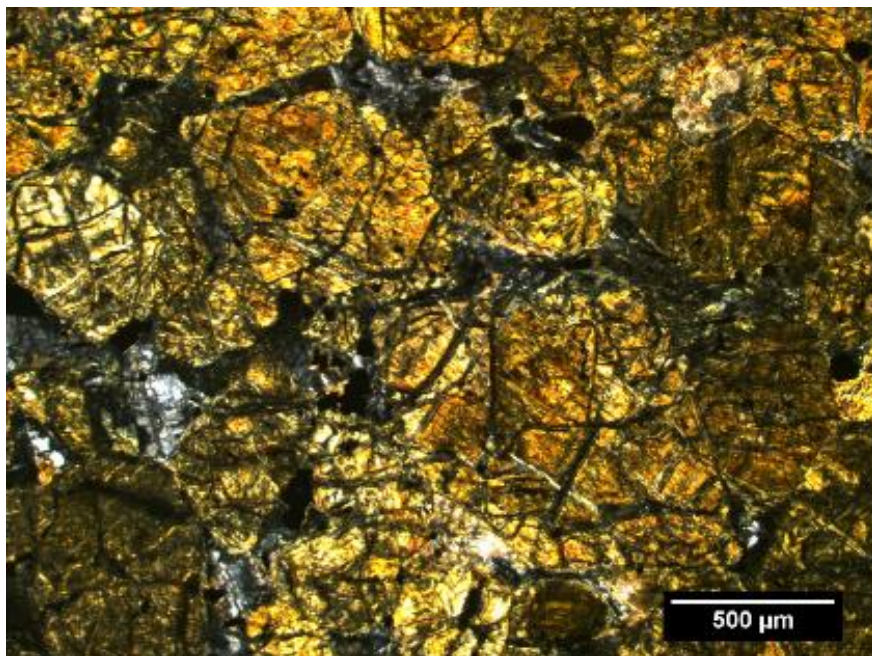


Figure 16

Photomicrograph of MQT-14-001

Serpentine after olivine pseudomorphs.

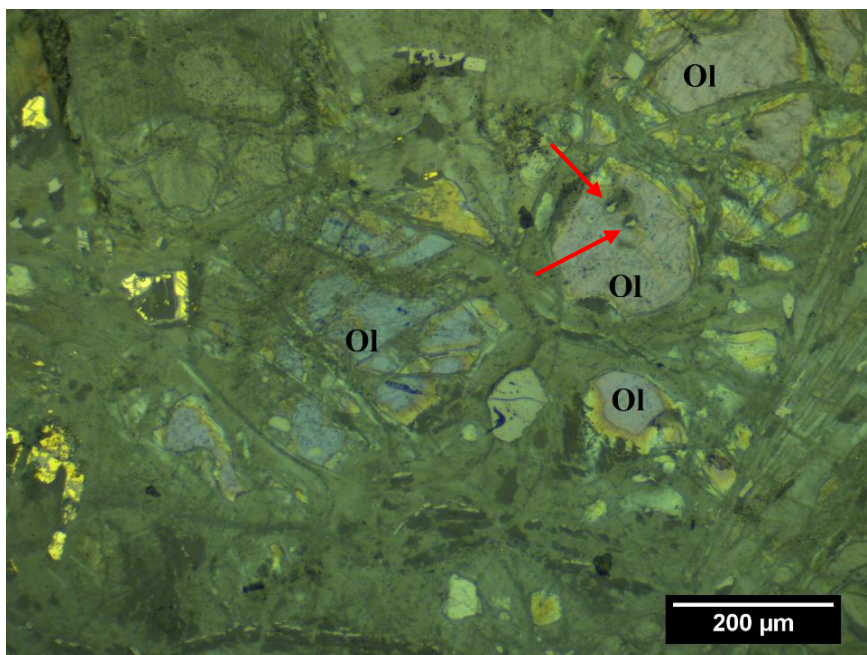


Figure 17
Reflected light photomicrograph of MQT-14-011.
Sulfide inclusions in olivine indicated by red arrows.

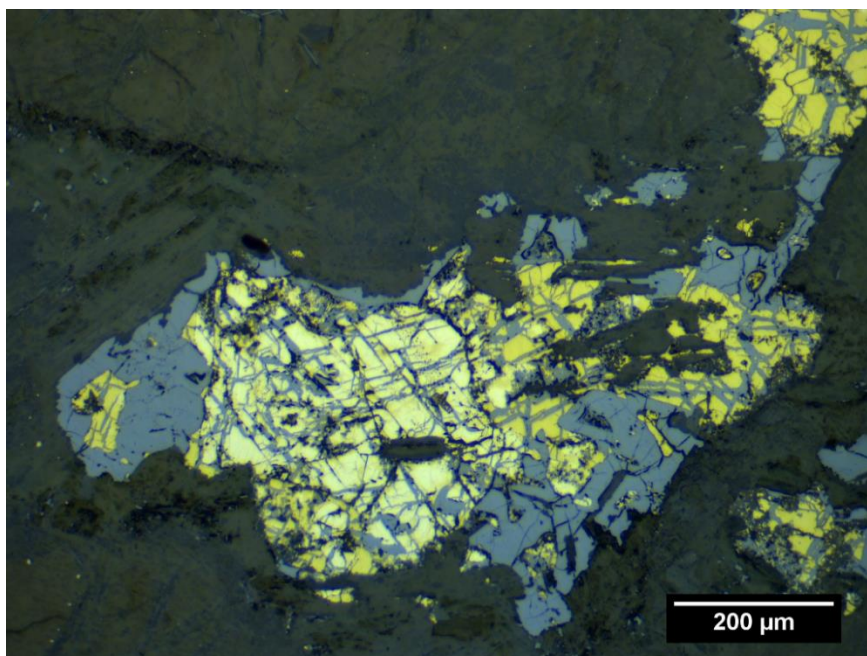


Figure 18
Reflected light photomicrograph of MQT-15-002.
magnetite (grey), chalcopyrite (dark yellow), pentlandite (bright yellow).

Deer Lake Peridotite

Deer Lake Peridotite, in its pre alteration state, would have been described as a medium grained peridotite. However, the majority of the unit has been highly altered. Collecting samples, at some locations, which retain their original crystallinity and texture is possible. However, the unit's primary minerals have invariably been replaced by serpentine pseudomorphs of olivine and pyroxene. Various other secondary and alteration minerals are also present in smaller amounts. Based on observations of these secondary mineral structures, it is apparent that the unit's original mineral assemblage was once dominated by olivine and pyroxene.



Figure 19

Photo of sample DLP-15-006.

Hand sample of low alteration Deer Lake Peridotite.



Figure 20
Deer Lake Peridotite outcrop, Verde Antique Quarry.
Highly altered portion of Deer Lake Peridotite.
Andrew Sasso (6') for scale.

Deer Lake Peridotite, in hand sample, appears to be fine to medium grained and is greenish to black in coloration. The unit typically weathers to a brown-grey color where it is exposed at the surface. Some samples are highly altered, making their crystallinity difficult to distinguish.

Thin sections, DLP-15-006, DLP, 1784ft, and DLP-562ft are Deer Lake Peridotite. Rossell (1983), notes that peridotite samples collected at Deer Lake appear to be of two varieties, both of which display nearly complete serpentinization. Type 1, is commonly found within outcrops of the peridotite. Samples of this rock type show no foliation; rather, they retain a relic igneous texture (observed in thin section, DLP-15-006). This relic igneous texture is characterized by pseudomorphs of serpentine after olivine, identified by rounded crystals and irregularly cracked texture. Serpentine after pyroxene pseudomorphs (known as bastite) are also present. Other minerals such as

magnetite, various carbonates, and talc comprise a smaller fraction of the unit. Similar to the Presque Isle Peridotite, serpentine after olivine pseudomorphs are often enclosed in anhedral bastite. Observation of these relic textures permits the interpretation, that in its pre-alteration state, the unit would have displayed a cumulate texture. There is a relic poikilitic texture observed in some areas, here pyroxene oikocrysts enclosed olivine chadacrysts. These pseudomorphs and associated textures, are exhibited in Figures 21 and 22. Small grains of spinel and sulfide minerals, can also be observed throughout thin sections of the Deer Lake Peridotite however, they account for only 1-2% of the rock unit.

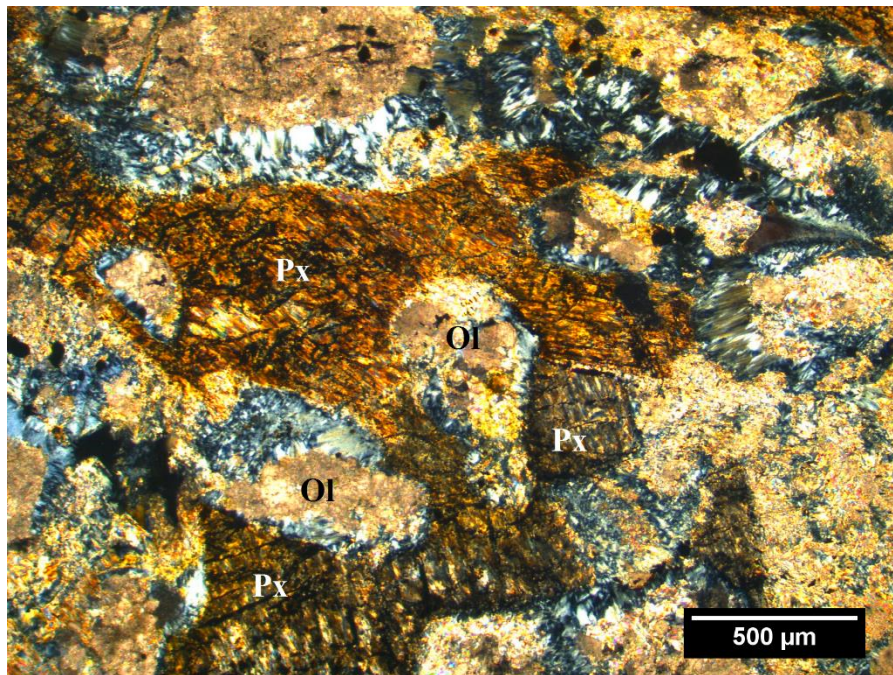


Figure 21

Photomicrograph of DLP-15-006.

Bastite oikocrysts (Px) surround serpentine after olivine chadacrysts (Ol).

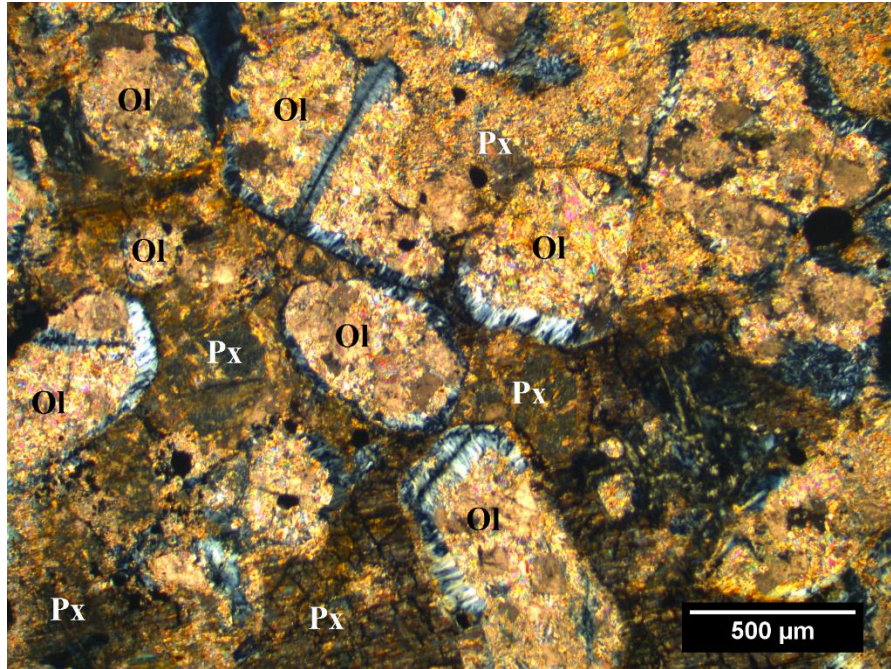


Figure 22

Photomicrograph of DLP-15-006

Bastite oikocrysts (Px) surround serpentine after olivine chadacrysts (Ol).

The second variety, or Type 2, of peridotite observed at Deer Lake has been observed only in drill core samples. These were originally obtained by Callahan Mining Company in the vicinity of the Ropes Gold Mine, and collected from the Michigan Department of Environmental Quality's core repository located in Harvey, Michigan. Type 2 are highly foliated. Serpentine is the most abundant mineral. Other minerals such as magnetite, various carbonates, and talc comprise a smaller fraction of the unit. The high degree of foliation has drastically distorts, or completely destroys any relic igneous texture. This makes it impossible to determine (through petrographic means) whether the primary mineralogy and texture of Type 2 samples would could be similar to that interpreted for Type 1 samples.

Black Rock Point Gabbro

Petrographic analysis of the Black Rock Point Gabbro allows for its classification as a medium-to-coarse grained gabbro. The unit is composed primarily of plagioclase feldspar and clinopyroxene. Sphene is also found in small quantities. This gabbro shows a substantial degree of alteration resulting in amounts of chlorite, quartz, and amphibole being present.

In hand sample, Black Rock Point Gabbro is bluish green in color and is medium to coarse grained in texture. It weathers to an unusual reddish tone where the unit is exposed to the surface.



Figure 23
Black Rock Point Gabbro.
Photo of hand sample BRP-14-005.



Figure 24
Black Rock Point Gabbro outcrop.

Thin sections BRP-14-005, BRP-14-006, and BRP-15-012 are Black Rock Point Gabbro. Petrographic analysis reveals the units to primarily have a hypidiomorphic texture in which the majority of crystal phases are subhedral to anhedral. Plagioclase crystals are subhedral, easily recognized by their: (1) First order interference color, (2) lath shape, and (3) albite twinning. Pyroxene can be identified by its: (1) High refractive index, (2) second order interference color, and (3) inclined extinction. Spene sparsely occurs throughout the unit as anhedral crystals of varying size. It can be identified by its very high positive relief, and cleavage. Small plagioclase laths are commonly found either partially or fully enclosed by clinopyroxene, giving the unit a subophitic to ophitic texture.

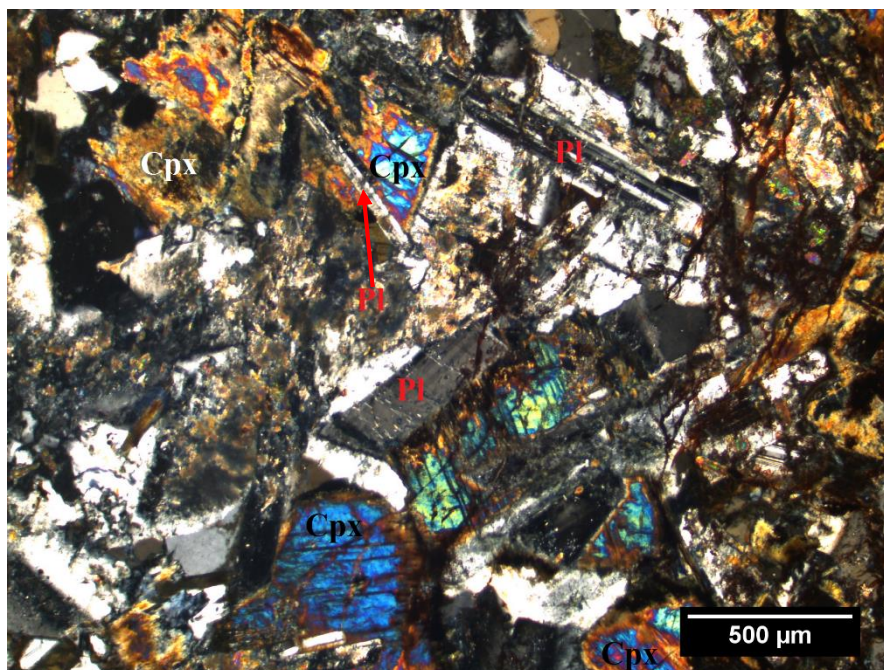


Figure 25

Photomicrograph from BRP-14-005 showing plagioclase and clinopyroxene crystals. Plagioclase lath indicated by red arrow is partially enclosed within clinopyroxene.

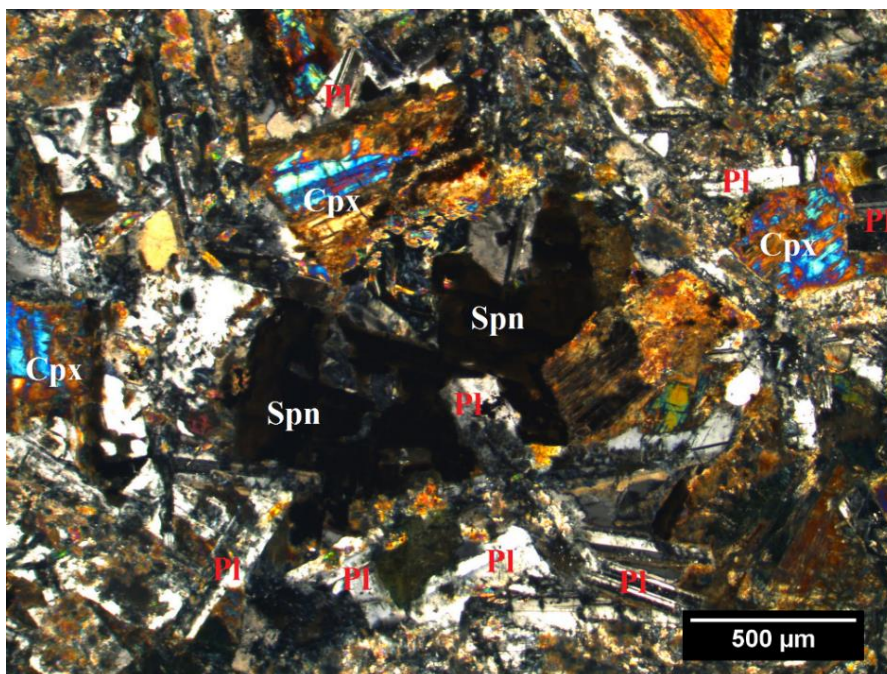


Figure 26

Photomicrograph from BRP-14-005. Sphene (Spn) is visible at center of image.

Yellowdog Peridotite

Yellowdog Peridotite found in both the eastern and western intrusions, is a medium to coarse-grained feldspathic lherzolite. This unit is composed primarily of olivine with clinopyroxene, orthopyroxene, and plagioclase feldspar. Yellowdog Peridotite is partially serpentinized, and alteration of both olivines and pyroxenes can be observed. The unit, a medium-to coarse-grained plagioclase lherzolite, has a composition of $\geq 40\%$ olivine, contains a significant fraction of both orthorhombic and monoclinic pyroxene. Substantial quantities of plagioclase feldspar can also be observed.

Yellowdog Peridotite, In hand sample, is dark grey to greenish colored and has a mottled white and black appearance due to the presence of plagioclase. The rock, in outcrop, is weathered brown to red due to of pyrrhotite (an iron sulfide) hosted within the unit.



Figure 27
Photo of sample EA-15-002.
Yellowdog Peridotite hand sample.

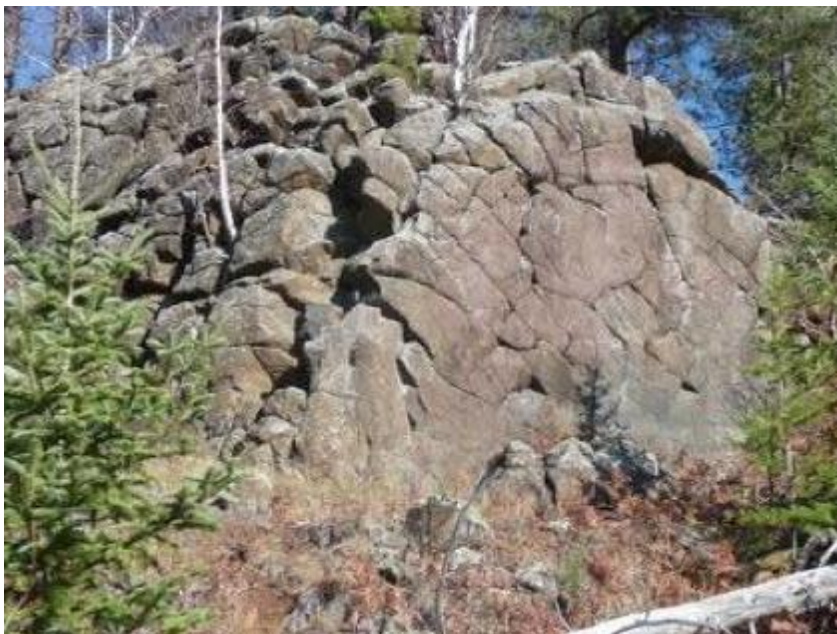


Figure 28
 Outcrop of Yellowdog Peridotite at “Eagle Rock”
 (Eastern intrusion at the Eagle Mine Site.)

Thin sections EA-15-001, EA-15-002, EA-15-003 and EAUG0012-86.43m are from the Yellowdog Peridotite. Olivine occurs here as rounded grains, and constitutes approximately 40-60% of the unit. After olivine, pyroxene is the next most abundant phase, constituting approximately 15-40%. Most samples contain a fraction of plagioclase ranging between 15-25% of the unit. Minor minerals, such as hornblende, biotite, and magnetite account for a small percentage of the unit (<5%). Samples taken from sulfide poor sections of the unit contain minor fractions of pyrrhotite, pentlandite, and chalcopyrite. These minerals occur either as inclusions within olivines, or as small crystals filling interstitial spaces. This unit displays a cumulate texture. Olivines are subhedral to euhedral, with interstitial spaces being filled by subhedral to anhedral grains of either pyroxene or plagioclase. Poikilitic texture, in which pyroxene oikocrysts enclose olivine chadacrysts, can occasionally be observed. One example of this textural

characteristic is displayed in Figure 30. Here a group of olivine chadacrysts can be observed, completely enclosed by a clinopyroxene oikocryst. Plagioclase occurs as anhedral to subhedral laths filling the remaining interstitial space. This suggests that it was the last phase to crystallize.

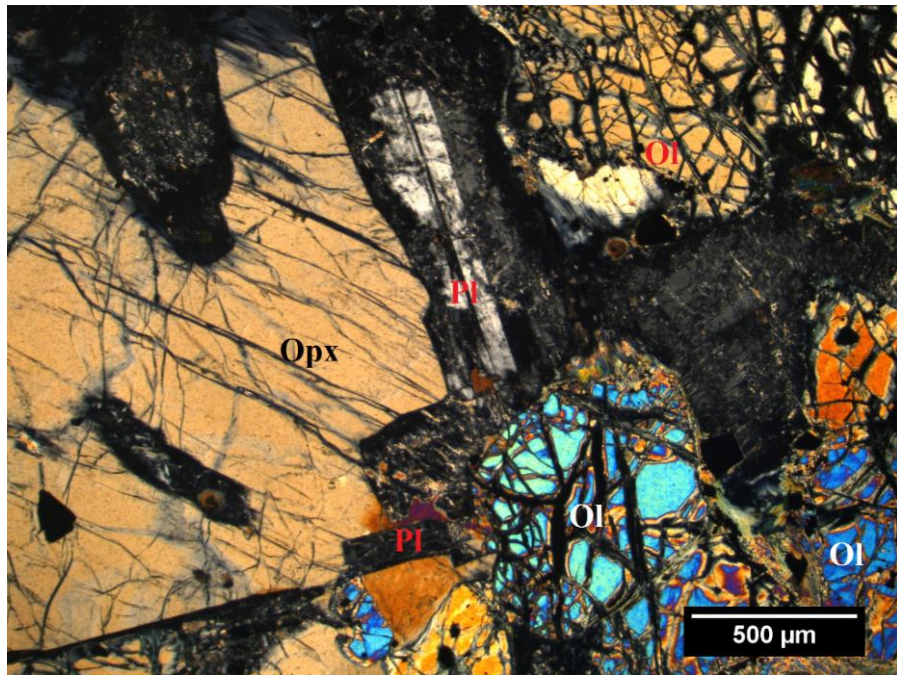


Figure 29

Photomicrograph of EA-15-001.

Showing olivine, and pyroxene with interstitial plagioclase.

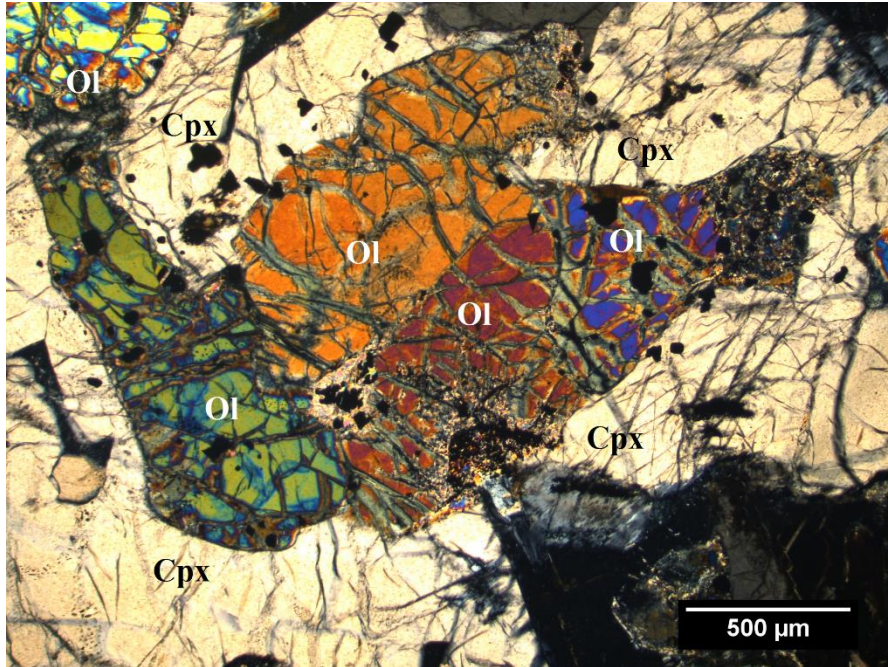


Figure 30

Photomicrograph from EA-15-001.

Poikilitic texture of pyroxene oikocrysts surrounding olivine chadacrysts.

Geochemistry

Bulk major and minor trace element data of selected samples from each study area are presented in tables 1, and 3. Table 2 displays base metal concentrations for selected samples from each site. Tables 4, 5, 6, 7, 8, 9, 10, 11, and 12 display electron microprobe data for selected samples from Presque Isle Peridotite, Yellowdog Peridotite, and Black Rock Point Gabbro. Major oxide geochemistry numbers are expressed as weight percent. Trace element and base metal concentrations are expressed in ppm.

X-ray Fluorescence Spectrometry

Table 6: Whole Rock Geochemistry

Sample		MQT-15-002	BRP-14-005	EA-15-001	DLP-1784
wt. %	Detection Limit				
SiO ₂	0.04	37.32	48.41	40.91	37.75
TiO ₂	0.01	0.39	0.83	0.67	0.02
Al ₂ O ₃	0.02	2.41	15.64	4.61	2.71
Cr ₂ O ₃	0.002	0.51	0.04	0.41	0.33
Fe ₂ O ₃	0.01	17.77	12.74	15.21	8.27
MnO	0.002	0.141	0.196	0.183	0.057
MgO	0.01	28.43	7.17	28.23	38.32
CaO	0.006	0.584	9.663	4.243	0.036
Na ₂ O	0.02	0.09	2.22	0.24	<0.02
K ₂ O	0.01	0.09	0.55	0.22	<0.01
P ₂ O ₅	0.002	0.04	0.096	0.054	<0.002
LOI	0.05	12.01	2.6	5.77	12.77
Total		99.79	100.15	100.76	100.23

Table 7: Select Base Metal Concentrations

Sample	Detection Limit	MQT-15-002	BRP-14-005	EA-15-001	DLP-1784
Co	12	196	54	139	131
Cu	14	776	127	113	19
Ni	9	1853	130	1572	3173
V	8	81	238	124	23
Zn	5	74	95	111	44

Values expressed in ppm.

Table 7 displays base metal concentrations obtained via XRF for samples of Presque Isle Peridotite (MQT-15-002), Black Rock Point Gabbro (BRP-14-005), Eagle East (EA-15-001), and Deer Lake Peridotite (DLP-1784). Note: Elevated nickel concentrations present in peridotite samples from Presque Isle, Eagle East, and Deer Lake. This enrichment may result either from the olivine chemistry of the unit or by inclusion of nickel rich sulfide minerals. Presque Isle Peridotite also appears enriched in copper when compared to the other three units.

Inductively Coupled Plasma Mass Spectrometry

Table 8: Trace Element Geochemistry

Sample	MQT-15-002	MQT-14-003	MQT-14-011	
	Detection Limit			
Ba	0.80	25.20	44.90	40.40
Be	0.04	0.30	0.25	0.34
Bi	0.47	<0.47	<0.47	<0.47
Cd	0.01	0.23	0.02	0.04
Ce	0.12	6.86	7.39	7.65
Co	0.13	181.38	150.38	154.99
Cr	3.00	3402.00	>4500	4250.00
Cs	0.01	0.25	0.24	0.21
Cu	1.40	738.60	45.70	216.60
Dy	0.01	0.91	1.08	1.01
Er	0.01	0.45	0.53	0.50
Eu	0.00	0.36	0.38	0.41
Ga	0.04	4.11	5.48	5.05
Gd	0.01	1.05	1.14	1.16
Hf	0.14	0.73	0.84	0.84
Ho	0.00	0.17	0.20	0.19
In	0.00	0.03	0.03	0.02
La	0.10	3.36	3.31	3.57
Li	0.40	11.60	17.00	23.90
Lu	0.00	0.06	0.07	0.06
Mo	0.08	0.51	0.57	0.36
Nb	0.03	1.53	1.66	1.82
Nd	0.06	4.35	4.72	5.06

Values expressed in ppm.

Table 8: Continued

Sample	MQT-15-002	MQT-14-003	MQT-14-011	
	Detection Limit			
Ni	0.70	1766.10	1830.50	1591.30
Pb	0.18	19.70	2.60	5.80
Pr	0.01	1.01	1.04	1.12
Rb	0.11	3.26	2.38	2.61
Sb	0.04	<0.04	0.06	<0.04
Sc	1.10	10.40	11.80	9.60
Sm	0.03	1.10	1.16	1.16
Sn	0.16	0.35	0.32	0.30
Sr	0.60	32.60	37.80	41.20
Ta	0.01	0.10	0.11	0.12
Tb	0.00	0.16	0.18	0.17
Th	0.02	0.42	0.53	0.53
Ti	7.00	2306.00	2691.00	2659.00
Tl	0.00	0.26	0.04	0.16
Tm	0.00	0.06	0.07	0.07
U	0.01	0.10	0.12	0.12
V	0.80	79.20	87.90	79.00
W	0.05	0.05	<0.05	0.05
Y	0.05	4.55	5.18	5.04
Yb	0.01	0.38	0.46	0.42
Zn	1.80	64.00	73.00	49.00
Zr	6.00	27.00	30.00	32.00

Values expressed in ppm.

Table 8: Continued

Sample	14EA331H 1141.9m	04EA054 86.05m	EA-15-001	EA-15-003	
	Detection Limit				
Ba	0.80	84.50	36.50	60.30	34.40
Be	0.04	0.51	0.40	0.42	0.36
Bi	0.47	2.45	0.59	<0.47	<0.47
Cd	0.01	2.36	0.60	0.07	0.08
Ce	0.12	14.91	6.71	9.36	8.87
Co	0.13	>187	>187	128.91	133.28
Cr	3.00	1762.00	3109.00	2749.00	2855.00
Cs	0.01	1.61	0.84	1.24	1.08
Cu	1.40	>2900	>2900	89.40	91.30
Dy	0.01	2.73	1.40	1.58	1.57
Er	0.01	1.28	0.70	0.84	0.81
Eu	0.00	0.98	0.45	0.58	0.52
Ga	0.04	12.20	7.38	7.79	7.71
Gd	0.01	2.91	1.41	1.67	1.67
Hf	0.14	1.87	0.85	1.18	1.10
Ho	0.00	0.49	0.26	0.31	0.29
In	0.00	0.16	0.07	0.03	0.04
La	0.10	6.56	2.86	4.23	3.94
Li	0.40	11.90	13.30	18.40	18.10
Lu	0.00	0.14	0.09	0.10	0.09
Mo	0.08	0.70	0.58	0.69	0.59
Nb	0.03	4.32	1.65	2.54	2.41
Nd	0.06	10.78	4.62	6.46	5.80

Values expressed in ppm.

Table 8: Continued

Sample	14EA331H 1141.9m	04EA054 86.05m	EA-15-001	EA-15-003	
	Detection Limit				
Ni	0.70	>4100	>4100	1490.80	1550.90
Pb	0.18	25.20	7.20	1.40	1.60
Pr	0.01	2.31	0.97	1.37	1.30
Rb	0.11	7.10	4.07	8.93	7.79
Sb	0.04	0.12	0.10	<0.04	0.06
Sc	1.10	18.80	14.70	13.50	14.40
Sm	0.03	2.84	1.22	1.64	1.48
Sn	0.16	2.96	0.59	0.48	0.65
Sr	0.60	142.50	60.50	66.40	37.90
Ta	0.01	0.29	0.11	0.17	0.16
Tb	0.00	0.45	0.22	0.26	0.26
Th	0.02	0.86	0.48	0.64	0.64
Ti	7.00	7319.00	3302.00	4032.00	3850.00
Tl	0.00	0.17	0.09	0.10	0.09
Tm	0.00	0.17	0.10	0.11	0.10
U	0.01	0.31	0.17	0.24	0.24
V	0.80	188.60	114.20	123.00	120.80
W	0.05	0.12	0.07	0.08	0.07
Y	0.05	12.87	6.97	7.89	7.73
Yb	0.01	1.09	0.60	0.68	0.68
Zn	1.80	110.00	109.00	99.00	98.00
Zr	6.00	70.00	31.00	43.00	40.00

Values expressed in ppm.

Table 8: Continued

Sample	BRP-15-012	BRP-14-005	DLP-15-006	DLP-1784	
	Detection Limit				
Ba	0.80	141.80	121.90	2.20	<0.8
Be	0.04	0.51	0.63	0.30	0.15
Bi	0.47	<0.47	<0.47	<0.47	<0.47
Cd	0.01	0.14	0.09	0.07	<0.013
Ce	0.12	16.62	18.31	4.17	0.41
Co	0.13	57.23	51.23	112.70	118.64
Cr	3.00	281.00	266.00	3469.00	2200.00
Cs	0.01	1.23	0.60	0.23	0.02
Cu	1.40	109.40	121.20	22.40	2.70
Dy	0.01	3.80	3.95	0.80	0.06
Er	0.01	2.42	2.55	0.52	0.04
Eu	0.00	0.92	0.99	0.18	0.03
Ga	0.04	16.60	16.72	5.85	1.58
Gd	0.01	3.18	3.51	0.68	0.05
Hf	0.14	1.96	2.06	0.51	<0.14
Ho	0.00	0.79	0.84	0.16	0.01
In	0.00	0.07	0.07	0.02	0.00
La	0.10	7.30	7.89	1.94	0.25
Li	0.40	15.70	18.10	6.40	<0.4
Lu	0.00	0.37	0.38	0.08	0.01
Mo	0.08	1.15	0.82	0.34	0.88
Nb	0.03	3.65	3.75	0.61	0.05
Nd	0.06	10.13	10.72	2.43	0.16

Values expressed in ppm.

Table 8: Continued

Sample	BRP-15-012	BRP-14-005	DLP-15-006	DLP-1784	
	Detection Limit				
Ni	0.70	138.80	130.90	1906.60	2969.50
Pb	0.18	3.80	3.10	1.80	0.40
Pr	0.01	2.25	2.48	0.58	0.05
Rb	0.11	32.17	20.91	2.51	0.16
Sb	0.04	0.10	0.06	1.54	4.51
Sc	1.10	40.50	38.40	17.60	3.80
Sm	0.03	2.66	2.87	0.58	0.04
Sn	0.16	0.76	0.82	0.20	<0.16
Sr	0.60	181.90	161.80	29.90	1.70
Ta	0.01	0.24	0.25	0.04	<0.007
Tb	0.00	0.56	0.60	0.12	0.01
Th	0.02	1.18	1.18	0.28	0.03
Ti	7.00	5645.00	5052.00	1336.00	99.00
Tl	0.00	0.13	0.08	0.08	0.01
Tm	0.00	0.37	0.36	0.08	0.01
U	0.01	0.33	0.36	0.08	0.01
V	0.80	281.20	236.20	83.70	12.90
W	0.05	0.12	0.14	0.16	0.72
Y	0.05	22.33	23.42	4.46	0.31
Yb	0.01	2.40	2.49	0.54	0.05
Zn	1.80	120.00	88.00	82.00	32.00
Zr	6.00		76.00	18.00	<6

Values expressed in ppm.

Electron Microprobe

Presque Isle Peridotite

Table 9: MQT-14-004 Olivine. Oxides expressed in wt. %

Mineral	OL1		OL 2		OL3		OL4		OL5		OL6	
Point	289	290	293	294	295	296	300	303	304	306	310	311
SiO ₂	39.14	39.21	39.29	39.25	39.14	39.33	39.45	39.04	39.19	39.33	39.37	39.55
FeO	16.62	16.44	16.26	16.41	16.73	16.22	16.22	16.55	16.60	16.16	16.24	16.40
MnO	0.25	0.19	0.14	0.18	0.11	0.21	0.19	0.08	0.10	0.11	0.13	0.16
MgO	43.40	43.41	43.77	43.42	43.19	43.46	43.73	43.54	43.30	43.45	43.44	43.20
NiO	0.32	0.39	0.39	0.29	0.26	0.35	0.32	0.33	0.31	0.27	0.29	0.25
CaO	0.15	0.17	0.10	0.18	0.20	0.20	0.09	0.20	0.19	0.25	0.24	0.23
Total	99.87	99.81	99.95	99.72	99.63	99.76	99.99	99.74	99.68	99.58	99.72	99.80
Stoichiometry normalized to 4 oxygens.												
Si	1.00	1.00	1.00	1.00	1.00	1.00	1.00	0.99	1.00	1.00	1.00	1.00
Fe(II)	0.35	0.35	0.34	0.35	0.36	0.34	0.34	0.35	0.35	0.34	0.35	0.35
Mn	0.01	0.00	0.00	0.00	0.00	0.00	0.00	0.00	0.00	0.00	0.00	0.00
Mg	1.64	1.65	1.65	1.65	1.64	1.65	1.65	1.65	1.64	1.65	1.65	1.64
Ni	0.01	0.01	0.01	0.01	0.01	0.01	0.01	0.01	0.01	0.01	0.01	0.01
Ca	0.00	0.00	0.00	0.00	0.01	0.01	0.00	0.01	0.01	0.01	0.01	0.01
Total	3.01	3.01	3.01	3.01	3.01	3.01	3.00	3.01	3.01	3.01	3.01	3.00
Mg#	82.32	82.48	82.75	82.50	82.14	82.69	82.77	82.42	82.30	82.73	82.66	82.44
Fo	82.10	82.32	82.63	82.35	82.05	82.51	82.61	82.36	82.22	82.64	82.55	82.30
Fa	17.63	17.48	17.22	17.46	17.83	17.27	17.19	17.56	17.68	17.25	17.31	17.53

"Point" refers to analysis number or probe position.

Mg-number = $100(\text{MgO}/(\text{MgO}+\text{FeO}))$ molar%

Table 9: Continued

Mineral Point	OL7		OL8		OL9		OL10		OL11		OL12	
	312	316	318	321	322	325	328	331	339	340	332	333
SiO ₂	38.89	39.10	39.35	39.26	39.30	39.39	39.58	39.45	39.22	39.33	39.59	39.32
FeO	16.63	17.30	16.32	16.54	16.86	16.35	16.27	16.35	16.15	16.19	16.52	16.30
MnO	0.20	0.13	0.25	0.20	0.21	0.13	0.22	0.22	0.16	0.18	0.20	0.15
MgO	43.47	42.20	43.30	43.77	42.84	43.74	43.54	43.54	43.86	43.91	43.27	43.10
NiO	0.40	0.30	0.35	0.35	0.30	0.34	0.33	0.28	0.39	0.27	0.32	0.37
CaO	0.22	0.17	0.22	0.14	0.51	0.20	0.18	0.20	0.23	0.22	0.21	0.15
Total	99.81	99.20	99.80	100.25	100.02	100.14	100.13	100.04	100.00	100.09	100.09	99.39
Stoichiometry normalized to 4 oxygens.												
Si	0.99	1.00	1.00	0.99	1.00	1.00	1.00	1.00	0.99	1.00	1.00	1.00
Fe(II)	0.35	0.37	0.35	0.35	0.36	0.35	0.34	0.35	0.34	0.34	0.35	0.35
Mn	0.00	0.00	0.01	0.00	0.00	0.00	0.00	0.00	0.00	0.00	0.00	0.00
Mg	1.65	1.61	1.64	1.65	1.63	1.65	1.64	1.64	1.66	1.66	1.63	1.64
Ni	0.01	0.01	0.01	0.01	0.01	0.01	0.01	0.01	0.01	0.01	0.01	0.01
Ca	0.01	0.00	0.01	0.00	0.01	0.01	0.00	0.01	0.01	0.01	0.01	0.00
Total	3.02	3.00	3.01	3.01	3.01	3.01	3.00	3.01	3.01	3.01	3.00	3.00
Mg#	82.32	82.48	82.75	82.50	82.14	82.69	82.77	82.42	82.30	82.73	82.66	82.44
Fo	82.15	81.20	82.32	82.34	81.73	82.56	82.47	82.41	82.74	82.70	82.19	82.37
Fa	17.63	18.66	17.41	17.45	18.05	17.31	17.29	17.36	17.09	17.11	17.60	17.47

"Point" refers to analysis number or probe position.

Mg-number = $100(\text{MgO}/(\text{MgO}+\text{FeO}))$ molar%

Table 10: MQT-14-004 Pyroxene. Oxides expressed in wt. %

Mineral	PX1		PX2		PX3	PX6		
	Point	344	348	349	354	364	384	389
SiO ₂		52.39	52.63	46.04	51.64	54.90	51.93	51.30
TiO ₂		0.67	0.60	2.87	0.99	0.28	0.76	0.77
Al ₂ O ₃		2.46	2.29	7.90	3.57	1.44	2.77	2.67
Cr ₂ O ₃		0.75	0.83	0.06	0.62	0.42	0.83	0.70
FeO		5.88	5.90	8.75	6.93	10.04	6.18	5.72
MnO		0.10	0.15	0.15	0.13	0.18	0.12	0.05
MgO		18.30	18.46	14.51	18.46	30.71	18.11	17.95
CaO		19.04	19.14	18.87	17.58	2.03	19.23	19.19
Na ₂ O		0.25	0.28	0.41	0.28	0.04	0.33	0.59
K ₂ O		0.02	0.01	0.02	0.00	0.02	0.01	0.17
NiO		0.00	0.05	0.02	0.08	0.10	0.00	0.11
Total		99.85	100.33	99.60	100.28	100.16	100.24	99.23
Stoichiometry normalized to 6 oxygens.								
Si		1.92	1.92	1.73	1.89	1.94	1.90	1.90
Ti		0.02	0.02	0.08	0.03	0.01	0.02	0.02
Al		0.02	0.02	0.07	0.04	0.00	0.02	0.01
Fe(III)		0.03	0.04	0.10	0.03	0.06	0.06	0.11
Cr		0.02	0.02	0.00	0.02	0.01	0.02	0.02
Fe(II)		0.15	0.14	0.17	0.18	0.24	0.13	0.07
Mn		0.00	0.00	0.00	0.00	0.01	0.00	0.00
Mg		1.00	1.00	0.81	1.00	1.62	0.99	0.99
Ca		0.75	0.75	0.76	0.69	0.08	0.75	0.76
Na		0.02	0.02	0.03	0.02	0.00	0.02	0.04
K		0.00	0.00	0.00	0.00	0.00	0.00	0.01
Total		4.01	4.01	4.03	4.01	4.02	4.02	4.03
Wo		38.38	38.25	40.42	35.67	3.85	38.52	38.61
En		51.33	51.33	43.23	52.13	80.96	50.47	50.27
Fs		9.39	9.40	14.74	11.16	15.05	9.81	8.98
Ac		0.90	1.02	1.60	1.04	0.15	1.20	2.13

"Point" refers to analysis number or probe position.

Table 10: Continued

Mineral	PX7		PX8		PX9		PX10		
	Point	393	396	397	398	417	422	410	411
SiO ₂		53.46	53.43	52.52	52.04	48.64	46.56	47.58	49.27
TiO ₂		0.45	0.47	0.52	0.66	1.78	2.42	2.45	1.87
Al ₂ O ₃		1.71	1.78	2.32	2.31	5.72	7.50	7.19	5.12
Cr ₂ O ₃		0.86	0.80	0.73	0.74	0.13	-0.01	0.04	0.31
FeO		5.72	5.78	6.08	6.10	7.81	8.04	7.99	7.42
MnO		0.15	0.20	0.07	0.14	0.16	0.14	0.12	0.15
MgO		19.15	19.25	18.65	18.85	16.44	14.75	14.88	15.98
CaO		18.51	18.60	18.90	18.81	18.47	19.42	19.50	19.69
Na ₂ O		0.26	0.23	0.34	0.32	0.28	0.40	0.31	0.31
K ₂ O		0.00	0.01	0.00	0.01	0.00	0.00	0.02	0.01
NiO		0.04	0.04	0.07	0.01	0.12	0.03	0.04	0.08
Total		100.31	100.60	100.19	100.01	99.54	99.25	100.12	100.22
Stoichiometry normalized to 6 oxygens.									
Si		1.94	1.94	1.92	1.91	1.81	1.75	1.76	1.82
Ti		0.01	0.01	0.01	0.02	0.05	0.07	0.07	0.05
Al		0.02	0.01	0.02	0.01	0.06	0.08	0.08	0.04
Fe(III)		0.02	0.03	0.06	0.08	0.08	0.11	0.06	0.07
Cr		0.02	0.02	0.02	0.02	0.00	0.00	0.00	0.01
Fe(II)		0.16	0.15	0.13	0.10	0.16	0.14	0.18	0.16
Mn		0.00	0.01	0.00	0.00	0.01	0.00	0.00	0.00
Mg		1.04	1.04	1.02	1.03	0.91	0.82	0.82	0.88
Ca		0.72	0.72	0.74	0.74	0.74	0.78	0.77	0.78
Na		0.02	0.02	0.02	0.02	0.02	0.03	0.02	0.02
K		0.00	0.00	0.00	0.00	0.00	0.00	0.00	0.00
Total		4.01	4.01	4.02	4.03	4.02	4.03	4.02	4.02
Wo		36.87	36.87	37.62	37.28	38.46	41.32	41.44	40.71
En		53.08	53.09	51.66	51.98	47.64	43.67	43.98	45.97
Fs		9.12	9.24	9.50	9.59	12.87	13.47	13.38	12.15
Ac		0.94	0.81	1.21	1.16	1.04	1.54	1.19	1.17

"Point" refers to analysis number or probe position.

Yellowdog Peridotite

Table 11: EA-15-002 Olivine. Oxides expressed in wt. %

Mineral	OL1		OL2		OL4		OL5		OL6	
Point	473	477	531	532	539	541	543	546	548	551
SiO ₂	38.82	39.03	39.17	38.97	38.76	38.82	38.14	38.74	38.52	38.36
FeO	18.92	19.09	18.05	18.29	18.94	19.17	18.76	18.96	18.71	19.07
MnO	0.18	0.28	0.26	0.29	0.20	0.22	0.16	0.17	0.24	0.22
MgO	41.54	41.19	41.98	42.06	41.60	41.42	42.28	41.53	41.28	41.96
NiO	0.26	0.26	0.26	0.33	0.32	0.38	0.31	0.25	0.29	0.33
CaO	0.20	0.17	0.18	0.21	0.16	0.17	0.20	0.23	0.23	0.23
Total	99.93	100.01	99.92	100.15	99.98	100.17	99.86	99.88	99.27	100.17
Stoichiometry normalized to 4 oxygens.										
Si	0.997	1.002	1.001	0.996	0.995	0.996	0.982	0.996	0.996	0.986
Fe(II)	0.406	0.410	0.386	0.391	0.407	0.411	0.404	0.408	0.405	0.410
Mn	0.004	0.006	0.006	0.006	0.004	0.005	0.004	0.004	0.005	0.005
Mg	1.590	1.576	1.600	1.603	1.592	1.584	1.623	1.592	1.591	1.607
Ni	0.005	0.005	0.005	0.007	0.007	0.008	0.006	0.005	0.006	0.007
Ca	0.006	0.005	0.005	0.006	0.005	0.005	0.005	0.006	0.006	0.006
Total	3.009	3.003	3.004	3.009	3.009	3.009	3.024	3.010	3.010	3.021
Mg#	79.65	79.36	80.56	80.39	79.65	79.38	80.07	79.61	79.72	79.68
Fo	79.50	79.13	80.34	80.14	79.48	79.20	79.93	79.47	79.52	79.50
Fa	20.31	20.57	19.38	19.55	20.30	20.56	19.89	20.35	20.22	20.26

"Point" refers to analysis number or probe position.

Mg-number = $100(\text{MgO}/(\text{MgO}+\text{FeO}))$ molar%.

Table 11: Continued

Mineral	OL7		OL8		OL9		OL10		
	Point	552	554	560	561	562	564	567	568
SiO ₂		38.51	38.92	38.68	38.80	38.79	38.92	38.62	38.61
FeO		18.58	18.83	19.18	18.96	18.96	19.27	19.52	19.27
MnO		0.21	0.20	0.20	0.17	0.16	0.17	0.16	0.14
MgO		42.13	41.55	41.49	41.39	41.57	41.32	41.32	41.37
NiO		0.22	0.29	0.25	0.22	0.33	0.35	0.33	0.35
CaO		0.19	0.17	0.17	0.22	0.11	0.12	0.15	0.16
Total		99.84	99.95	99.97	99.75	99.93	100.15	100.10	99.90
Stoichiometry normalized to 4 oxygens.									
Si		0.989	0.998	0.994	0.998	0.996	0.998	0.993	0.994
Fe(II)		0.399	0.404	0.412	0.408	0.407	0.413	0.420	0.415
Mn		0.005	0.004	0.004	0.004	0.003	0.004	0.003	0.003
Mg		1.613	1.589	1.590	1.587	1.591	1.580	1.584	1.587
Ni		0.005	0.006	0.005	0.004	0.007	0.007	0.007	0.007
Ca		0.005	0.005	0.005	0.006	0.003	0.003	0.004	0.004
Total		3.016	3.006	3.010	3.008	3.007	3.005	3.011	3.011
Mg#		79.65	79.36	80.56	80.39	79.65	79.38	80.07	79.61
Fo		79.98	79.56	79.24	79.41	79.49	79.12	78.91	79.16
Fa		19.79	20.23	20.54	20.40	20.34	20.70	20.91	20.68

"Point" refers to analysis number or probe position.

Mg-number = $100(\text{MgO}/(\text{MgO}+\text{FeO}))$ molar%.

Table 12: EA-15-002 Pyroxene. Oxides expressed in wt. %

Mineral Point	PX2	PX5	PX8		PX9	
	485	497	513	514	518	519
SiO ₂	53.78	52.09	51.67	51.42	54.79	54.28
TiO ₂	0.54	0.10	1.12	0.91	0.53	0.49
Al ₂ O ₃	2.07	29.63	2.66	3.33	1.11	1.09
Cr ₂ O ₃	0.34	0.00	0.45	0.74	0.15	0.22
FeO	11.78	0.74	6.53	6.55	11.79	11.58
MnO	0.13	0.00	0.11	0.14	0.16	0.25
MgO	30.10	0.07	17.44	17.45	30.43	30.90
CaO	2.04	12.92	19.34	19.15	1.79	1.72
Na ₂ O	0.01	3.90	0.31	0.28	0.04	0.06
K ₂ O	0.00	0.18	0.02	0.01	0.02	0.01
NiO	0.09	0.00	0.00	0.02	0.09	0.11
Total	100.88	99.56	99.65	100.01	100.90	100.72
Stoichiometry normalized to 6 oxygens.						
Si	1.904	1.784	1.904	1.888	1.936	1.923
Ti	0.014	0.003	0.031	0.025	0.014	0.013
Al	0.000	0.980	0.019	0.033	0.000	0.000
Fe(III)	0.101	0.000	0.037	0.043	0.081	0.119
Cr	0.010	0.000	0.013	0.021	0.004	0.006
Fe(II)	0.245	0.023	0.164	0.158	0.265	0.221
Mn	0.004	0.000	0.003	0.004	0.005	0.007
Mg	1.589	0.003	0.958	0.955	1.603	1.632
Ca	0.077	0.474	0.763	0.754	0.068	0.065
Na	0.001	0.259	0.022	0.020	0.003	0.004
K	0.000	0.008	0.001	0.001	0.001	0.000
Total	3.944	3.534	3.915	3.902	3.979	3.991
Wo	3.84	62.46	39.20	38.97	3.35	3.19
En	78.79	0.45	49.19	49.40	79.18	79.68
Fs	17.34	2.97	10.47	10.58	17.32	16.95
Ac	0.04	34.11	1.13	1.05	0.15	0.19

"Point" refers to analysis number or probe position.

Table 13: EAUG0012-86.43m Olivine

Mineral Point	OL4		OL6	
	621	623	630	632
SiO ₂	38.76	38.79	39.31	38.99
FeO	17.88	17.45	16.70	17.40
MnO	0.16	0.11	0.12	0.12
MgO	42.87	42.93	43.16	43.13
NiO	0.35	0.35	0.25	0.26
CaO	0.18	0.14	0.17	0.15
Total	100.21	99.77	99.71	100.04
Stoichiometry normalized to 4 oxygens.				
Si	0.99	0.99	1.00	0.99
Fe(II)	0.38	0.37	0.36	0.37
Mn	0.00	0.00	0.00	0.00
Mg	1.63	1.64	1.64	1.64
Ni	0.01	0.01	0.01	0.01
Ca	0.01	0.00	0.00	0.00
Total	3.01	3.01	3.01	3.01
Mg#	81.03	81.43	82.17	81.54
Fo	80.90	81.34	82.06	81.44
Fa	18.93	18.54	17.81	18.43

"Point" refers to analysis number or probe position.

Mg-number = $100(\text{MgO}/(\text{MgO}+\text{FeO}))$ molar%

Table 14: EAUG0012-86.43m Pyroxene. Oxides expressed in wt. %

Mineral	PX2		PX3		PX4		PX5	
	Point	647	649	651	652	654	656	661
SiO ₂		52.63	52.99	50.49	50.36	52.04	51.50	54.63
TiO ₂		0.49	0.59	1.50	1.27	0.57	0.66	0.51
Al ₂ O ₃		2.10	2.26	3.37	3.45	2.15	2.54	2.11
Cr ₂ O ₃		0.55	0.77	0.27	0.27	0.61	0.65	0.04
FeO		7.47	6.92	8.74	8.42	7.40	7.21	9.55
MnO		0.08	0.13	0.17	0.09	0.14	0.06	0.15
MgO		19.37	18.69	16.57	16.94	18.60	17.94	19.48
CaO		16.94	18.28	18.43	18.34	17.23	18.67	11.47
Na ₂ O		0.28	0.23	0.31	0.31	0.28	0.28	0.65
K ₂ O		0.00	0.00	0.00	0.01	0.01	0.00	0.12
NiO		0.04	0.02	0.06	0.03	0.10	0.00	0.08
Totals		99.93	100.86	99.90	99.49	99.13	99.51	98.78
Stoichiometry normalized to 6 oxygens.								
Si		1.93	1.92	1.87	1.87	1.92	1.90	2.00
Ti		0.01	0.02	0.04	0.04	0.02	0.02	0.01
Al		0.02	0.02	0.02	0.02	0.02	0.01	0.09
Fe(III)		0.05	0.03	0.05	0.07	0.04	0.07	0.00
Cr		0.02	0.02	0.01	0.01	0.02	0.02	0.00
Fe(II)		0.18	0.18	0.22	0.19	0.18	0.15	0.29
Mn		0.00	0.00	0.01	0.00	0.00	0.00	0.00
Mg		1.06	1.01	0.92	0.94	1.03	0.99	1.06
Ca		0.66	0.71	0.73	0.73	0.68	0.74	0.45
Na		0.02	0.02	0.02	0.02	0.02	0.02	0.05
K		0.00	0.00	0.00	0.00	0.00	0.00	0.01
Total		4.02	4.01	4.02	4.02	4.01	4.02	3.97
Wo		33.71	36.41	37.64	37.37	34.81	37.49	24.20
En		53.62	51.81	47.09	48.04	52.31	50.14	57.19
Fs		11.68	10.93	14.14	13.46	11.84	11.33	16.11
Ac		1.00	0.85	1.13	1.13	1.03	1.03	2.50

"Point" refers to analysis number or probe position.

Black Rock Point Gabbro

Table 15: BRP-14-006 Pyroxene. Oxides expressed in wt. %

Mineral Point	PX1		PX2		PX3	
	226	231	181	182	195	236
SiO ₂	52.25	51.04	52.57	51.47	52.21	52.76
TiO ₂	0.22	0.53	0.24	0.30	0.30	0.31
Al ₂ O ₃	2.13	2.30	2.45	2.88	2.90	2.33
Cr ₂ O ₃	0.31	0.03	0.28	0.39	0.41	0.35
FeO	9.22	14.32	10.54	10.79	9.29	8.56
MnO	0.30	0.23	0.29	0.24	0.21	0.15
MgO	15.27	14.04	17.02	15.82	17.61	17.66
CaO	19.66	16.94	16.86	17.81	16.94	17.62
Na ₂ O	0.22	0.26	0.23	0.21	0.25	0.25
K ₂ O	0.01	0.00	0.00	0.00	0.00	0.01
NiO	0.00	0.03	0.03	0.01	0.03	0.01
Total	99.58	99.72	100.51	99.91	100.14	100.00
Stoichiometry normalized to 6 oxygens.						
O	6.00	6.00	6.00	6.00	6.00	6.00
Si	1.95	1.93	1.94	1.92	1.92	1.94
Ti	0.01	0.02	0.01	0.01	0.01	0.01
Al	0.04	0.03	0.04	0.04	0.05	0.04
Fe(III)	0.01	0.03	0.02	0.04	0.03	0.02
Cr	0.01	0.00	0.01	0.01	0.01	0.01
Fe(II)	0.28	0.42	0.30	0.30	0.25	0.25
Mn	0.01	0.01	0.01	0.01	0.01	0.00
Mg	0.85	0.79	0.93	0.88	0.97	0.97
Ca	0.79	0.69	0.67	0.71	0.67	0.69
Na	0.02	0.02	0.02	0.01	0.02	0.02
K	0.00	0.00	0.00	0.00	0.00	0.00
Total	4.00	4.01	4.01	4.01	4.01	4.01
Wo	40.34	35.09	34.13	36.50	34.37	35.64
En	43.61	40.48	47.94	45.13	49.71	49.71
Fs	15.24	23.47	17.08	17.60	15.00	13.74
Ac	0.81	0.96	0.85	0.77	0.91	0.90

"Point" refers to analysis number or probe position.

Table 15: Continued

Mineral Point	PX4		PX5		PX6	
	237	242	247	251	252	255
SiO ₂	51.73	52.26	51.87	52.23	51.69	50.73
TiO ₂	0.26	0.31	0.25	0.26	0.33	0.56
Al ₂ O ₃	2.69	2.99	2.73	2.48	2.74	2.61
Cr ₂ O ₃	0.31	0.22	0.34	0.35	0.37	0.05
FeO	9.48	10.02	9.74	9.52	9.18	14.06
MnO	0.17	0.29	0.19	0.25	0.29	0.27
MgO	16.28	16.59	17.89	16.14	17.42	15.10
CaO	18.54	17.58	16.62	18.91	17.55	15.96
Na ₂ O	0.23	0.26	0.20	0.19	0.24	0.21
K ₂ O	0.02	0.02	0.01	0.01	0.02	0.01
NiO	0.03	0.01	0.09	0.04	0.00	-0.03
Total	99.76	100.55	99.92	100.38	99.81	99.53
Stoichiometry normalized to 6 oxygens.						
O	6.00	6.00	6.00	6.00	6.00	6.00
Si	1.92	1.92	1.92	1.93	1.91	1.92
Ti	0.01	0.01	0.01	0.01	0.01	0.02
Al	0.04	0.05	0.04	0.04	0.03	0.03
Fe(III)	0.05	0.03	0.06	0.03	0.06	0.05
Cr	0.01	0.01	0.01	0.01	0.01	0.00
Fe(II)	0.25	0.28	0.24	0.26	0.22	0.39
Mn	0.01	0.01	0.01	0.01	0.01	0.01
Mg	0.90	0.91	0.99	0.89	0.96	0.85
Ca	0.74	0.69	0.66	0.75	0.70	0.65
Na	0.02	0.02	0.01	0.01	0.02	0.02
K	0.00	0.00	0.00	0.00	0.00	0.00
Total	4.01	4.01	4.02	4.01	4.02	4.01
Wo	37.74	35.75	33.52	38.33	35.39	32.90
En	46.12	46.97	50.19	45.54	48.90	43.34
Fs	15.28	16.34	15.56	15.43	14.84	22.98
Ac	0.86	0.95	0.72	0.70	0.87	0.78

"Point" refers to analysis number or probe position.

Table 15: Continued

Mineral Point	PX7		PX8		PX9	
	258	259	260	262	264	268
SiO ₂	51.75	51.08	51.42	51.73	51.76	52.76
TiO ₂	0.26	0.44	0.45	0.34	0.34	0.22
Al ₂ O ₃	2.74	3.53	2.41	2.87	2.70	2.26
Cr ₂ O ₃	0.47	0.49	0.04	0.55	0.34	0.44
FeO	9.46	8.66	12.80	8.97	10.15	8.07
MnO	0.28	0.16	0.34	0.26	0.22	0.23
MgO	16.37	16.39	15.81	16.99	16.23	17.04
CaO	17.93	18.86	16.43	18.15	17.78	18.61
Na ₂ O	0.27	0.24	0.25	0.26	0.22	0.22
K ₂ O	0.01	0.01	0.00	0.00	0.02	0.01
NiO	0.05	0.07	0.07	0.03	0.01	0.06
Total	99.59	99.94	100.01	100.16	99.78	99.92
Stoichiometry normalized to 6 oxygens.						
O	6.00	6.00	6.00	6.00	6.00	6.00
Si	1.92	1.89	1.93	1.91	1.92	1.94
Ti	0.01	0.01	0.01	0.01	0.01	0.01
Al	0.04	0.05	0.03	0.04	0.04	0.04
Fe(III)	0.03	0.06	0.05	0.06	0.03	0.01
Cr	0.01	0.01	0.00	0.02	0.01	0.01
Fe(II)	0.26	0.21	0.35	0.22	0.28	0.24
Mn	0.01	0.01	0.01	0.01	0.01	0.01
Mg	0.91	0.91	0.88	0.94	0.90	0.94
Ca	0.71	0.75	0.66	0.72	0.71	0.73
Na	0.02	0.02	0.02	0.02	0.02	0.02
K	0.00	0.00	0.00	0.00	0.00	0.00
Total	4.01	4.02	4.02	4.02	4.01	4.00
Wo	36.76	38.52	33.46	36.71	36.40	37.83
En	46.70	46.58	44.80	47.83	46.23	48.20
Fs	15.55	14.00	20.82	14.51	16.54	13.16
Ac	0.99	0.89	0.92	0.96	0.83	0.81

"Point" refers to analysis number or probe position.

Table 16: BRP-14-006 Plagioclase. Oxides expressed in wt. %

Mineral	PLAG1		PLAG2		PLAG3		PLAG5		PLAG6	
Point	176	178	186	187	190	191	201	203	204	206
SiO ₂	52.16	51.98	52.25	53.11	53.18	52.05	53.58	53.21	55.35	55.58
TiO ₂	0.00	0.00	0.00	0.00	0.00	0.00	0.00	0.00	0.00	0.00
Al ₂ O ₃	30.33	29.92	28.98	29.23	29.68	30.18	28.89	29.22	26.99	27.63
Cr ₂ O ₃	0.00	0.00	0.00	0.00	0.00	0.00	0.00	0.00	0.00	0.00
FeO	0.74	0.88	1.59	0.96	0.94	0.83	0.90	0.91	1.15	0.65
CaO	13.54	14.02	12.65	12.71	13.21	13.33	12.24	12.28	10.27	10.77
Na ₂ O	3.62	3.33	4.01	4.25	4.08	3.85	4.25	4.33	5.45	5.62
K ₂ O	0.10	0.16	0.19	0.20	0.25	0.13	0.22	0.20	0.30	0.31
MgO	0.00	0.00	0.00	0.00	0.00	0.00	0.00	0.00	0.00	0.00
MnO	0.00	0.00	0.00	0.00	0.00	0.00	0.00	0.00	0.00	0.00
NiO	0.00	0.00	0.00	0.00	0.00	0.00	0.00	0.00	0.00	0.00
Total	100.48	100.29	99.66	100.46	101.34	100.37	100.08	100.15	99.51	100.56
Stoichiometry normalized to 8 oxygens.										
Si	9.45	9.45	9.58	9.63	9.57	9.45	9.72	9.66	10.07	10.01
Ti	0.00	0.00	0.00	0.00	0.00	0.00	0.00	0.00	0.00	0.00
Al	6.48	6.41	6.26	6.24	6.29	6.46	6.18	6.25	5.79	5.86
Fe(II)	0.11	0.13	0.24	0.14	0.14	0.13	0.14	0.14	0.18	0.10
Ca	2.63	2.73	2.48	2.47	2.55	2.59	2.38	2.39	2.00	2.08
Na	1.27	1.18	1.42	1.49	1.42	1.36	1.50	1.53	1.92	1.96
K	0.02	0.04	0.04	0.05	0.06	0.03	0.05	0.05	0.07	0.07
Total	19.96	19.95	20.03	20.02	20.03	20.01	19.96	20.00	20.03	20.08
An	67.01	69.24	62.86	61.57	63.25	65.15	60.63	60.32	50.12	50.52
Ab	32.41	29.81	36.04	37.25	35.32	34.07	38.10	38.53	48.12	47.73
Or	0.59	0.95	1.10	1.18	1.43	0.78	1.27	1.15	1.77	1.75

"Point" refers to analysis number or probe position.

Table 16: Continued

Mineral Point	PLAG7		PLAG8		PLAG9		PLAG10		PLAG11	
	208	209	215	216	218	220	221	225	243	244
SiO ₂	53.95	51.51	55.41	53.25	52.49	51.28	55.33	63.22	50.55	50.97
TiO ₂	0.00	0.00	0.00	0.00	0.00	0.00	0.00	0.00	0.00	0.00
Al ₂ O ₃	28.90	30.17	27.59	29.13	29.50	29.97	28.33	19.65	31.20	30.53
Cr ₂ O ₃	0.00	0.00	0.00	0.00	0.00	0.00	0.00	0.00	0.00	0.00
FeO	0.84	0.61	1.53	0.86	0.81	0.89	0.85	4.33	1.13	1.21
CaO	11.37	13.84	10.41	12.34	13.15	13.65	11.14	0.76	14.84	14.58
Na ₂ O	5.01	3.54	5.18	4.37	4.16	3.68	5.28	10.67	3.26	3.27
K ₂ O	0.27	0.14	0.13	0.23	0.11	0.20	0.27	0.07	0.16	0.10
MgO	0.00	0.00	0.00	0.00	0.00	0.00	0.00	0.00	0.00	0.00
MnO	0.00	0.00	0.00	0.00	0.00	0.00	0.00	0.00	0.00	0.00
NiO	0.00	0.00	0.00	0.00	0.00	0.00	0.00	0.00	0.00	0.00
Total	100.34	99.81	100.25	100.17	100.22	99.66	101.21	98.71	101.14	100.67
Stoichiometry normalized to 8 oxygens.										
Si	9.76	9.41	10.01	9.66	9.54	9.40	9.91	11.49	9.17	9.28
Ti	0.00	0.00	0.00	0.00	0.00	0.00	0.00	0.00	0.00	0.00
Al	6.16	6.49	5.87	6.23	6.32	6.47	5.98	4.21	6.67	6.55
Fe(II)	0.13	0.09	0.23	0.13	0.12	0.14	0.13	0.66	0.17	0.18
Ca	2.20	2.71	2.01	2.40	2.56	2.68	2.14	0.15	2.88	2.84
Na	1.76	1.25	1.81	1.54	1.47	1.31	1.83	3.76	1.15	1.15
K	0.06	0.03	0.03	0.05	0.03	0.05	0.06	0.02	0.04	0.02
Total	20.07	19.99	19.97	20.01	20.04	20.04	20.05	20.29	20.08	20.03
An	54.78	67.85	52.20	60.16	63.18	66.43	53.00	3.78	70.93	70.73
Ab	43.68	31.36	47.01	38.52	36.18	32.41	45.45	95.79	28.17	28.72
Or	1.54	0.79	0.79	1.32	0.64	1.16	1.54	0.44	0.90	0.55

"Point" refers to analysis number or probe position.

Data Analysis

Tables 9 through 16 display geochemical data collected via electron microprobe for samples of: (1) Presque Isle Peridotite, (2) Yellowdog Peridotite (from both the Eagle and Eagle East intrusions), and (3) Black Rock Point Gabbro. Stoichiometry has been calculated for each crystal that was probed, and normalized to the number of oxygens in the chemical formula of that mineral.

End member compositions of each probed mineral were also calculated, and are presented as a molar percentage in tables 9 through 16. This was done according to the procedure outlined by the serc.carleton.edu website by Brady and Perkins. The weight percentage of each oxide was divided by the formula weight of that oxide. Secondly, the resulting "mole number" of each oxide was multiplied by the number of oxygens in the oxide formula. The resulting "oxygen number" of each oxide was then multiplied by a normalization constant (equal to the number of oxygens in the desired formula divided by the sum of the "oxygen numbers"). Finally, the "normalized oxygen numbers" of each oxide were multiplied by the number of cations per oxygen in the oxide formula. Only then could the percentages of each end member, present in each probed crystal, be calculated according to their elemental makeup.

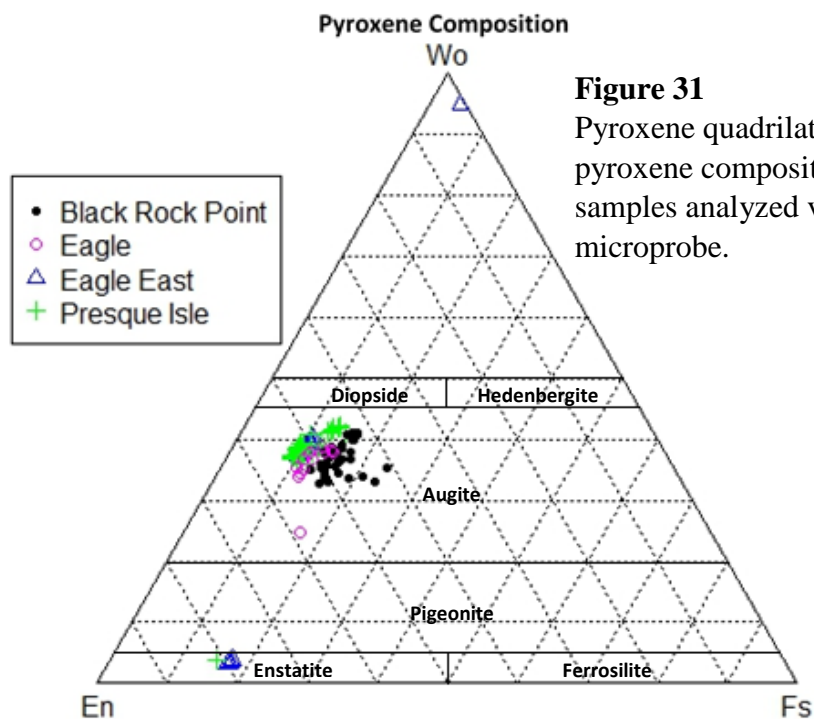
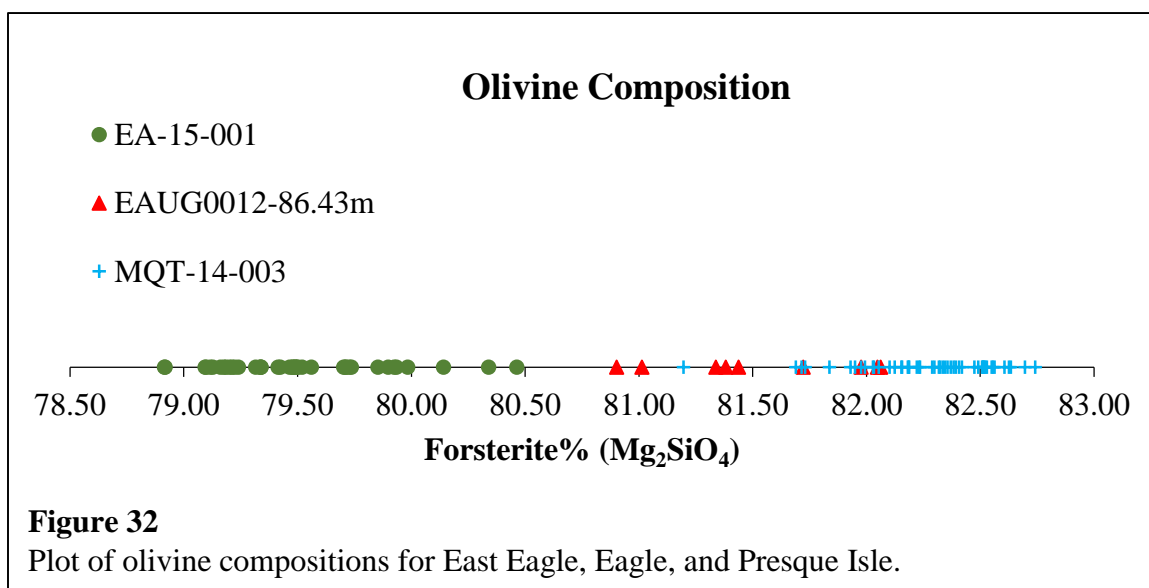


Figure 31
Pyroxene quadrilateral showing pyroxene compositions for all samples analyzed via electron microprobe.

Figure 31 is the ternary diagram known as a “pyroxene quadrilateral”. The diagram displays the distribution of pyroxene compositions for the individual crystals probed in each sample. According to the diagram, all of the probed pyroxenes from Black Rock Point Gabbro, and the majority of those from Eagle, Eagle East, and Presque Isle Peridotites can be identified as augite (a clinopyroxene mineral). Additionally, several probe points from Eagle East, and one from Presque Isle, can be identified as enstatite (an orthopyroxene mineral).

Figure 32 shows the distribution of olivine end member compositions among three samples from East Eagle, Eagle, and Presque Isle. Olivine from all three sites shows a predominately forsteritic composition with East Eagle, or the eastern intrusion of Yellowdog Peridotite showing the highest average fayalite concentration per olivine

crystal probed, and Presque Isle Peridotite showing the lowest. Despite the observed differences in forsterite content, the average end member composition of probed olivines from all three sites fall within a range of less than 4% forsterite. Given the relatively small sampling of probe points from each site, this variation would be expected to decrease further were the sample size to be increased.



CHAPTER V

DISCUSSION

Petrology

All three peridotite units have been observed to exhibit a cumulate texture, consisting of a fabric of interlocking subhedral to euhedral olivine with interstitial spaces filled by pyroxene (or, as in the case of the Yellowdog Peridotite, pyroxene and plagioclase). These three peridotites also exhibit poikilitic texture, in which pyroxene oikocrysts, fully or partially enclose olivine chadacrysts. Both textures are common features of cumulate type peridotite units (Wagner et al., 1960). Therefore it can be assumed that these three peridotite units resulted from fractional crystallization of an intrusive magma, and are not examples of mantle peridotite that was tectonically emplaced.

All three peridotite units display different degrees of serpentinization. Deer Lake Peridotite has been almost entirely serpentinized. Presque Isle Peridotite has been partially to mostly serpentinized depending upon where the unit is sampled. Yellowdog Peridotite displays by far the lowest degree of serpentinization. Serpentinization results from the interaction of high temperature and pressure minerals (such as olivine and pyroxene, which are unstable at near surface conditions) with water and oxygen. Oxidation and hydrolysis reactions occur, resulting in alteration of primary olivine and pyroxene, into secondary serpentine. Differing degrees of alteration may be attributed to: (1) Differences in time since formation, (2) exposure to near surface conditions of temperature and pressure, and (3) variance in the number of episodes, duration, and intensity of these hydrothermal interactions.

Yellowdog Peridotite, in contrast to Marquette County's other two peridotite units, contains a substantial fraction of plagioclase feldspar (primarily as interstitial crystals). Findings of Saper and Yang (2014) suggest that the mineralogy of this unit may result from the "refertilization" of residual peridotite with mafic melt. If the Yellowdog Peridotite is considered to have formed as a cumulate (as concluded above). Any secondary reaction of the peridotite with its remaining parental melt could explain the feldspathic composition of the unit.

In Presque Isle Peridotite, pentlandite and chalcopyrite were observed in association with magnetite. Nickel sulfide is present as the hypogene mineral, pentlandite, not its supergene equivalent, violarite, which is common in hydrothermal deposits, therefore, it is likely that these mineral assemblages are representative of primary magmatic sulfides, hosted within this peridotite unit.

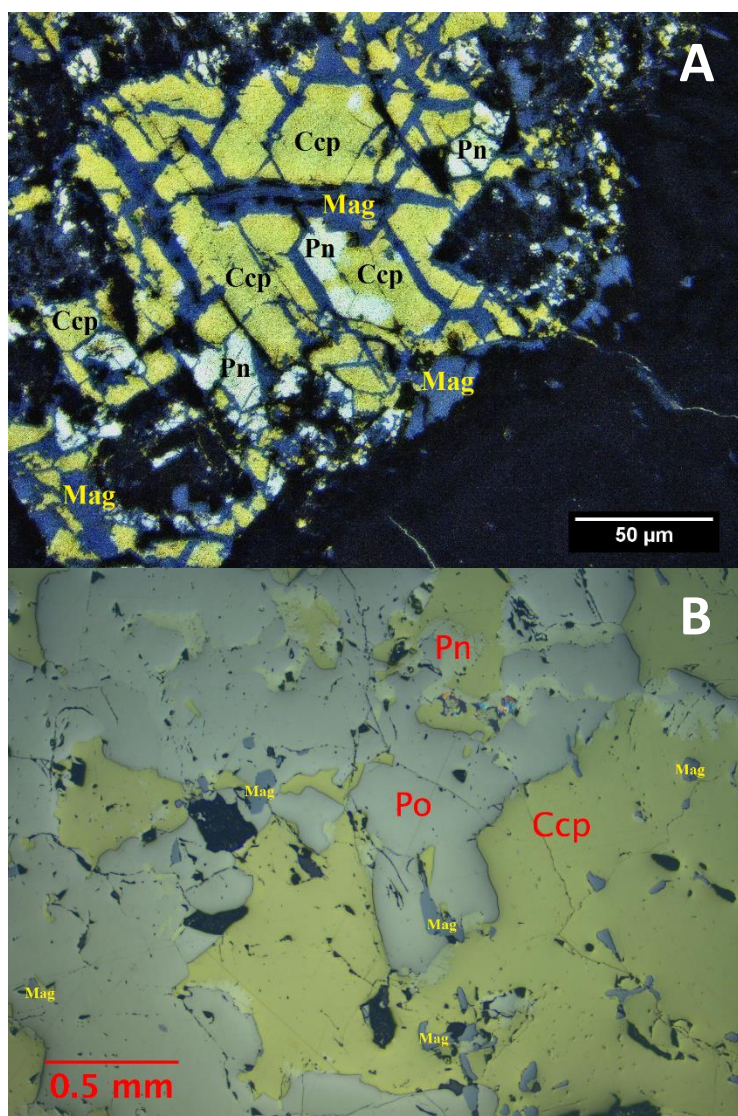


Figure 33
Comparison of sulfides from Presque Isle Peridotite (A) and Yellowdog Peridotite (B).

In Yellowdog Peridotite, pyrrhotite, in addition to pentlandite, and chalcopyrite can be observed in association with magnetite. A comparison of sulfide mineral assemblages from both units can be viewed in Figure 33.

Black Rock Point Gabbro is composed primarily of augite and plagioclase feldspar. The unit also contains only a small percentage of sphene, and no olivine is present. These characteristics allow the major mafic unit found at Black Rock Point to be classified as a gabbro (per the IUGS classification scheme, shown in Figure 34).

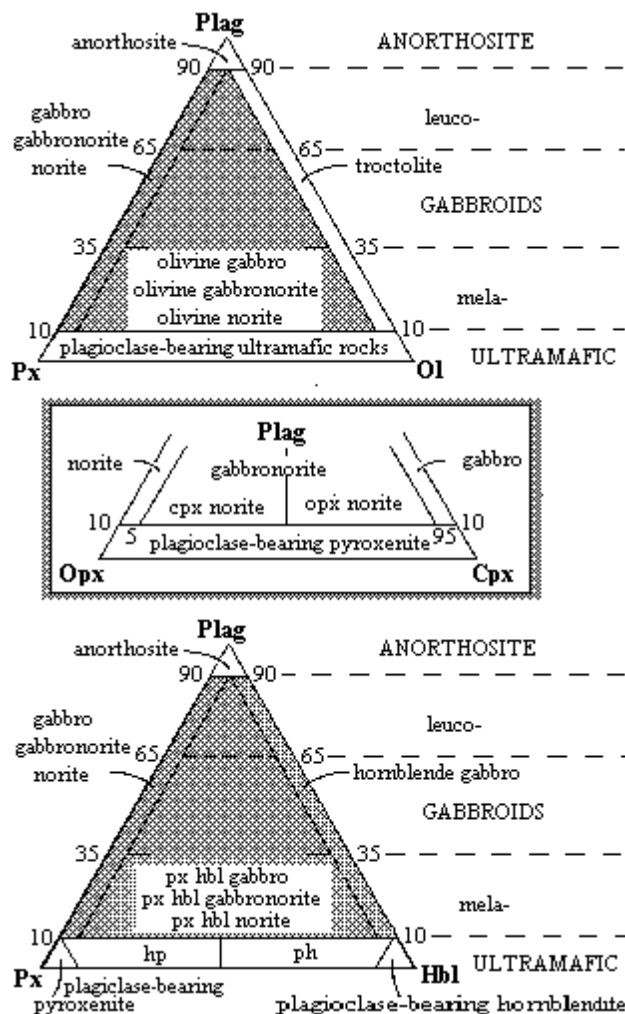


Figure 34
IUGS classification scheme for gabbro.
(Woolley, 1996)

Geological Mapping

Maps of each field area were created using hand drawn field maps based on data collected at each site. These maps were then used in conjunction with previously published maps, for Presque Isle by, Gair and Thaden (1968), and for Deer Lake by, Clark, Cannon, and Klasner (1975). Finally, field maps were digitized using Esri ArcMap software to produce the final maps for each area.

Presque Isle Peridotite

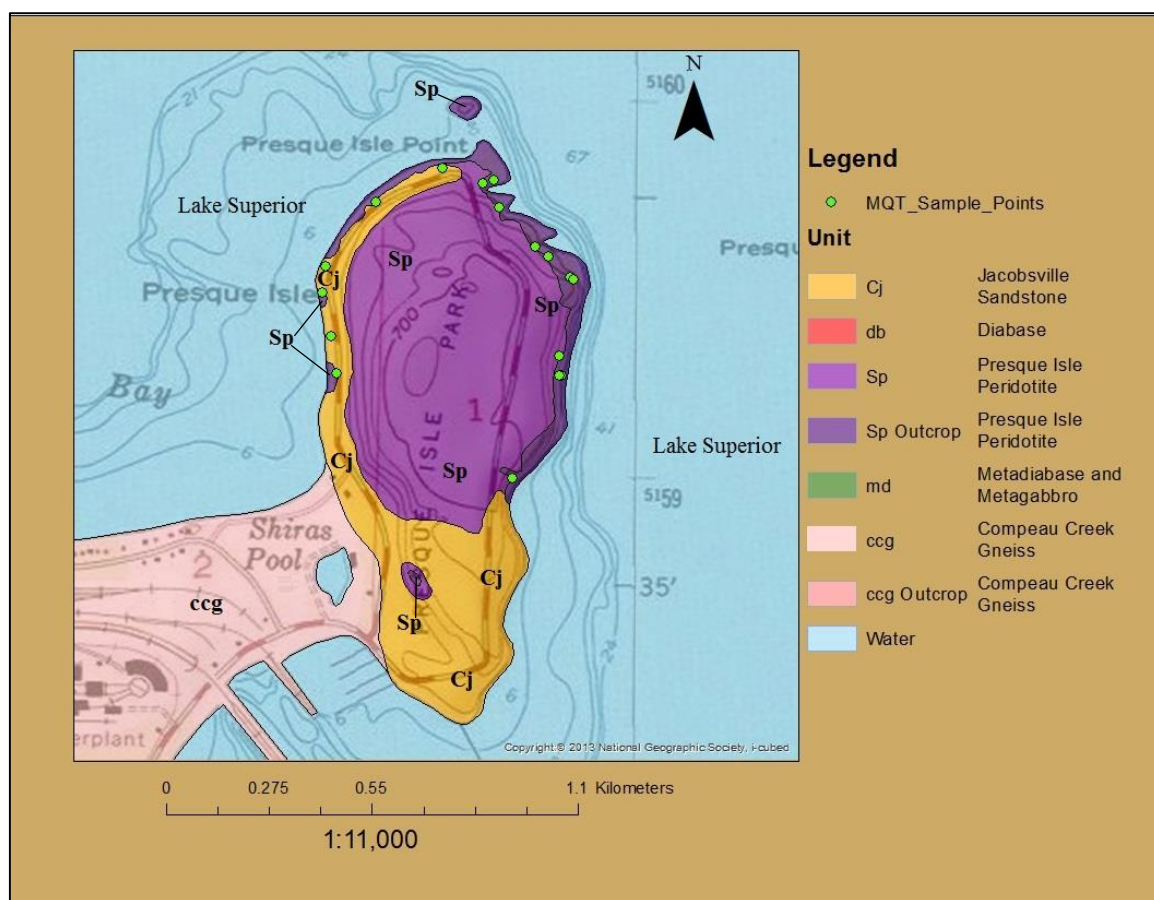


Figure 35
Geological map-Presque Isle.
Adapted from Gair and Thaden (1968).

Deer Lake Peridotite

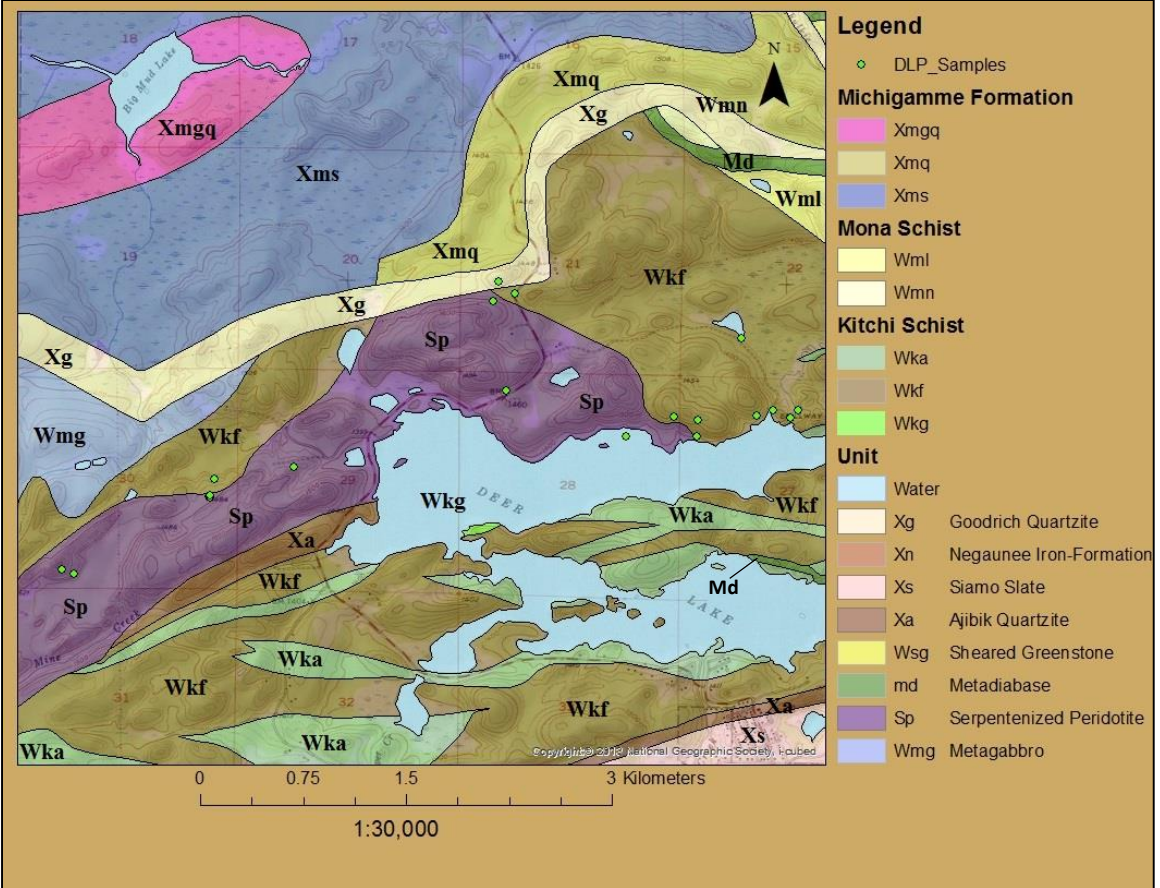


Figure 36
Geological map-Deer Lake area.
Adapted from Clark, Cannon, and Klassner (1975).

Black Rock Point Gabbro

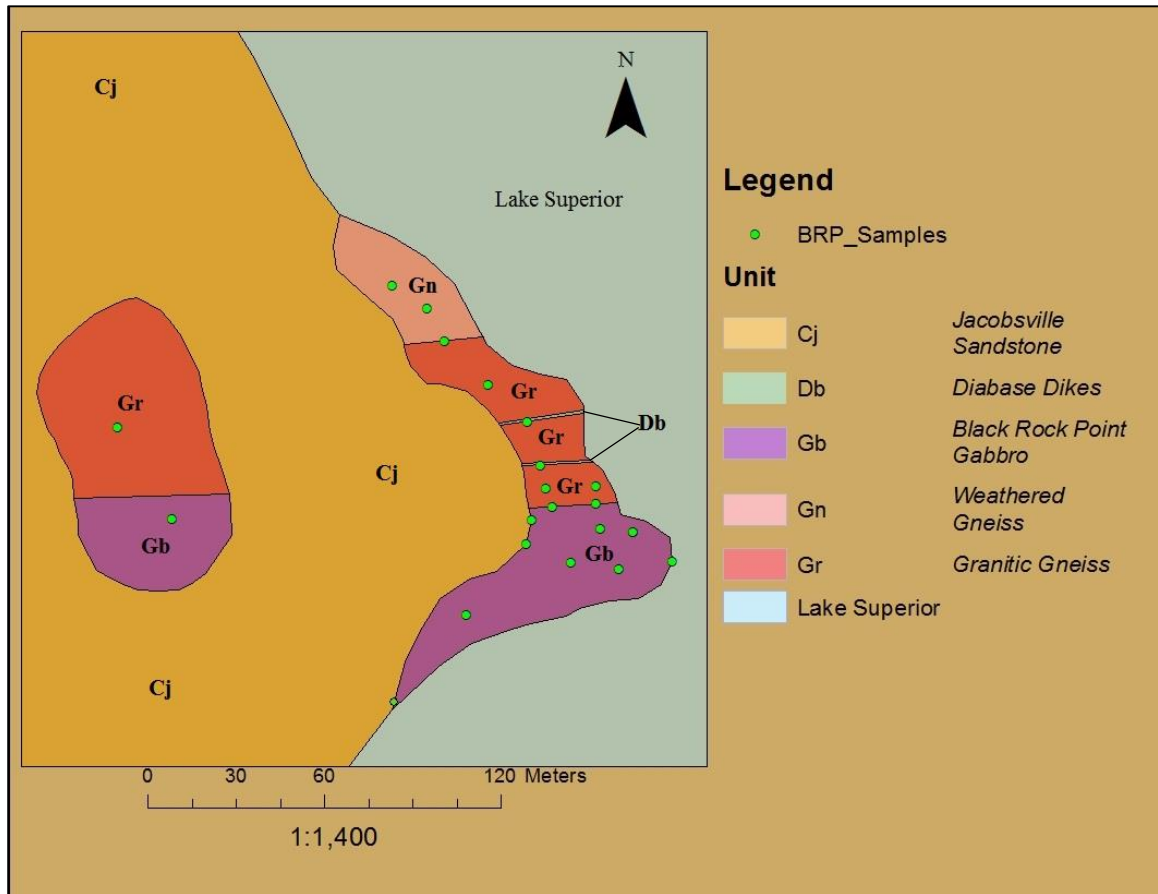


Figure 37

Geological map-Black Rock Point showing sample locations from May 2014 and 2015.

Geochemistry

Electron Microprobe

Olivine Data collected via electron microprobe can be used to determine the MgO/(MgO+FeO) ratio of each crystal's parental magma. The results of these calculations, averaged for each sample, appear in Table 13. According to Tatsumi et al (1983), the MgO/(MgO+FeO) ratio of a parental mantle magma can be expected to fall between 0.63 and 0.73.

Sample	Average MgO/(MgO+FeO)
Presque Isle (MQT-14-003)	0.72
Eagle East (EA-15-001)	0.69
Eagle East (EUG0012-86.43m)	0.71

Major element analysis has revealed that all three peridotite units appear to be anomalously rich in nickel (Table7). This is not surprising in the case of Yellowdog Peridotite. The unit is already observed to host a rich Cu-Ni magmatic sulfide deposit. High nickel concentrations in the other peridotite units may also be due to nickel-rich sulfides. However, the high nickel anomalies may also result from a high concentration of nickel contained in the crystal structure of olivines. This can be determined by using data collected from electron microprobe analysis. Figure 37 displays a plot of Ni-content vs. Forsterite molar percent. This comparison can be used to determine if nickel depletion of olivine, in the presence of an immiscible sulfide liquid, has occurred.

Maier et al. (2015) suggests that intrusions whose olivines show a steep trend from high Fo and Ni toward low Ni content, when plotted in this manner, are prospective. This trend suggests that sulfide segregation has taken place within the intrusion. Any intrusion which contains only Ni depleted olivine suggests that the nickel depletion must have occurred prior to the final emplacement of the intrusive body. There is a low probability that any such body would be able to host a magmatic sulfide deposit.

Ding et al. (2010) used a plot similar to Figure 38, to model olivine compositions from both intrusions of the Yellowdog Peridotite. Crystallization curves were also constructed based on the olivine composition of the Keweenaw, Mamainse Point Formation. This model has been applied to data collected by this study (Figure 37).

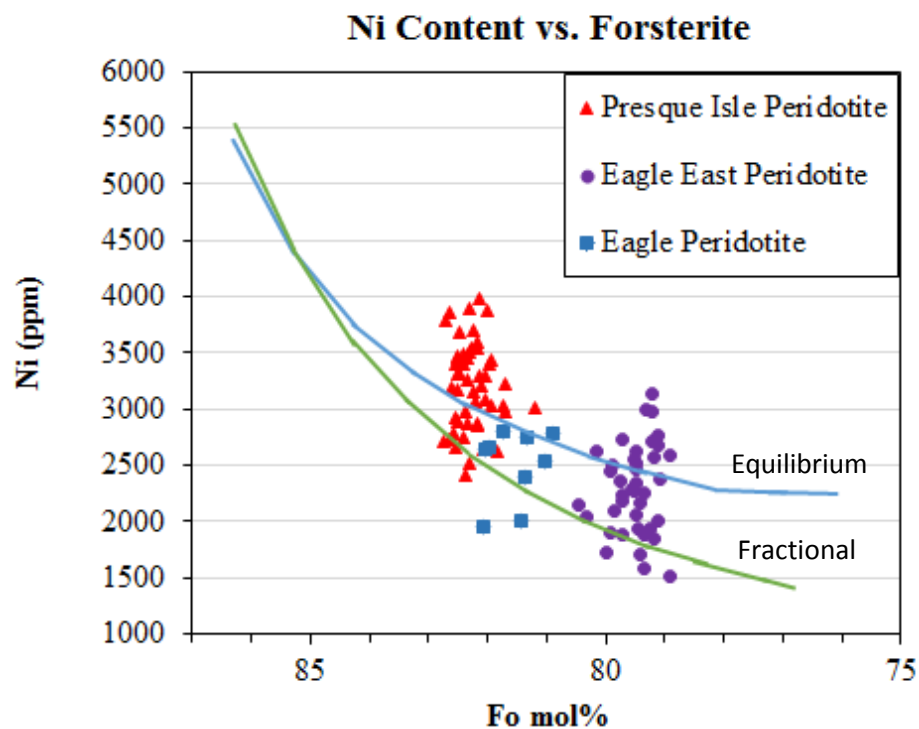


Figure 38

Ni-content vs. Fo mol% plot. After, Ding et al. (2010).

Blue curve: Equilibrium crystallization.

Green curve: Fractional crystallization.

Olivine compositions samples MQT-14-003, EA-15-001, and EUG0012-86.43m which were analyzed using electron microprobe, display a range of nickel contents which spread across both the fractional and equilibrium crystallization curves. Compositions of olivine ranged from high Fo/high Ni, to high Fo/low Ni. Olivine which plotted above the fractional crystallization curve shows Ni enrichment, while those which plot below show Ni depletion.

Similar trends are displayed by all three intrusions. Both Eagle and Eagle East host massive sulfide deposits. This fact, along with the similar Ni/Fo trends of the three intrusions, suggests that these intrusions have all experienced Ni depletion of olivine, in the presence of an immiscible sulfide liquid. Additionally, the findings suggest that Presque Isle Peridotite may also host Ni-Cu-PGE sulfide mineralization, and should be considered prospective. However, the small sample size utilized in cannot be relied upon as a basis for absolute conclusions.

Major and Minor Trace Elements

Figures 39, 40, and 41 compare of all four rock units targeted by this study in terms of minor and trace element composition.

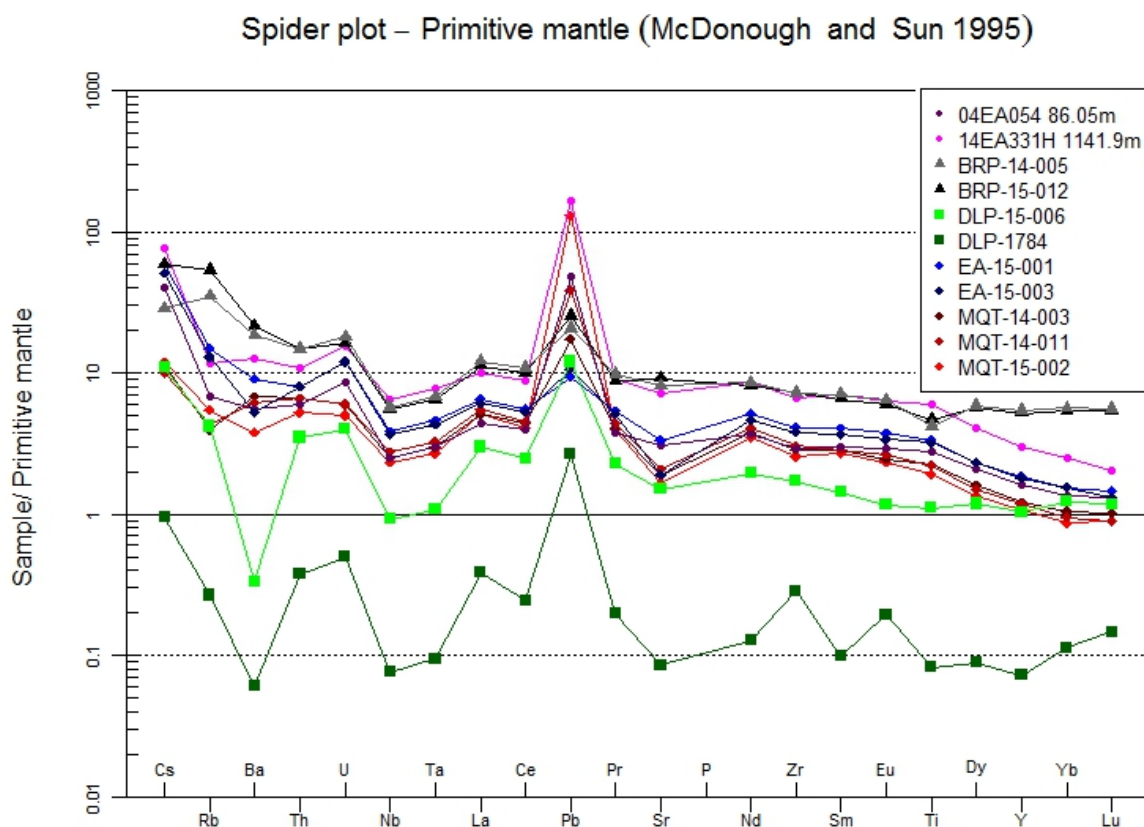
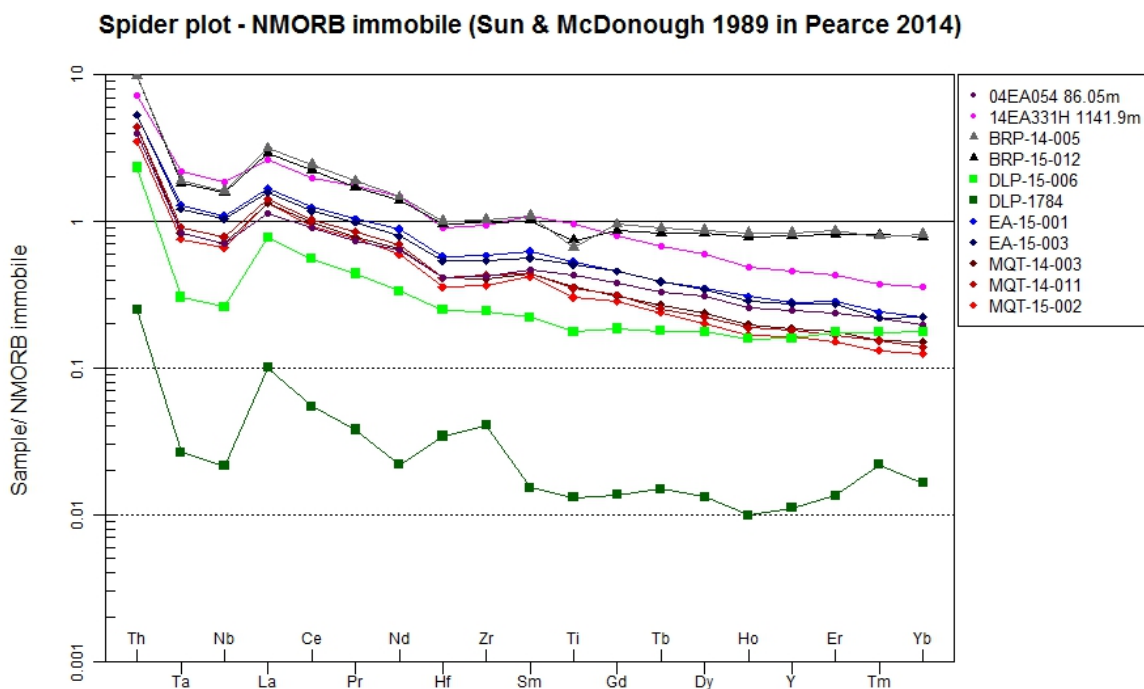


Figure 39

Minor trace element spider plot normalized to primitive mantle.
After McDonough and Sun (1995).

A high degree of variation, in terms of minor trace element composition, seems to exist between samples of Deer Lake Peridotite. When viewing only Figure 39, one might consider this pattern as the product of the extensive alteration which has occurred in the Deer Lake Peridotite. However, when only the immobile elements are considered (as shown in Figure 40) variations continue to be apparent. Type 2 Deer Lake Peridotite (sample DLP-1784) shows enrichment in Hf, Zr, and Tm which is not present in Type 1

Deer lake Peridotite (sample DLP-15-006). Geochemical variations between samples taken from the Deer Lake Peridotite may imply that the unit was not formed by a single magmatic pulse. Formation of this unit may actually have resulted from multiple episodes of magmatic intrusion.



Due to their incompatibility, rare earth elements are particularly useful for identification of a suite of rocks formed as a result of crystal fractionation (Nelson, 2012). Such a suite should plot as a group of nearly parallel lines showing varying degrees of rare earth element enrichment. Figure 41 shows a data plot for these elements. Four distinct suites can be identified on this graph. Samples of Black Rock Point Gabbro appear to plot as one suite at the top of the graph. Samples of Type 1 and Type 2 Deer

Lake Peridotite plot as two separate suites. Samples of both Presque Isle Peridotite and Yellowdog Peridotite plot as a fourth suite of seven nearly parallel lines.

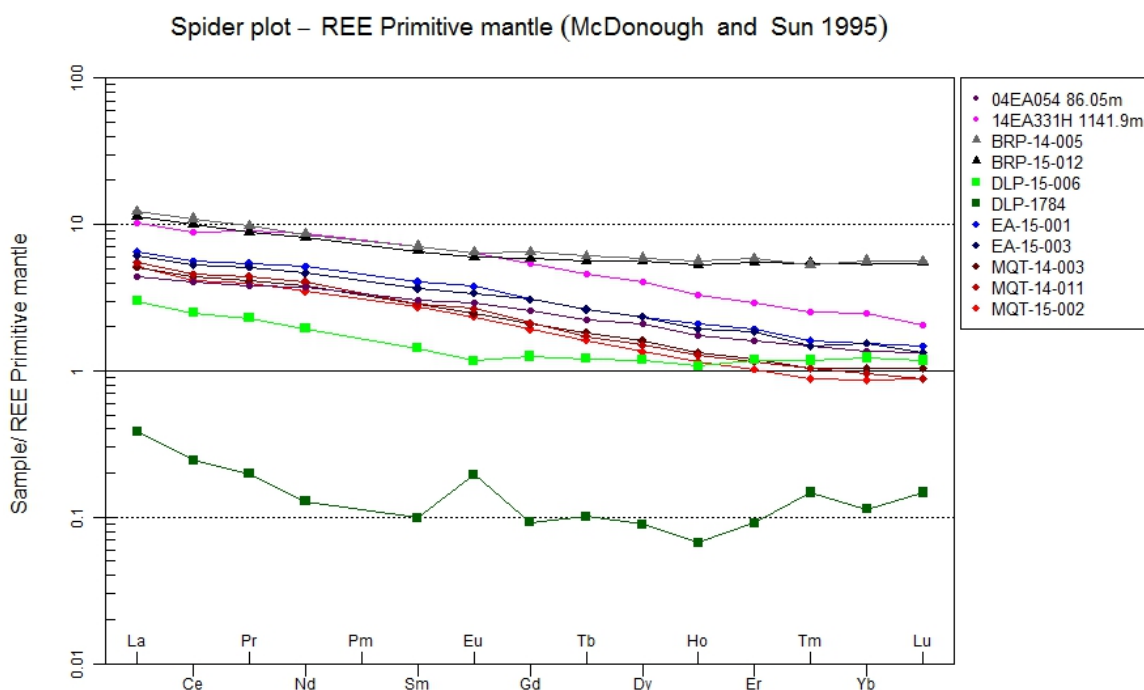


Figure 41

Rare earth element spider plot. After McDonough and Sun (1995).

The suite discussed (Black Rock Point Gabbro) was entirely composed of multiple samples from a single unit; therefore, their geochemical relationship is expected. Trace element variation between Type 1 and Type 2 Der Lake Peridotite is not entirely unexpected, and may constitute additional evidence suggesting that this unit was formed by two separate magmatic events. The Nearly identical trends displayed by samples from both Eagle, and Presque Isle are significant. The geochemical similarity between these units is not isolated to rare earth elements, but can also be observed in both Figure 39 and Figure 40. There is a clear geochemical relationship in terms of minor-trace elements

between these two rock units. This similarity exists despite the fact that the dates of formation for these units are conventionally thought to be nearly 1 billion years apart.

Geotectonic Proxies

Two geotectonic proxies were applied to the geochemical data in an effort to determine the origin of each unit. These are the Th-Nb proxy for crustal input and the Ti-Yb proxy for melting depth. This was conducted according to the methodology established by Pearce (2008). The proxies are based on the following principles which can be observed by plotting a range of samples on a MORB normalized trace element similar to Figure 38. These proxies function according to the following principles (shown visually in Figure 42).

(1) Crustal contamination of a mafic melt by continental lithosphere will result in selective Th and LREE enrichment and thus negative Nb anomalies. This allows for the use of Th-Nb as a proxy for crustal input. Such an Nb

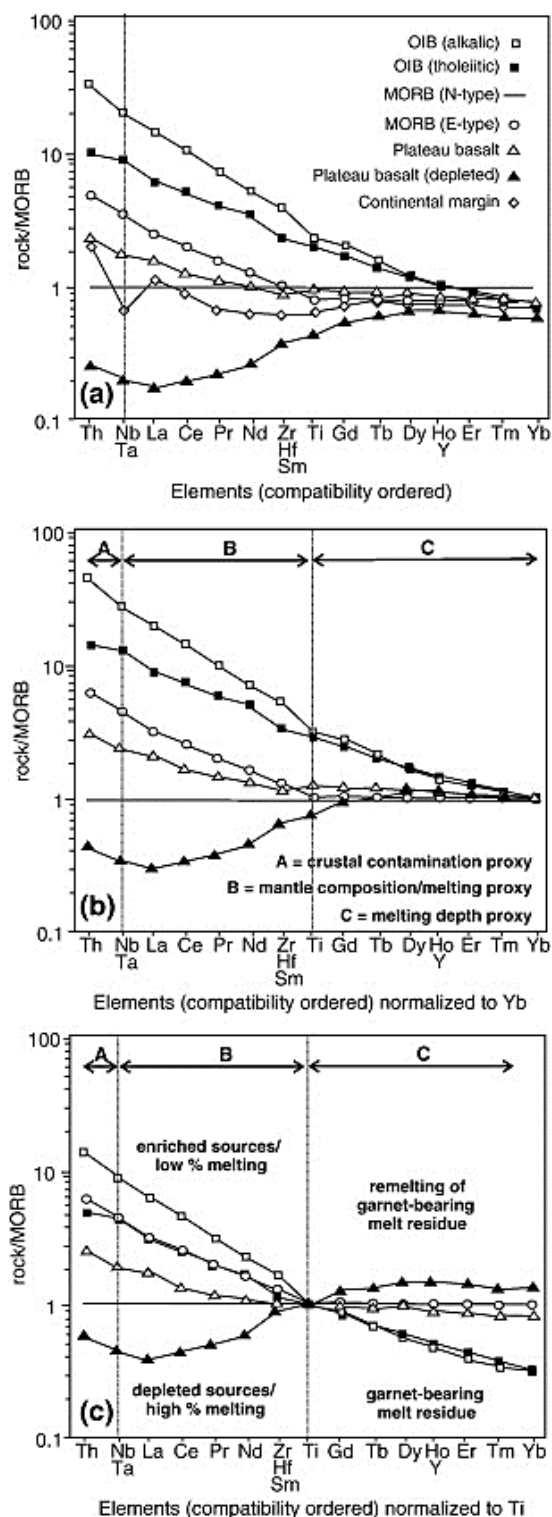


Figure 42

Visual explanation of Th-Nb, Nb-Ti, and Ti-Yb proxy indicators. From Pearce (2008).

depletion can be observed for all samples in Figure 39.

(2) Source and melting effects result in Nb-Ti gradients. Nb-Ti gradients are indicative of incompatible enrichment which cannot be explained by HREE compatibility in garnet.

This gradient increases from tholeiitic to alkalic compositions.

(3) Presence of garnet residue will result in negative Ti-Yb gradient. Ti and Yb are partitioned similarly in spinel peridotite, while Yb is much more strongly partitioned into garnet. This allows for Ti/Yb to be used as a proxy for melting depth.

Figure 43 and Figure 44 display ratio plots designed to highlight crustal input, and melting depth proxies by focusing on Yb normalized ratios (refer to Figure 42b). Figure 43 is an Nb/Yb-Th/Yb plot based on Pearce (2008). This diagram is a graphical representation of the Th-Nb crustal input proxy. Present day MORB and OIB form a diagonal array with average N-MORB, E-MORB, and OIB at its center. This array contains >98% of analyzed oceanic basalts. Melts which have interacted with continental crust during ascent, display higher Th/Yb values (Pearce, 2008). Samples from all four research areas plot above the diagonal array. This indicates that the melts from which they formed were subjected to crustal contamination either during their intrusion, or as the result of subduction related input prior to crystallization of each, individual unit.

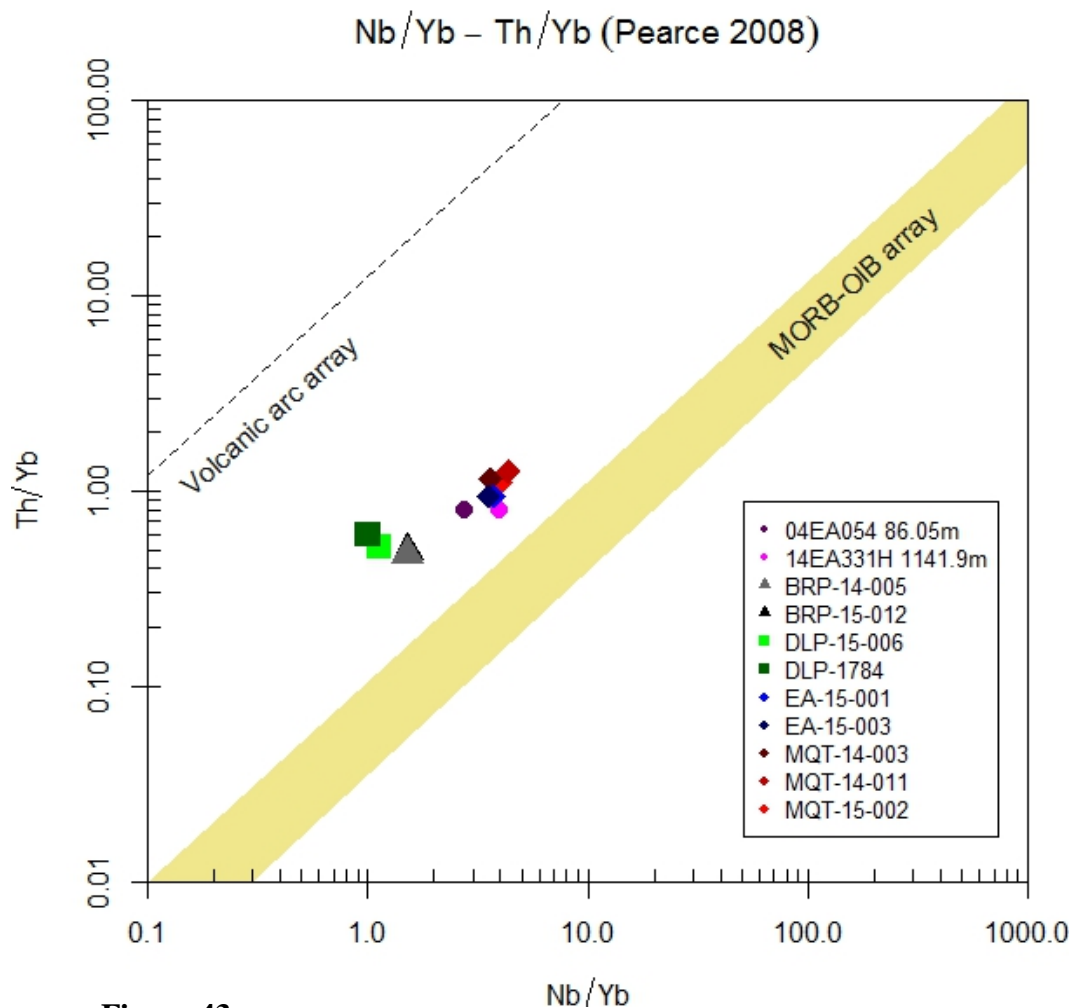
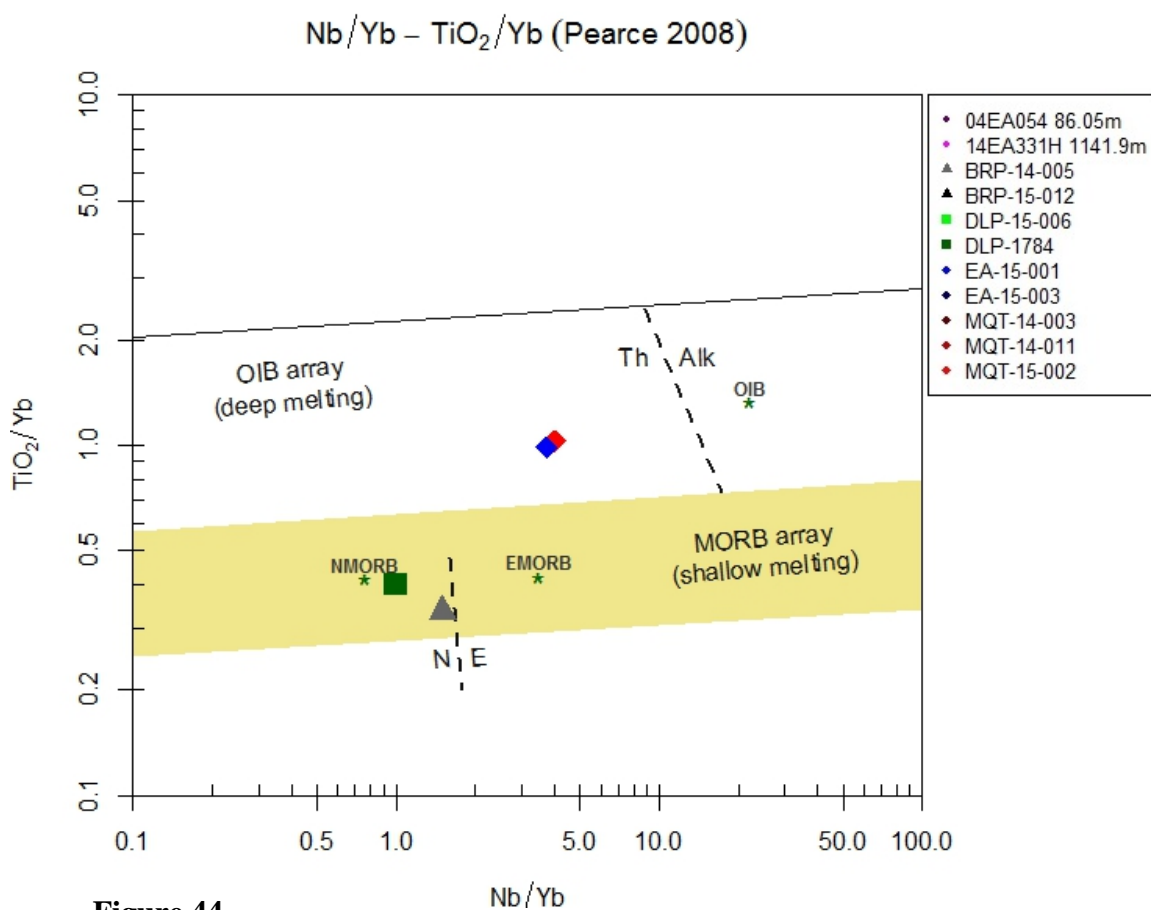


Figure 43
Nb/Yb-Th/Yb plot. Ratio plot highlighting Th-Nb proxy.

Figure 44 is a $\text{TiO}_2/\text{Yb-Nb}/\text{Yb}$ plot based on Pearce (2008). This plot is a graphical representation of the Ti-Yb melting depth proxy. TiO_2/Yb values which plot above the MORB array are indicative of melting which has occurred beneath thicker lithosphere. Data acquired from samples taken from each research area in this study are included on this plot. These data split into two distinct groupings. Both Deer Lake Peridotite and Black Rock Point Gabbro plot within the shallow melting array. Samples

of Yellowdog Peridotite and Presque Isle Peridotite Plot with in the deep melting zone as indicative of their elevated TiO_2/Yb values.



The environment of formation for each unit can be proposed when both the Th-Nb crustal input proxy and the Ti-Yb melting depth proxy are considered. Samples of both Deer Lake Peridotite and Black Rock Point Gabbro display elevated Th/Yb values indicating of crustal contamination of their parental magmas. However, neither unit displays elevated TiO_2/Yb values. This suggests that both are products of shallow melting. The parental melts of these units were most likely formed as a result of shallow dipping ocean-ocean or ocean-continent subduction. Samples of Yellowdog Peridotite

and Presque Isle Peridotite display elevated Th/Yb values indicating crustal contamination. Elevated TiO_2/Yb indicative of deep melting is also present in both units. Evidence, in this case, suggests that parental magmas were probably formed as a result of plume-initiated melting deep beneath the continental lithosphere. When the melts intruded through the upper mantle and continental crust, they became contaminated, prior to their crystallization.

Conclusion

Deer Lake Peridotite

Mineralogical compositions and textural characteristics of Deer Lake Peridotite are similar to those observed in the Presque Isle Peridotite and Yellowdog Peridotite. Prior to alteration, the unit's mineralogical composition was dominated by olivine and pyroxene. This rock type displays a cumulate texture in some cases, a poikilitic texture in which pyroxene oikocrysts enclose olivine chadacrysts is also present. However these similarities are not sufficient to conclude that this unit shares a common origin with either of the other peridotite units. Also, it is noteworthy that the degree of serpentinization and hydrothermal alteration observed in the Deer Lake Peridotite is different, being far greater than that observed in either of Marquette County's other peridotite units.

Geochemical comparison of Deer Lake Peridotite with the other three units addressed in this study reveals obvious differences in chemical composition. Geochemical analysis also reveals that the Deer Lake Peridotite crystallized from a

magma which formed as a result of shallow melting; whereas, the parent magmas of Presque Isle Peridotite and Yellowdog Peridotite formed as a result of deep melting.

Truncation of the Deer Lake Peridotite along its south-western margin by the Great Lakes Tectonic Zone suggests that the unit must have been formed either during, or prior to the formation of the GLTZ (2.7-1.85 Ga). This window of time for this formational event proves that the Deer Lake Peridotite predates the Yellowdog Peridotite's age (1.1 Ga) by no less than 750 Ma.

Trace element, and petrographic analysis also suggests that Deer Lake Peridotite may actually represent two separate peridotite units emplaced during two separate events. Type 2 Deer Lake Peridotite displays foliation which is not present in Type 1 Deer Lake Peridotite. Possibly, Type 2 Deer Lake Peridotite was emplaced early in the formation of the GLTZ, and later deformed during the Penokean Orogeny (1.86-1.83 Ga), with Type 1 crystallizing during this later compressive phase. Bornhorst et al. (1993) postulated that the Deer Lake Peridotite may represent the subvolcanic base of the Mona Formation. Deer Lake Peridotite also appears to be associated with the metavolcanics of the Kitchi Formation. It is possible that these successive metavolcanic units may correspond to the two ultramafic units of Deer Lake Peridotite.

Based on geochemical analysis, in conjunction with the geologic setting of the Deer Lake Peridotite, it is reasonable to conclude that the Deer Lake Peridotite was formed independently, and substantially earlier, than Presque Isle Peridotite and Yellowdog Peridotite. It is likely that this unit crystallized from a parent magma which resulted from shallow melting during the formation of the Great Lakes Tectonic Zone.

Black Rock Point Gabbro

Petrological comparison of Black Rock Point Gabbro with the other three units addressed by this study yielded little similarity. Unlike Marquette County's three peridotite units, Black Rock Point Gabbro contains no olivine. The unit's primary minerals include augite and plagioclase feldspar, with small amounts of sphene. Additionally, no shared textural characteristics were identified between the Black Rock Point Gabbro, and any of the Marquette County peridotites.

Geochemical comparison of Black Rock Point Gabbro with the Marquette County Peridotites reveals a substantially different minor trace element signature. Geochemical analysis also leads to the conclusion that the unit crystallized from a parent melt which resulted from shallow melting before becoming contaminated by crustal material. This environment of formation suggests it is likely that the Black Rock Point Gabbro also dates from the formation of the Great Lakes Tectonic Zone (2.7-1.85 Ga).

Due to the limited extent of the Black Rock Point Gabbro's outcrop, very little can be concluded based on its geologic setting. It does intrude the Late-Archean granite of the "Northern Complex", and it is overlain by the Jacobsville Sandstone nonconformably.

Based on petrographic analysis, no relationship can be established between the Black Rock Point Gabbro and the other three units addressed in this study. Although geochemical analysis suggests that both the Black Rock Point Gabbro and Deer Lake Peridotite crystallized from parent melts formed under similar circumstances, their

substantially different geochemical compositions give no indication that these melts were similar or directly related.

Presque Isle Peridotite and Yellowdog Peridotite

Presque Isle Peridotite and Yellowdog Peridotite, upon first examination, appear to be very different units. Presque Isle Peridotite is more finely grained, and lacks visible plagioclase feldspar crystals, such as those observed in the Yellowdog Peridotite. Presque Isle Peridotite has also undergone a notably higher degree of serpentinization, as is evidenced by a greater density of hydrothermal veins.

Additional examination also reveals that primary mineral assemblages in both units include a large fraction of olivine. Pyroxene, mostly in the form of augite, with a much smaller fraction of enstatite, also constitutes a substantial fraction of both units. They both display a cumulate texture. Additionally, a poikilitic texture in which rounded olivine chadacrysts are partially, or fully enclosed by pyroxene oikocrysts can be observed in both the Presque Isle Peridotite and Yellowdog Peridotite. Petrographic analysis of both units also reveals olivine hosted sulfide inclusions. Such inclusions may indicate the presence of an immiscible sulfide liquid at the time of crystallization.

Geochemical comparison of the Presque Isle Peridotite and Yellowdog Peridotite indicates that both formed from a parent melt of mantle origin, and became contaminated by crustal material prior to crystallization. Minor trace element analysis of the two units, reveals that they share a very similar geochemical composition. Samples from both sites plot as a tightly spaced group of nearly parallel lines (Figures 39, 40, and 41).

Limited outcrop exposure of the Yellowdog Peridotite, and the lack of accessibility to host rock contacts at the Presque Isle Peridotite, make it difficult to draw conclusions based strictly on geologic setting relationships at both sites. However, Yellowdog Peridotite has intruded through the Late-Archean granite basement of the “Northern Complex”, and Paleoproterozoic sediments of the Baraga Basin (as confirmed by the exploration teams of both Kennecott and Lundin Mining). Ding et al. (2010), by the use of U-Pb baddeleyite dating, has confirmed that this unit crystallized at 1107.2 ± 5.7 Ma. This date allows for the reasonable conclusion that the Yellowdog Peridotite formed during the Midcontinent Rift event. The only unit which has been observed in direct contact with the Presque Isle Peridotite is the uppermost member of the Keweenawan series, the Jacobsville Sandstone. Here, it is clear that Presque Isle Peridotite is nonconformably overlain. Radiometric dating of zircons from Jacobsville Sandstone confirms that the unit is no younger than 960 Ma (Malone et al., 2015). Observation of the peridotite’s contacts with other units is not possible because they are concealed beneath Lake Superior. However, it can be safely assumed that the Presque Isle Peridotite has also intruded through the Archean granite basement of the “Northern Complex”. No geochronological dates have ever been obtained for the Presque Isle Peridotite.

In summary, Presque Isle Peridotite and Yellowdog Peridotite share similar mineralogical and textural characteristics. Geochemical analysis reveals that both units crystallized from parent magmas of a mantle origin, which were contaminated by crustal material during their intrusion and prior to crystallization. Analysis of minor trace

elements also reveals that the units share a very similar chemical signature, and can easily be classified as a single suite of rocks.

The findings also suggest the possibility that the Presque Isle Peridotite may also date to the Mesoproterozoic, at which time, it may have been formed contemporaneously with the Yellowdog Peridotite, during the early stages of the Midcontinent Rift event (1.1 Ga). Geochemical similarities between these units also suggest the likelihood that the plume induced, parent melts of both units were very similar, and may have been directly related.

Presque Isle Peridotite is shown to display the following: (1) High nickel content, comparable to that of the Yellowdog Peridotite (as shown by XRF analysis). (2) Sulfide inclusions within olivine. (3) Primary magmatic sulfide assemblages of chalcopyrite and pentlandite. (4) Incompatible element enrichment. Comparison of Ni content with Fo molar percentage, also yields results similar to those observed in both the “Eagle” and “Eagle East” intrusions of Yellowdog Peridotite. All these factors make Presque Isle Peridotite a prime target for future exploration, as they suggest the possibility that the unit has the potential to host magmatic sulfide deposit similar to those hosted by both intrusions of the Yellowdog Peridotite. It can be concluded from the available data, that peridotite units of Keweenawan age, located in the Lake Superior region should be considered high priority targets for magmatic sulfide exploration.

Future Work

Geochronologic analysis of Presque Isle Peridotite should be the top priority. If age dates can be obtained using U-Pb baddeleyite dating, as was accomplished for the Yellowdog Peridotite, the debate over the age of the Presque Isle Peridotite can finally be put to an end. Dates returned will greatly solidify any concepts concerning the origin of the Presque Isle Peridotite.

Additional geochemical analysis should also be conducted using XRF and ICP-MS for both Presque Isle Peridotite and Yellowdog Peridotite. This new data should be combined with data developed in this study, in an effort to determine if the geochemical similarity between Presque Isle Peridotite and Yellowdog Peridotite can be further supported by a larger, more statistically valid, sample size.

Expanded electron microprobe studies of Presque Isle Peridotite should also be undertaken. Additional data from a wide range of samples will allow for improved modeling of nickel depletion currently observed in olivines of Presque Isle Peridotite. This will allow for a better assessment of this unit as a potential magmatic sulfide host.

Sulfur isotope analysis of primary magmatic sulfides from Presque Isle Peridotite and Yellowdog Peridotite should be conducted. This analysis would allow for the origin of sulfur to be determined for these sites.

Metallic ore bodies are associated with significant magnetic anomalies. Aeromagnetic surveys played a role in the discovery of the Eagle magmatic sulfide deposit, hosted within the Yellowdog Peridotite, and have continued to be employed by subsequent exploration efforts in the area. Aeromagnetic survey data which includes the

Presque Isle area has never been made publically available. Analysis of Presque Isle Peridotite's associated magnetic anomaly would not only help to define the most promising locations for magmatic sulfide exploration, but would also reveal the full extent of the unit, which is concealed beneath Lake Superior.

References

- Blatt, Harvey, Tracy Robert J., and Brent E. Owens, 2006, *Petrology: Igneous, Sedimentary and Metamorphic*. New York: Freeman.
- Bornhorst, T. J. and R. C. Johnson, 1993, *Geology of Volcanic Rocks in the South Half of the Ishpeming Greenstone Belt, Michigan*. United States Geological Survey. USGS Publication Warehouse.
- Brady, John, and Dexter Perkins, 2015, "Mineral Formulae Recalculation." *Teaching Phase Equilibria*.
http://serc.carleton.edu/research_education/equilibria/mineralformulaerecalculation.html.
- Case, James and Gair, Jacob, 1965, *Aeromagnetic Map of Parts of Marquette, Dickinson, Baraga, Alger, and Schoolcraft Counties, Michigan, and Its Geologic Interpretation*. United States Geological Survey. USGS Publication Warehouse.
- Clark, Lorin D., William F. Cannon, and J. S. Klasner., 1975, *Bedrock Geologic Map of the Negaunee SW Quadrangle, Marquette County, Michigan*. United States Geological Survey. USGS Publication Warehouse.
- Coleman, R. G., 1977, *Ophiolites*. Berlin, Heidelberg, New York: Springer-Verlag.
- Dilek, Yildirim, 2003, "Ophiolite Concept and Its Evolution." *Ophiolite Concept and the Evolution of Geological Thought*. Vol. Special Paper 373. Geological Society of America. 1-14.
- Ding, Xin, Chusi Li, Edward M. Ripley, Dean Rossell, and Sandra Kamo, 2010, "The Eagle and East Eagle Sulfide Ore-bearing Mafic-ultramafic Intrusions in the Midcontinent Rift System, Upper Michigan: Geochronology and Petrologic Evolution." *Geochemistry Geophysics Geosystems* 11.3.
- Dunlop, Matthew, 2013, *The Eagle Ni-Cu-PGE Magmatic Sulfide Deposit and Surrounding Mafic Dikes and Intrusions in the Baraga Basin, Upper Michigan: Relationships, Petrogenesis, and Implications for Magmatic Sulfide Exploration*. Thesis. Indiana University, Department of Geological Sciences.
- Evans, B. W., 1977, "Metamorphism of Alpine Peridotite and Serpentinite." *Annu. Rev. EarthPlanet. Sci. Annual Review of Earth and Planetary Sciences* 5.1: 397-447.

- Foose, Michael P., Michael L. Zientek, and Douglas P. Klein, 1996, "Chapter 4: Magmatic Sulfide Deposits.". Reliminary Compilation of Descriptive Geoenvironmental Mineral Deposit Models. Ed. Edward A. Du Bray. United States Geological Survey. USGS Publication Warehouse.
- Gair, Jacob Eugene, and Robert E. Thaden, 1968, Geology of the Marquette and Sands Quadrangles, Marquette County, Michigan. United States Geological Survey. USGS Publication Warehouse.
- Janoušek, V., Farrow, C. M. & Erban, V., 2006, Interpretation of whole-rock geochemical data in igneous geochemistry: introducing Geochemical Data Toolkit (GCDkit). *Journal of Petrology* 47(6):1255-1259.
- King, H., 2016, Peridotite: Igneous Rock - Pictures, Definition & More. *Geology.com*. Retrieved 17 February 2016. <http://geology.com/rocks/peridotite.shtml>
- Klasner, J.S., 1979, The Yellowdog Peridotite and a Possible Buried Igneous Complex of Lower Keweenaw Age in the Northern Peninsula of Michigan. State of Michigan, Dept. of Natural Resources, Geological Survey Division.
- Lantz, Rik E, 1982, The Presque Isle Serpentinized Peridotite a Chemical and Petrographic Study. Thesis. University of Illinois at Urbana-Champaign.
- Lewan, Michael Donald, 1972, Metasomatism and Weathering of the Presque Isle Serpentinized Peridotite, Marquette, Michigan. Thesis. Michigan Technological University.
- Maier, Wolfgang D., Raimo Lahtinen, and Hugh O'Brien, 2015, "Litho-geochemistry." *Mineral Deposits of Finland*. Elsevier.
- Malone, David H., Carol A. Stein, John P. Craddock, Jonas Kley, Seth Stein, and John Malone, 2015, "Maximum Depositional Age of the Neoproterozoic Jacobsville Sandstone, Michigan: Implications for the Evolution of the Midcontinent Rift." *Jacobsville/MCR*. Illinois State University. <http://www.earth.northwestern.edu/people/seth/Texts/mcrfail.pdf>
- Marquette County Map Tour Lakes Snowmobile ATV River Hike Hotels Motels Michigan Interactive™. Marquette County Map Tour Lakes Snowmobile ATV River Hike Hotels Motels Michigan Interactive™, 2014, <http://www.fishweb.com/maps/marquette/>

- Mineralogical Spreadsheet Download Page, 2015, Gabbrosoft Mineralogical Spreadsheet. gabbrosoft.org/spreadsheets.html
- Naldrett, A. J., 1999, "World-class Ni-Cu-PGE Deposits: Key Factors in Their Genesis." *Mineralium Deposita* 34.3: 227-40.
- Naldrett, A. J., 2004, *Magmatic Sulfide Deposits: Geology, Geochemistry and Exploration*. Berlin: Springer.
- Nelson, Stephen A, 2012, "Magmatic Differentiation." Tulane University. <http://www.tulane.edu/~sanelson/eens212/magmadiff.htm>
- Owen, M. L., and L. H. Meyer, 2013, Lundin Mining Corporation NI 43-101 Technical Report on the Eagle Mine, Upper Peninsula of Michigan. Wardell-Armstrong.
- Pearce, Julian A, 2008, "Geochemical Fingerprinting of Oceanic Basalts with Applications to Ophiolite Classification and the Search for Archean Oceanic Crust." *Lithos* 100.1-4: 14-48. Science Direct.
- Pracejus, Bernhard, 2008, *The Ore Minerals under the Microscope: An Optical Guide*. Amsterdam: Elsevier Science. Elsevier Science.
- Richard Van Hise, William Bayley, and Henry Lloyd Smyth, 1895, Preliminary Report on the Marquette Iron-bearing District of Michigan. Washington, Govt. print. off.
- Rose, Bill, 1999, "Age of Jacobsville SS." Age of Jacobsville Sandstone. Michigan Tech University. <http://www.geo.mtu.edu/KeweenawGeoheritage/Sandstone/Age.html>.
- Rossell, Dean and Coombes, Steven, 2005, *The geology of the Eagle Nickel-Copper Deposit Michigan, USA*. Kennecott Minerals Co. Kennecott Minerals Co.
- Saper, Lee, and Yan Liang, 2014, "Formation of Plagioclase-bearing Peridotite and Plagioclase-bearing Wehrlite and Gabbro Suite through Reactive Crystallization: An Experimental Study." *Contributions to Mineralogy and Petrology* 167.3.
- Schmus, W. Van, 1985, "The Midcontinent Rift System." *Annual Review of Earth and Planetary Sciences* 13.1: 345-83.

- Schulz, Klaus J., Val W. Chandler, Suzanne W. Nicholson, Nadine Piatak, Robert R. Seal, II, Laurel G. Woodruff, and Michael L. Zientek, 2010, Magmatic Sulfide-Rich Nickel-Copper Deposits Related to Picrite and (or) Tholeiitic Basalt Dike-Sill Complexes: A Preliminary Deposit Model. Rep. no. 2010-1179. United States Geological Survey. USGS Publication Warehouse.
- Sims, P. K., and W. C. Day, 1993, The Great Lakes Tectonic Zone-Revisited. Rep. no. 1904-S. United States Geological Survey. USGS Publication Warehouse.
- Sims, P.K., 1991, Great Lakes Tectonic Zone in Marquette Area, Michigan Implications for Archean Tectonics in North-Central United States. Rep. no. 1904-E. N.p.: United States Geological Survey. USGS Publication Warehouse.
- Stein, Carol A., Seth Stein, and Miguel Merino, 2014, "April 2014 LIP of the Month." International Association of Volcanology and Chemistry of the Earth's Interior, Apr. 2014. <http://www.largeigneousprovinces.org/14apr>
- Tatsumi, Yoshiyuki, Masanori Sakuyama, Hiroyuki Fukuyama, and Ikuo Kushiro, 1983, "Generation of Arc Basalt Magmas and Thermal Structure of the Mantle Wedge in Subduction Zones." *J. Geophys. Res. Journal of Geophysical Research* 88.B7: 5815.
- Wadsworth, M. Edward, 1884, "Presque Isle, Michigan." *Lithological Studies: A Description and Classification of the Rocks of the Cordilleras*. Cambridge.
- Wager, L. R., G. M. Brown, and W. J. Wadsworth, 1960, "Types of Igneous Cumulates." *Journal of Petrology* 1.1: 73-85.
- Woolley, A.R, 2014, "A Web Browser Flow Chart for the Classification of Igneous Rocks." *Classification of Igneous Rocks - Flow Chart*. <http://www.geol.lsu.edu/henry/Geology3041/lectures/02IgneousClassify/IUGS-IgneousClassFlowChart.htm>